# Carbon fluxes and productivity regimes in Alpine streams

## Marta BOIX CANADELL

École
polytechnique
fédérale
de Lausanne

2020

# Acknowledgements

# Abstract

High-altitude catchments have a major role in the transport of organic matter to streams due to the storage of dissolved organic carbon (DOC) in soils and glacier ice and the subsequent mobilization during the melting processes. Yet, stream function goes beyond the conveying downstream of the terrestrial and glacier derived DOC since they are also highly active in the mineralization, retention and production of organic matter. Stream ecosystem metabolism integrates the processes that regulate the conversion between the organic and inorganic forms of carbon in streams and is a fundamental measure to determine whether carbon accumulates or it is lost within the ecosystem. In a global warming scenario, high-mountain stream ecosystems are faced to modifications in their structure and function as a result of climate-driven hydrological changes. Thus far, despite the active role of alpine streams in the global carbon cycle, studies on the impacts from changes in snowmelt, glacier ice melt and groundwater contribution to streamflow have been largely focusing on alterations in hydrological regimes, water availability, geomorphology and biodiversity. To fill this gap, the aim of this thesis is to examine DOC fluxes dynamics and productivity regimes across a range of glacierized and non-glacierized alpine catchments to anticipate the possible consequences of projected hydrological changes on alpine stream biogeochemistry and ecosystem functioning.

This thesis is supported by the collection and analysis of high-frequency time series of physicochemical parameters, geomorphological data and streamwater samples from different Alpine streams with contrasting glacier coverage. The first part of the thesis investigates the response across all the streams of the annual DOC export to runoff primarily driven by snowmelt and glacier melt. In the second part, with the use of dissolved oxygen time series, the ecosystem energetics regimes in a glacier-, groundwater- and snowmelt-fed stream are explored during two years and related to their physical template. The third and last part is focused on providing estimates of gross primary production (GPP) rates for the energetic regimes established in the three Alpine stream types.

The obtained results show a varied response of DOC export to runoff across the catchments which was related to the degree of glaciation and vegetation cover. Our findings also reveal different stream ecosystem energetic regimes among the streams and highlight discharge as the major modulator of drivers, such as light, gas exchange rate or stability, on the seasonal and daily dissolved oxygen dynamics. Lastly, the magnitude and the temporal patterns of ecosystem GPP are the result of the light and streambed disturbance conditions that are largely determined by the hydrological and turbidity regime.

I argue that glacier shrinkage together with changes in snowmelt hydrology will alter the response of DOC yield to discharge, with consequent impact on the timing and magnitude of the lateral DOC fluxes from terrestrial to stream ecosystems. Also, an eventual reduction in glacier runoff and snowpack duration and content will alter the physical template for primary producers, which may lead to a greater production of autochthonous organic matter across high-mountain streams. Overall, I assume that climate-driven hydrological changes would cause a shift in the magnitude and temporal patterns of energetic inputs, with consequences for the stream ecosystem biogeochemistry and function and therefore for the role of alpine streams in the global carbon cycle.

*Keywords : Alpine streams, Hydrological regimes, DOC fluxes, Productivity regimes, Global warming*

# Résumé

Les bassins versants d'altitude jouent un rôle majeur dans le transport du carbone organique vers les cours d'eau en raison du stockage du carbone organique dissous (COD) dans les sols et dans la glace et de la mobilisation subséquente pendant les processus de fonte. Pourtant, la fonction des cours d'eau ne se limite pas au transport en aval du COD d'origine terrestre et glaciaire. Les ruisseaux sont, en effect, également très actifs dans la minéralisation, la rétention et la production de matière organique. Le métabolisme de l'écosystème d'un cours d'eau intègre les processus qui régulent la conversion entre les formes organiques et inorganiques du carbone dans les cours d'eau et constitue une mesure fondamentale pour déterminer si le carbone s'accumule ou se perd dans l'écosystème. Face au réchauffement climatique, les écosystèmes aquatiquede haute montagne sont confrontés à des modifications de leur structure et de leur fonction, suite aux changements hydrologiques liés au climat. Malgré le rôle actif des cours d'eau alpins dans le cycle global du carbone, les etudes sur les effets en cascade et les implications potentielles d'un changement dans la contribution de la fonte des neiges, de la fonte des glaciers et des eaux souterraines à l'écoulement fluvial ont été axés sur les modifications des régimes hydrologiques, la disponibilité en eau, la géomorphologie et la biodiversité. En ce sens, le but de la thèse est d'examiner la dynamique des flux de COD et les régimes de productivité dans une gamme de bassins versants alpins, glaciaires et non glaciaires, afin d'anticiper les conséquences possibles des changements hydrologiques prévus sur la biogéochimie et le fonctionnement de ces écosystèmes.

Cette thèse se base sur la collecte et l'analyse de séries chronologiques à haute fréquence de paramètres physico-chimiques, de données géomorphologiques et d'échantillons d'eau provenant de différents cours d'eau Alpins avec une couverture glaciaire différente. La première partie de la thèse porte sur la réaction de ces flux à l'exportation annuelle de COD au ruissellement, causé principalement par la fonte des neiges et des glaciers. Dans la deuxième partie, à l'aide de séries chronologiques sur l'oxygène dissous, les régimes énergétiques de l'écosystème d'un glacier, des eaux souterraines et d'un cours d'eau alimenté par la fonte des neiges ont été explorés pendant deux ans et reliés à leur modèle physique. La troisième et dernière partie de ce travail est axée sur l'estimation des taux de production primaire brute (PPA) pour les régimes énergétiques établis dans les trois types de flux alpins.

Les résultats obtenus montrent une réponse variée de l'exportation du COD au ruissellement à travers les bassins versants. Cela varie en fonction du degré de glaciation et de la couverture végétale. Nos résultats révèlent également différents régimes énergétiques de l'écosystème cours d'eau parmi les ruisseaux étudiés, et soulignent que le débit est le principal modulateur de plusieurs facteurs tels que la disponibilité de lumière au fond du cours d'eau, la stabilité de son lit ou le taux de ses échanges gazeux. Enfin, l'ampleur et le profil temporel des PPA écosystémique étaient le résultat des conditions de perturbation de la lumière et du lit de chaque cours d'eau et étaient déterminés par le régime hydrologique et le régime de turbidité.

Je soutiens que le rétrécissement des glaciers, ainsi que les changements de l'hydrologie de la fonte des neiges, entraineront une modification du rendement en COD. Ces changements auront un impact sur le temps et l'ampleur des flux de COD entre les écosystèmes terrestres et fluviaux. De plus, la réduction du ruissellement glaciaire et de la durée et du contenu de l'accumulation de neige modifiera le modèle physique des producteurs primaires, ce qui pourrait entraîner une production accrue de matière organique autochtone dans ces cours d'eau de haute montagne. Par conséquent, je suppose que les changements hydrologiques dictés par le climat entraîneraient un changement dans l'ampleur et la structure temporelle des apports énergétiques, ce qui aurait

des conséquences sur la biogéochimie et la fonction de l'écosystème étudié et sur son le rôle dans le cycle global du carbone.

# Contents

# List of Figures

# List of Figures Supporting Information

# List of Tables

# List of Tables Supporting Information

# List of Equations

# Chapter 1 Introduction

## 1.1    High-mountain regions and climate change

Global warming is possibly the most severe challenge facing our planet during the 21st century. Anthropogenic interference with the climate system as a consequence of land use changes and greenhouse gas emissions are estimated to have caused an increase of approximately 1.0 ºC of the global mean surface temperature relative to pre-industrial levels (years 1850-1900) (IPCC 2014). Continued increase in atmospheric concentrations of carbon dioxide, methane, and nitrous oxide will cause further warming and long-lasting changes in all components of the climate system, increasing the likelihood of irreversible impacts for people and ecosystems (IPCC 2018). The ecological responses to climate change are evident and span an array of ecosystems and levels of organization (Walther et al. 2002). However, nowhere are the impacts of anthropogenic climate change more evident than in polar and high-mountain regions (Beniston 2005).

The mountain cryosphere, which includes glaciers, permafrost, and snow, is one of the Earth's ecosystems most strongly affected by climate change. Observations show that mountain glaciers around the globe are responding to recent climate change and are in retreat and losing mass (Zemp et al. 2015) since its maximum attained during the Little Ice Age (years 1450 - 1850). Changes in glacier length, area, volume and mass have been accelerating since the 1980s (IPCC 2019) as a consequence of increased temperature (i.e. acceleration of glacier ablation) or changes in solid precipitation (i.e. changes in accumulation rate). In the tropical Andes, which hosts more than 99% of all tropical glaciers, air temperature increased 0.10 ºC per decade since 1939 (Vuille et al. 2008). This caused an unprecedented glacier retreat since the late 1970s as glacier mass loss increased from -0.2 m water equivalent year$^{-1}$ (-200 kg m$^{-2}$ year$^{-1}$) over the 1964-1795 period to -0.76 m w.e. year$^{-1}$ (-760 kg m$^{-2}$ year$^{-1}$) over the 1976-2010 period (Rabatel et al. 2013). Comparable glacier mass loss in high mountain Asia (-220 ± 100 kg m$^{-2}$ year$^{-1}$) or the Rocky Mountains (-930 ± 230 kg m$^{-2}$ year$^{-1}$) have also been documented by Gardner et al. (2013). Seasonal snow covers over 46 million km$^2$ or about 31% of Earth's land each year, with 98% this cover located in the Northern Hemisphere (Rutgers University Global Snow Laboratory (GSL)). The relative amount of precipitation falling as snow in snow-influenced regions depends on intra-annual precipitation variability and the relationship between precipitation seasonality and the annual air temperature cycle (Willmott et al. 1985; Woods 2009). In a warmer climate, the percent precipitation falling as snow and spring snow cover duration and extent in the Northern Hemisphere will likely decrease (Beniston et al. 2018; IPCC 2018). Declines in spring snowpack have already occurred in much of the North American West since 1915 (Mote et al. 2018), in some regions of High Mountain Asia from 1987 to 2009 (Smith and Bookhagen 2018), and it seems to be an overall tendency in the Northern Hemisphere (Connolly et al. 2019). A shift towards an earlier onset of snowmelt due to warmer temperatures has also been observed (Cayan et al. 2001; Stewart et al. 2004; Choi et al. 2010).

## 1.2    Climate change in the Alps

In the highest and most extensive mountain range system in Europe, the Alps, mean annual air temperatures have been increasing (Serquet et al. 2011; CH2018), and various studies demonstrate the effect of this rising on snowfall (Serquet et al. 2011), snowpack duration and content (Durand et al. 2009; Klein et al. 2016; Marty et al. 2017a), and deglaciation rates (Huss 2012). For both conservative and extreme emission scenarios, snowfall projections over most parts of the Alps reveal a signal of decreasing snowfall amounts (Frei et al. 2017) that will further reduce

snowpack duration and content (Marty et al. 2017b; CH2018). Glaciers in the Alps cover an estimated area and volume of 2003 $km^2$ and 115 $km^3$ respectively (Beniston et al. 2018), with the Swiss Alps hosting the highest percentage of both measures (i.e., 47% and 58%) compared to Austrian, Italian, or French Alps. By the start of the twenty-first century, Alpine glaciers had lost almost two-thirds of their volume compared to 1850 (Zemp et al. 2006), and evidence suggests that glacier mass loss will accelerate in the next decades (Huss and Fischer 2016).

## 1.3     Hydrological regimes of high-mountain streams

In glacierized and snowmelt-dominated catchments (a.k.a. nival catchments), snow and glacial melt waters are critical for maintaining hydrologic baseflow, freshwater availability, solutes and sediment transport, and aquatic ecosystem structure and function (Milner et al. 2017; Beniston et al. 2018). Annual runoff in temperate nival catchments is dominated by snowmelt and displays a pronounced annual cycle of discharge with a runoff peak occurring in spring (Beria et al. 2018). At a daily scale, snowmelt runoff shows a clear diurnal cycle due to daily snow fusion (Brown et al. 2003). For glacierized catchments, high levels of runoff from snowmelt are sustained by glacier-melt-induced flows occurring later in the melt season (Schaner et al. 2012). Glacier runoff displays a particular regime with strong temporal variability at the inter-annual, seasonal, and diurnal time scale (Milner et al. 2009). Inter-annual variation in the glacier hydrological contribution are determined by climatic conditions (i.e., air temperature and precipitation regime) that regulate glacier mass-balance regime (Hock 2005). Seasonal discharge patterns with maximum discharge occurring in summer is a result of melting ice and snow stored during previous accumulation processes (Hock 2005). During the melting season, runoff exhibits repeated daily cyclic fluctuations in response to diurnal cycles of temperature (Clifford et al. 1995; Hannah et al. 2000). The degree to which glacier runoff contributes to overall stream runoff varies greatly from catchment to catchment (Schaner et al. 2012), with glacier contributions in individual months that reach > 25%, even in catchments with < 1% glacierization (Huss 2011). Glacier meltwater released during summer periods typically results in a water temperature decrease and an increase in turbidity, suspended solids concentrations, and sediment transport (Clifford et al. 1995). In both glacierized and nival catchments, stream flows are very low from the end of autumn to the beginning of spring, when stream channels can be covered by snow, freeze, or fall dry.

## 1.4     Effects of climate change on stream ecosystems

Under global warming scenarios, climate-driven changes in snow and ice melt will cause a shift in the timing and magnitude of discharge maxima (Stewart et al. 2004; Lane and Nienow 2019), a reduction of catchment runoff (Berghuijs et al. 2014; Beniston et al. 2018), and an increase in inter-annual flow variability as a result of a reduction in the predictability of the characteristic seasonal runoff fluctuations (Fleming and Clarke 2005 ; Horton et al. 2006). As glaciers shrink through time, runoff generated from ice melt initially increases until a peak is reached, beyond which it diminishes until the ice mass has disappeared (Huss and Hock 2018). As total runoff from glaciers diminishes, summer runoff will become more sensitive to precipitation events (Milner et al. 2017). Ultimately during the coming centuries, there will be a gradual transition of runoff regimes from glacial to nival and from nival to pluvial (Beniston et al. 2018).

 Associated impacts of glacier and snowpack alterations are especially relevant in the downstream systems whose streamflow is sustained by seasonal melt. The implications of these hydrological changes in lowland systems include changes in water availability, energy production, geomorphology, and ecological changes in downstream ecosystems (Huss et al. 2017). With more than one-sixth of Earth's population relying on glaciers and seasonal snowpack for their water supply, potential water scarcity resulting from glacier runoff and seasonal snowpack reductions has already been claimed as one of the most critical impact affecting mountain societies (Barnett et al. 2005; Kaser et al. 2010). In addition, changes in water resources will represent a future challenge to hydropower production globally (Finger et al. 2012). Glacial systems are an important source of sediments to downstream

areas, with a significant fraction transported as bedload (Gurnell et al. 2000). Glacier extent reduction will uncover and leave exposed unconsolidated sediments, enhancing sediment connectivity, and eventually leading to an increase in sediment export. However, river reworking and accumulation of glacial sediment in the now expanded proglacial zone may counterbalance the potential increase in sediment transport due to higher sediment availability (Lane et al. 2017).

High altitude streams tend to have high slopes, high water velocities, turbulent and well-oxygenated waters, and predominantly bedrock, boulder, and cobble substrata (Wohl 2010). Also, the relative contribution of snowmelt, glacier ice melt, and groundwater to the streamflow of nival and glacier-fed streams also results in a unique signature of physicochemical properties, including water temperature, suspended sediments, conductivity, solute concentrations, and channel stability (Füreder et al. 2001; Robinson et al. 2002; Battin et al. 2004; Sertić Perić et al. 2015). The physical isolation and the rather harsh conditions of these streams confers them with a singular stream habitat and biotic characteristics that is translated into a unique stream biota and stream ecosystem processes (Ward 1994). This uniqueness has motivated several studies and topic specific reviews on the different components of the biota and function (Ward 1994; Zah et al. 2001; Hieber et al. 2005; Clitherow et al. 2013; Slemmons et al. 2013; Wilhelm et al. 2013), with the most recent focusing on their response to shifts in stream runoff and physicochemical regimes due to global warming (Jacobsen et al. 2014; Cauvy-Fraunié et al. 2016; Hotaling et al. 2017; Milner et al. 2017; Fell et al. 2018; Brighenti et al. 2019).

Stream biofilms dominate microbial life in nival and glacier-fed streams, either in benthic biofilm or glacial snow and ice (Wilhelm et al. 2013; Battin et al. 2016 ; Smith et al. 2016). The structure and function of these microbial communities vary depending upon environmental conditions provided by the hydrological regime (Battin et al. 2004). In Swiss alpine floodplains, microbial community structure and enzymatic function were influenced by sediment pH, conductivity, and other physicochemical conditions derived from glacial meltwater (Freimann et al. 2013, 2014). Additional studies on glacier-fed streams suggest that as glacial runoff decreases there will be a homogenization of microbial diversity among glacier-fed streams (Wilhelm et al. 2013) and bacterial communities will resemble those from non-glacierized catchments. Research on benthic macroinvertebrate communities show that taxonomic richness and total abundance of individuals may increase, and experience a shift in longitudinal organization as snow melt and glacier melt contributions to stream runoff decrease (Brown et al. 2007; Finn et al. 2010; Jacobsen et al. 2014; Cauvy-Fraunié et al. 2016). However, expected homogenization across high-mountain streams due to the vanishing of glaciers will probably lead to a decrease in beta biodiversity due to the substitution of glacier-fed specialists by generalists (Jacobsen et al. 2012; Khamis et al. 2016).

In high-mountain streams, primary producers generally are associated with benthic substrates, and include diatoms, cyanobacteria, chrysophytes, and green and red algae which colonize microbial biofilms (Hieber et al. 2001; Fell et al. 2018; Niedrist et al. 2018), but also lichens and mosses (Rott et al. 2006). The fundamental controllers of temporal and spatial patterns of benthic algal communities in high-mountain streams are light availability and physical disturbance by high flow events (Peterson 1996 ; Uehlinger et al. 1996; Biggs et al. 1999). The principal mechanisms for flow disturbance to influence benthic communities is via shear stress, abrasion, and scouring (Biggs et al. 2001). If there is not sufficient energy to move bedload, the shear stress applied on benthic biota by increased flows may be sufficient to disrupt communities (Lancaster and Hildrew 1993; Biggs et al. 1999; Bond and Downes 2003), causing damage or removing flora and fauna from the substrate (Biggs and Thomsen 1995). As velocity and shear stress increase, sediment transport starts when fine sediments are mobilized, leading to an increase in the quantity of suspended sediments, and mechanical abrasion for benthic biofilms (Biggs et al. 2001). At a critical flow velocity (critical discharge), the movement of larger particles occurs, initiating bedload transport. High flow events which induce bedload transport are often associated with the most dramatic changes in streambed habitat structure, density and biomass of benthic algae (Segura et al. 2011). In glacier-fed streams, an increase in shear stress through greater suspended solids during summer can inhibit development of benthic

algae, and episodes of complete biomass loss in summer are often related to sediment shifting (Rott et al. 2006). Despite being above the tree line, where the seasonal canopy does not interfere, light availability for primary producers in high-mountain streams is highly seasonal. In winter, the streams may be completely covered by snow, reducing incident PAR by 99 % (Uehlinger et al. 2010). During the highest periods of discharge (i.e., melting periods), and as water depth increases, light availability to the streambed can be strongly reduced. High turbidity from suspended solids, like in summer flows in glacier-fed streams, will enhance light attenuation with increases in depth (Uehlinger et al. 1998). Considering all the above, biomass accumulation of benthic algae is constrained to those periods where there is an overlap of favourable conditions for primary production to occur. In nival streams, the snowmelt onset and recession are characterized by low turbidity and streambed stability and consequently represent crucial periods for recovery of benthic algae from winter and snowmelt harsh conditions respectively (Ward 1994; Füreder et al. 2001; Battin et al. 2004; Hieber et al. 2001). However, algal growth in clear waters and low flow may be inhibited due to an excess of UV and photosynthetic active radiation, already aggravated with the high altitude of these streams (Wellnitz and Ward 2000; Uehlinger et al. 2010). In glacier-fed streams, along with the onset of snowmelt, favourable growth conditions are encountered at the end of summer (Battin et al. 2004; Rott et al. 2006; Uehlinger et al. 2010), when the contribution of glacier melt to streamflow has been reduced with the colder autumn temperatures.

In face of global warming, currently autumnal conditions of low turbidity and sediment stability may be expanded into earlier days, linked to the eventual reduction of glacial meltwater. A change towards more favourable conditions into summer in glacier-fed streams may result in an increase in algal biomass, as seen experimentally by Cauvy-Fraunié et al. 2016, or a shift in benthic algal composition (Fell et al. 2018; Niedrist et al. 2018). Shallower snowpacks along with warmer temperatures will affect the timing and magnitude of snowmelt peak with a consequent displace and extension of the favorable growth conditions. However, in a scenario in which both snow and ice meltwaters have been reduced, stream runoff will be still influenced by stochastic and periodic high-flow events that will scour benthic algae and reduce algae biomass (Rinke et al. 2001).

## 1.5    Dissolved organic matter export and function in streams

One phenomenon highly coupled to discharge is the lateral export of organic carbon from terrestrial ecosystems. High-altitude catchments have a major role in carbon fluxes downstream due to the organic carbon storage in adjacent soils and glacial ice, and the subsequent mobilization during seasonal melt (Boyer et al. 1997; Brooks et al. 1999; Pellerin et al. 2012; Hood et al. 2015; Li et al. 2018). From all the soil organic carbon fractions, dissolved organic carbon (DOC) is widely recognized as the most mobile form of soil organic matter (Tank et al. 2018). Besides allochthonous inputs from degrading plant and soil material (Meyer and Wallace 1998), stream dissolved organic matter (DOM) originates from autochthonous sources, such as in-stream primary production (Lovett et al. 2006). DOM is operationally defined as the organic matter that passes through a membrane with a pore size of ~0.7 mm or a glass fiber filter. DOM is an essential resource for fluvial ecosystems as it serves as a carbon and energy source to heterotrophic bacteria in streams (Lovett et al. 2006). Furthermore, the transport of dissolved organic matter not assimilated or mineralized by the bacterial community represents the greatest flux downstream of organic carbon. It is well recognized that most DOM export in a stream occurs during precipitation events when large quantities of DOM are flushed from the soil profile and delivered to the streams (Boyer et al. 1997; Ågren et al. 2010). During rainy events and snowmelt, shallow flowpaths connecting the soil horizons with the stream are activated and terrestrial derived organic carbon is transferred to the stream (Boyer et al. 1997). Also, the activation of additional groundwater flowpaths may enhance this export (Sawyer et al. 2014). A significant positive correlation between DOC and discharge has been found in a broad range of catchments in different climatic areas, hydrological characteristics, and land uses attributed to the 'flushing effect' (Hood et al. 2006; Vidon et al. 2008). Together with hydrology, concentration and fluxes of dissolved organic carbon are controlled by factors such as climate, biological productivity and decomposition in the catchment (Hope et al.

1994; Hornberger et al. 1994; Boyer et al. 1997; Dawson et al. 2008). In streams above the tree line with minimal riparian vegetation, lower DOC concentrations compared to the ones encountered downstream (with higher forest coverage) are expected (Sertić Perić et al. 2015). Also, alternative sources of DOC may gain importance because of poorly developed soils. For instance, glacial ice and melt water can also release carbon and contribute to the allochthonous pool of organic matter (Hood et al. 2015; Li et al. 2018).

Once imported into the stream, DOM either supports bacterial production and respiration, is physically retained, or is exported to downstream reaches. In some streams, readily labile DOM might support > 50 % of the community respiration near the point of input, whereas intermediately labile DOM might be an important subsidy to downstream ecosystems (Wiegner et al. 2005). Seasonal patterns of DOC export from different catchment sources can control temporal variations of bacterial growth in streamwater (Berggren et al. 2009). Also, the traditional assumption that terrestrially derived dissolved organic carbon is generally not highly biologically degradable is changing (Holmes et al. 2008; Bianchi et al. 2012; Ward et al. 2013). In Berggren and del Giorgio (2015), the highest bacterial growth efficiency was supported by terrestrial DOC across a range of streams draining peat bogs and forest soils. Lapierre et al. (2013) tested the potential for the degradation of terrestrially-derived DOC from natural water samples from a wide range of aquatic systems (lakes, rivers and wetlands) in the boreal and temperature landscapes. Their results indicated that increasing terrestrial influence implies higher potential for dissolved organic carbon to be degraded across all the different aquatic systems, and eventually to increase $CO_2$ in streams. In glacierized catchments, old glacier-derived organic carbon proves to be also bioavailable to aquatic bacterial communities (Singer et al. 2012) and to have the capacity to sustain higher trophic levels in the food web (Fellman et al. 2015). The transport of DOC across the terrestrial-aquatic interface is thus relevant for stream ecosystem functioning and its export from the catchment is critical for the carbon balance at catchment scale (Tank et al. 2018). Despite this, our ability to predict the impact of climate change on DOC export is relatively limited at present (Zarnetske et al. 2018).

## 1.6    Stream ecosystem metabolism

Streams function goes beyond being merely a conduit for the transport of organic carbon and other solutes from upstream to downstream (Cole et al. 2007). In fact, streams are active components involved in the production, processing and retention of organic carbon (Battin et al. 2009). Of the stream ecosystem functions, ecosystem metabolism plays a fundamental role in controlling the rate at which organic matter is produced, respired, and stored (Staehr et al. 2012), and thus provides critical information about the role of stream ecosystems in the global carbon cycle (Battin et al. 2009).

Ecosystem metabolism includes gross primary production (GPP) and ecosystem respiration (ER). GPP is defined as the total autotrophic conversion through photosynthesis of inorganic carbon to organic forms. ER is the total oxidation of organic carbon to inorganic carbon by both heterotrophic and autotrophic organisms. The balance of these two processes is net ecosystem production (NEP) such that NEP = GPP + ER (considering ER a negative flux). NEP has long been used to indicate the relative importance of energy fixed by primary producers within the stream versus allochthonous organic matter derived from terrestrial plant production. NEP is positive when GPP > ER and negative when GPP < ER. Positive NEP means that energy to the system is supplied through in-stream photosynthesis and that an ecosystem must be accumulating or exporting organic carbon. Negative NEP means that ecosystem respiration is based on the utilization of imported organic matter and microbial production (Lovett et al. 2006).

Light is the ultimate energy source and a key driver for primary producers (Mulholland et al. 2001; Roberts et al. 2007). Variations in light can come from shading, turbidity, or seasonal variation in solar angle. The photosynthetically active radiation (PAR) explained 64% of the variation in GPP and 54% of the variation in chlorophyll *a* in spring in a headwater forested stream (Acuña et al. 2004). When canopy closure occurred, it

caused a 78% reduction in PAR, which was accompanied by remarkable decrease in GPP. Rates of GPP in a headwater forested stream were positively correlated with PAR over the two years of ecosystem metabolism study in Roberts et al. (2007), with PAR explaining over 70% of the variance in daily GPP rates. Turbidity was the strongest covariate with primary production in a series of continuous GPP data from 21 streams in Spain where benthic algae was the main primary producer (Izagirre et al. 2008). In the Colorado River, under high PAR conditions, GPP declined with turbidity (Hall et al. 2015). Characteristic seasonality in light availability in high latitudes was found to be the major driver of the annual patterns of GPP in one artic stream in Huryn et al. 2014.

Disturbance in stream ecosystems can be defined as any relatively discrete event in time that is characterized by a frequency, intensity, and severity outside a predictable range, and that disrupts ecosystem, community, or population structure and changes resources or the physical environment (Resh et al. 1988). Stream disturbance is primarily determined by the forces that flowing water exercises on streambed substratum. Physical disturbance of the streambed is a major factor controlling in-stream metabolic rates as it can cause the burial and removal of benthic producers from the substrate to which they are attached. The effects of high bed-moving spates on ecosystem stability were assessed by Uehlinger (2000) in two reaches of a pre-alpine river in Switzerland. In this study, ER was more resistant to bed movement events than GPP. Similarly, photosynthesis and respiration also exhibited a differential response to bed movement in Cronin et al. (2007). This study also identified a clear discharge threshold at which photosynthesis was suppressed to negligible rates. Respiration, however, was only weakly affected by change in discharge and did not show a clear threshold. After the disturbance event, differences between the recovery rates found in Uehlinger (2000) were driven by differences in light and temperature present during the recovery period. Post-spate recovery of GPP and ER was also found to be positively correlated with temperature and light availability in Uehlinger and Naegeli (1998). In comparison, in Segura et al. (2011), the absence of optimal environmental conditions in a snowmelt-dominated stream didn't allow GPP to recover to the initial state before perturbation.

Streamwater temperature is driven by strong seasonal variation and can also explain much of the temporal variability in primary production and ecosystem respiration (Uehlinger 2000). Temperature can control the rate of metabolism in part due to the direct control via temperature dependent kinetics of enzymes (Yvon-Durocher et al. 2012). Effects of temperature from metabolism studies show strong positive relations with temperature and GPP across a range of chemically similar, geothermally altered streams in Iceland (Demars et al. 2011; Rasmussen et al. 2011). Temperature is also a principal control of ecosystem respiration. Indeed, respiration is more sensitive to temperature than primary production (Allen et al. 2005): with a temperature increase from 0 to 30 °C, primary production increases 4-fold, while respiration increases 6-fold (Enquist et al. 2003; Allen et al. 2005). Water temperature along the thickness of the benthic biofilm influenced the temperature dependence of respiration in an Alpine river network (Acuña et al. 2008). Increases in water temperature stimulated respiration of benthic algae of incubated stones from mountain streams to a larger extent than did increases in nutrients concentrations (Rosa et al. 2013). Temperature was also identified as regulator of ER across streams from different geographic regions and with different land use (Bernot et al. 2010).

Finally, both nitrogen (N) and phosphorous (P) can be limiting nutrients in Alpine streams, with the limiting capacity varying seasonally and between glacier-fed or nival dominated streams (Robinson et al. 2002). The primary sources of N in high-mountain streams is atmospheric deposition or from organic soil processes such as nitrification (Rhim 1996; Kuhn 2001; Sebestyen et al. 2008). During snowmelt, N accumulated from atmospheric deposition and terrestrial sources areas during winter is transferred to the streamwater increasing stream $NO_3$ concentration values. In autumn, baseflow is when the lowest $NO_3$ levels are found. Sources of P in high-mountain streams include weathering of phosphate-containing minerals and potentially atmospheric inputs (Hodson 2007; Camarero and Catalan 2012). Glacial flour is also a supplier of P to alpine streams, mainly through the physical erosion and weathering of rocks (Hodson 2007). However, its availability for biological uptake may be reduced

due to absorption by glacial particles (Hodson et al. 2004). Overall, P rather than N is the element likely to be limiting benthic algae growth in high-mountain streams (Ren et al. 2019). Yet, physical disturbance and light may still play a dominant role determining activity and biomass of primary producers (Rinke et al. 2001).

## 1.7 Modelling ecosystem metabolism

GPP and ER can be estimated by monitoring the diel change in dissolved oxygen (DO) concentration using either a chamber-based approach or by open-channel methods (Hall et al. 2016; Staehr et al. 2012). Much of the metabolism in streams occurs in the benthic and hyporheic zone, for which it is difficult to use chambers to calculate scaled-up estimates of ecosystem metabolism. Thus, much of the recent research on metabolism has been via the open-channel method (Hall 2016). The open channel technique derives from Odum's first metabolic rates calculations based on the analysis of the mass balance of DO in a stream reach (Odum 1956). This technique requires information of temporal changes of DO concentration, water temperature, discharge and the air-water exchange of oxygen in one (single station method) or two points (two-station method) within a stream reach. In order to adequately estimate ecosystem metabolism from diel DO concentration, four processes that affect DO concentration in streamwater need to be considered: (1) release of DO into the water from primary production (2) uptake of DO because of ecosystem respiration (3) exchange of $O_2$ with the air (4) inputs of low DO from groundwater, which affects estimates of ER (Hall and Tank 2005). Therefore, the mass balance for dissolved $O_2$ in a stream, which is the basis for the ecosystem metabolism calculation method is:

$$\frac{dO}{dt} = GPP + ER + K(O_{SAT} - O_t)$$

Equation 1.1

Where GPP increases DO concentrations and ER (a negative flux) decreases DO concentrations. Gas exchange flux between water and atmosphere is the product of the gas exchange rate $K$ ($d^{-1}$) and oxygen deficit, which is the difference between DO concentration in water at saturation for a given temperature and atmospheric pressure ($O_{SAT}$) and DO concentration at time $t$ ($O_t$).

Modifications of Equation 1.1 have been proposed in order to better capture the underlying complexity of the metabolic processes. Examples of this are found in Hanson et al. 2008 where a non-linear response of GPP to light is proposed as a result of photoinhibition processes. On the other hand, a response more closely approximating a linear relationship is suggested by Van de Bogert et al. 2007. In addition to that, the inclusion in the model of a temperature-correction term that takes into account the diel variation of temperature may lead to better metabolic rates estimates (Holtgrieve et al. 2010 ; Riley and Dodds 2013). Over the last decades, researchers have also relied on a variety of techniques in order to estimate the best-fit metabolism parameters from a model given DO data. These techniques can be divided on the one hand between the earlier ones in which rates are calculated directly from DO concentrations and which are optimized by minimizing an objective function, such the residuals sum of squares between modelled and collected oxygen data (Marzolf et al. 1994; Izagirre et al. 2007; Riley and Dodds 2013). With these techniques the gas exchange rate needs to be previously estimated. On the other hand, most recent one are based on Bayesian inverse modeling or maximum likelihood estimation methods (Holtgrieve et al. 2010; Appling et al. 2018a). These two techniques allow the assessment of the fit by calculating the uncertainty of the parameters estimated and to solve for gas exchange rate if necessary. In addition, Bayesian estimation allows prior information, which is especially useful in case the estimation of $K$ from the model is also needed.

Today's accessibility of modelling programs (e.g., streamMetabolizer) and the availability of reliable and affordable DO sensors is allowing us the study of GPP and ER dynamics over long periods of time and multiple temporal

scales. Studies covering long periods include those focusing on the impact of anthropogenic alterations of river flow on ecosystem metabolism (15 years; Val et al. 2016) or on the response of water quality and ecosystem functioning to management practices (20 years; Arroita et al. 2018). Metabolic rates over long periods have been also estimated to assess the impact of streambed moving events on primary production and ecosystem respiration variability (Uehlinger 2006), the influence of season on annual in-stream productivity (Roberts et al. 2007), the effect of turbidity on primary productivity in large rivers (Hall et al. 2015) or how the influence of stream metabolism on nutrient biogeochemistry (Roberts and Mulholland 2007). On a larger scope, Appling et al. (2018b) estimated daily GPP and ER rates up to 9 years to help to reveal the metabolic regimes across multiple (i.e., 365) river and stream types. Thus, currently, with the acquisition of time series of metabolic rates we are not only able to study and classify stream ecosystems in terms of its rates of production and consumption of organic matter but also by their seasonal patterns of productivity or productivity regimes (Savoy et al. 2019). Ultimately, the metabolic regimes that streams exhibit are a response of the physicochemical pattern that each stream experience, which is mostly controlled by its hydrological regime and catchment properties (Bernhardt et al. 2018). In high-mountain streams, the melting of snow and glacial ice imparts a typical signature on the physicochemical properties of the streamwater, including temperature, turbidity and related light attenuation, solute composition and concentration, as well as streambed stability (Ward 1994; Robinson et al. 2002; Uehlinger et al. 2010; Gabbud et al. 2020). The interactions between these parameters over daily and seasonal scales create scenarios in which biological and physical processes play roles of alternating relevance in shaping stream ecosystem functioning. Studies on metabolic regimes in mountain regions are focused on pre-alpine or subalpine catchments (e.g., Uehlinger and Naegeli 1998; Ulseth et al. 2018). In this sense, the less abundant studies on metabolic rates in alpine streams contrast with the wider knowledge on benthic algae dynamics and their physical template in these ecosystems. Stream consumers depend on both allochthonous inputs of organic matter from terrestrial ecosystems and the autochthonous inputs by those primary producers (Lovett et al. 2006). Since it has been stated that autochthonous primary production is considered the main energy resource to higher trophic levels in streams above the tree line (Milner and Petts 1994; Ward 1994), the lack of knowledge of GPP rates in high-mountain streams is remarkable. Establishing the characteristic temporal pattern of ecosystem GPP and its magnitude is therefore critical to better understand the impact on carbon fluxes of the hydrological and physicochemical changes that high-mountain streams are facing.

## 1.8 Thesis aims and outline

Climate change is a complex global issue that is driving countless shifts in the structure and function of alpine stream ecosystems. Yet, in this instance, our capacity to anticipate the response of carbon fluxes and stream ecosystem functioning to climate-driven hydrological change is limited. Within the perspective of the decisive role that streams have in the fate of organic and inorganic carbon in aquatic systems, there is a need to push forward our understanding of how global warming is altering the role of alpine streams in the global carbon cycle.

This thesis therefore aims at improving the knowledge regarding dissolved organic carbon fluxes and productivity regimes in high-mountain catchments to better evaluate the consequences of global warming on alpine streams biogeochemistry and energetic regimes.

The content of this thesis is organized as follows:

**Chapter 2:** In this chapter, I investigated how runoff, as mediated by snowmelt and glacier-melt, affected the DOC yield from glacierized and non-glacierized catchments. For this, I used high-frequency (every 10 minutes) measurements of discharge, streamwater temperature, turbidity and chromophoric dissolved organic matter (CDOM) during one year to estimate DOC concentrations and yields from twelve Alpine streams with different levels of glacier coverage. Using a space-for-time substitution approach, I identified a change in DOC yield response to runoff as glaciers recede.

**Chapter 3:** In order to reveal stream ecosystem energetic regimes at daily and seasonal scales in high-mountain streams, the dissolved oxygen concentration dynamics of different Alpine streams and its potential drivers were explored in this chapter. For this, I monitored dissolved oxygen concentration (in percent of saturation) at 10-min frequency over two years in three major stream types in high-mountain regions: a glacier-fed, a groundwater-fed and a snowmelt-fed stream. Later, I derived a Shannon entropy index to quantify daily patterns of dissolved oxygen. Potential drivers of daily entropy included light availability at the streambed, gas exchange and streambed stability inferred from 10-min frequency measurements of turbidity, light reaching the stream surface, discharge and the geomorphological analysis of the studied streams. The approach used revealed different energetic regimes across the streams, and paves the way for a better understanding of the possible consequences of global warming on ecosystem productivity periods in high-mountain streams.

**Chapter 4:** Within the framework of Chapter 3, gross primary production (GPP) estimations for the different energetic regimes identified are provided. For each of the three streams, daily GPP was modelled based on the open channel diel oxygen method. I used changes in streamwater dissolved oxygen concentration, temperature, light at the streambed, depth and discharge times series to estimate daily GPP. Later, the response of GPP to light availability and streambed disturbance is assessed.

In the following, I introduce the study sites and the Alpine sensor network from which I obtained the data used in this thesis.

## 1.9    Swiss Alpine sensor network

The fieldwork undertaken for this thesis was done in the Swiss Alps, within the framework of the Swiss Science Foundation project 'Metabolic regimes in Alpine stream networks (SNF, 200021_163015). The execution of the project included a creation of a sensor network to monitor at high temporal resolution streamwater physicochemical parameters. For this, twelve streams within the canton of Valais and Vaud were selected (Figure 1.1). Among the twelve streams, six are not fed by glacier and six are glacier-fed streams. With this selection, we covered non-glacierized and glacierized catchments where the latter had glacier coverage ranging from 2% to 28%. Spring run-off is dominated by snowmelt in non-glacierized catchments and the combination of both snow and ice melt in glacierized catchments, peaking in spring and summer respectively. Additional information of the study stream sites will be given in detail in each chapter.

During May and June 2016, we equipped each stream with sensors measuring streamwater dissolved oxygen (DO, mg $O_2$/L), water temperature (ºC), conductivity (µS/cm), turbidity (NTU), chromophoric dissolved organic carbon (CDOM/FDOM) and water depth (mm). We also installed photosynthetically active radiation (PAR) sensors to measure the light that reaches both the stream surface and the streambed. Atmospheric sensors to measure barometric pressure were also included.

High-frequency streamwater monitoring it has been complemented by regular field surveys on geomorphology (i.e., stream reach width), hydrology (i.e., discharge) and biogeochemistry (i.e., nutrients, dissolved organic carbon concentration, total suspended solids and benthic biomass). Visits of the site included sensor maintenance and data downloading and in situ parameter readings with external probes. Those visits were reduced in some streams in winter when the danger of avalanches and heavy snow pack did not allow access. Sensor calibration procedure and the analytical methods for grab samples analysis will be described in details in the corresponding chapters.

All the data used and shown in this thesis comes from the sensor network and the field surveys including the drone imaginery (see Section 1.10 below). Additional data used for the characterization of the study streams drainage area are 2 x 2 m Swiss digital elevation models ALTI3D from Geodata Swisstopo and Corine Land Cover Inventory from Copernicus Land Monitoring Service (European Environment Agency). We also obtained daily precipitation

data for the study period from the Automatic Monitoring Network of MeteoSwiss (SwissMetNet, Federal Office of Meteorology and Climatology MeteoSwiss) closest to the four areas of study (maximum 8 km).

The time period studied range from October 2016 to October 2017 (Chapter 2), from October 2016 to October 2018 (Chapter 3) and from February 2017 to October 2018 (Chapter 4).
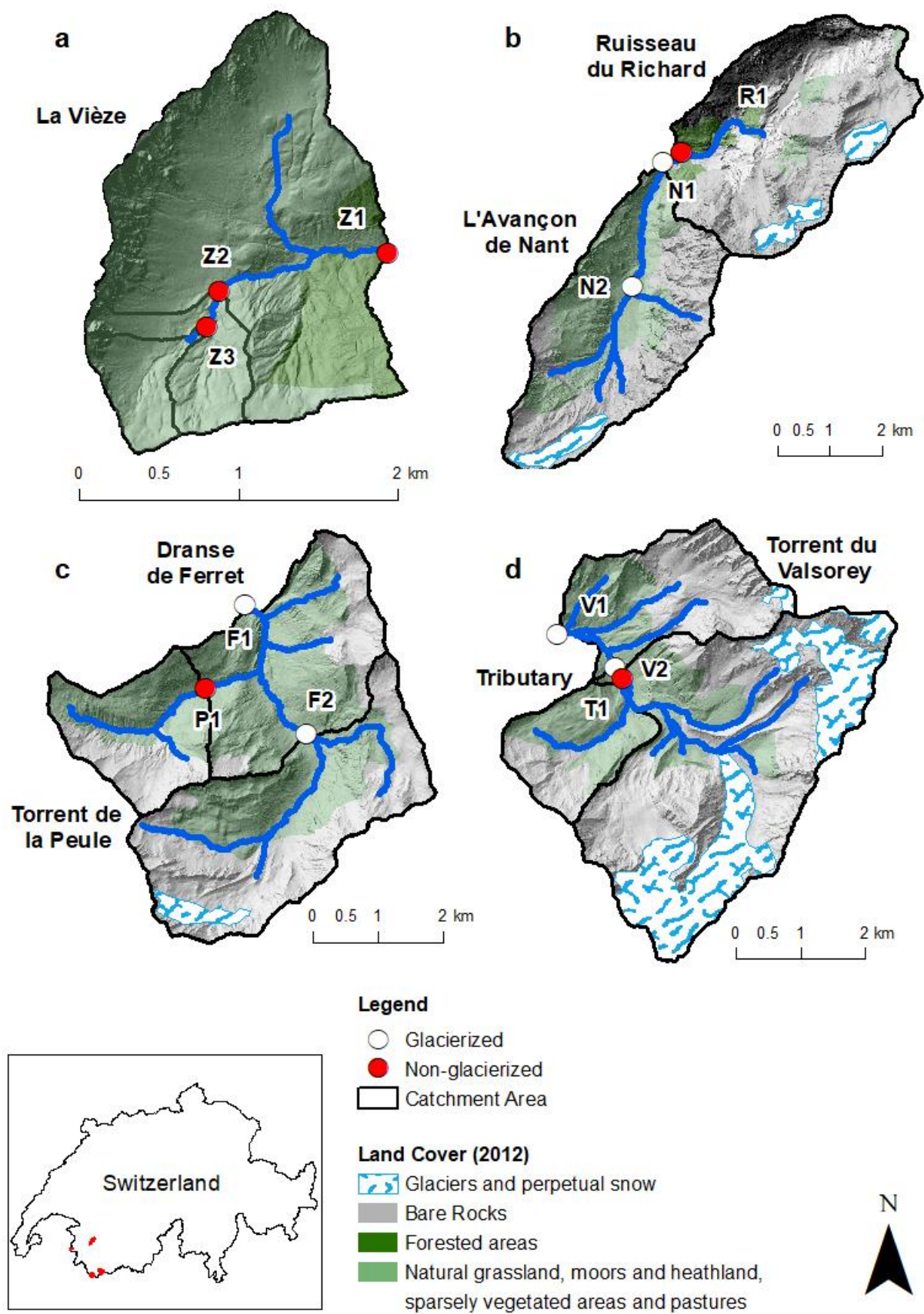
Figure 1.1 Map with the sensor network installed in the Swiss Alps.

Z1

Z2

Z3

R1

N1

N2

F1

F2

P1

V1

V2

T1

Figure 1.2 Picture of study streams and sensor stations.

# 1.10    Stream geomorphological characterization

A reach immediately upstream from each sensor station was surveyed for the sedimentological and bathymetric characterization using high-resolution orthoimaginery and digital elevation models (DEMs). Recent developement in photogrammetry using Structure from Motion (SfM) algorithms were applied for quantifying both dry and wet fluvial topography. Aerial images of the reaches were be collected with a small, unmanned aerial system (UAS) during baseflow periods. All the reaches presented Ground Control Points (GCP) whose position was determined using Differential GPS. An example of orthoimages and DEMs extracted from the drone surveys are shown in Figure 1.3. A complete description of the image processing and the computation of streambed stability time series is given in the Methods section of Chapter 3.
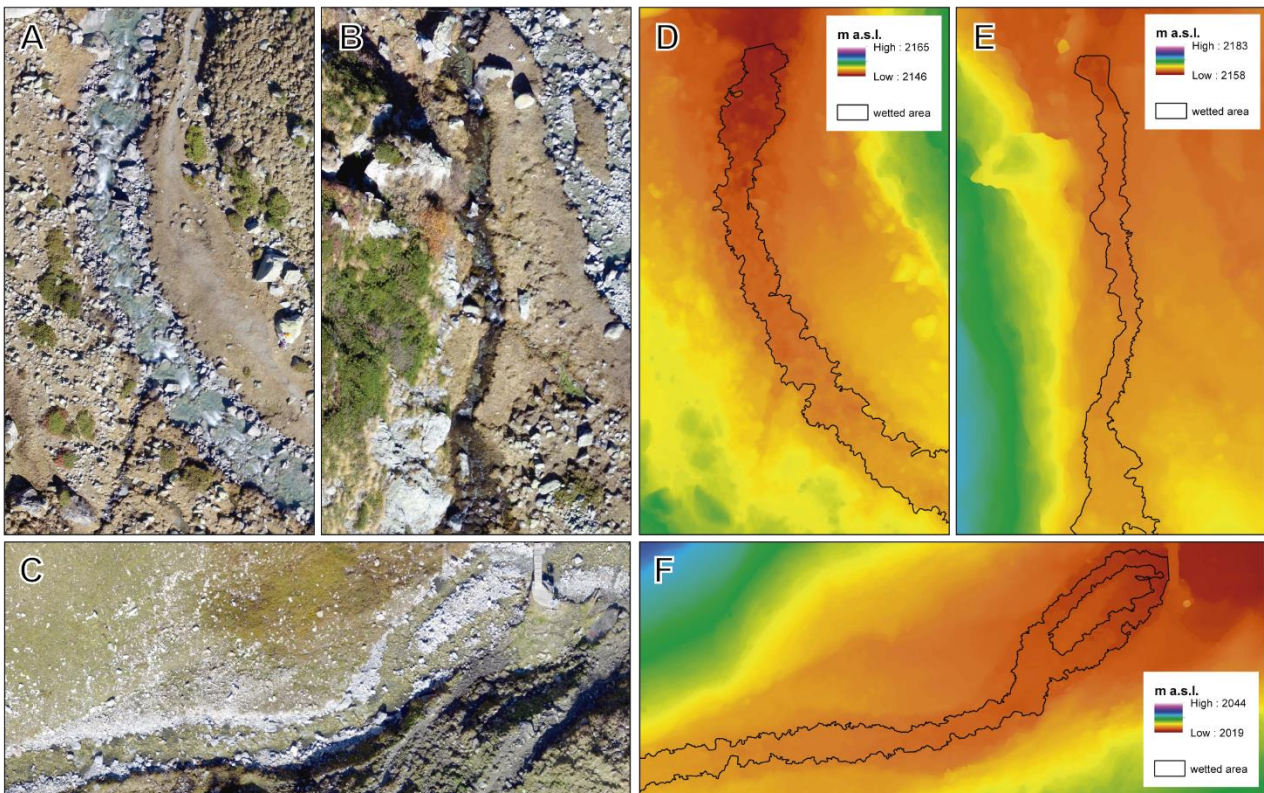


Figure 1.3 Ortophotos and digital elevation models (DEMs) collected in October 2017 from site V2 (image A and D), T1 (image B and E) and P1 (image C and F).

# 1.11    References

Acuña, V., A. Giorgi, I. Muñoz, U. Uehlinger, and S. Sabater. 2004. Flow extremes and benthic organic matter shape the metabolism of a headwater Mediterranean stream. Freshw. Biol. 49: 960–971. doi:10.1111/j.1365-2427.2004.01239.x

Acuña, V., A. Wolf, U. Uehlinger, and K. Tockner. 2008. Temperature dependence of stream benthic respiration in an Alpine river network under global warming. Freshw. Biol. 53: 2076–2088. doi:10.1111/j.1365-2427.2008.02028.x

Ågren, A., M. Haei, S. J. Köhler, K. Bishop, and H. Laudon. 2010. Regulation of stream water dissolved organic carbon (DOC) concentrations during snowmelt; the role of discharge, winter climate and memory effects. Biogeosciences 7: 2901–2913. doi:10.5194/bg-7-2901-2010

Allen, A. P., J. F. Gillooly, and J. H. Brown. 2005. Linking the global carbon cycle to individual metabolism. Funct. Ecol. 19: 202–213. doi:10.1111/j.1365-2435.2005.00952.x

Appling, A. P., R. O. Hall, C. B. Yackulic, and M. Arroita. 2018a. Overcoming Equifinality: Leveraging Long Time Series for Stream Metabolism Estimation. J. Geophys. Res. Biogeosciences 123: 624–645. doi:10.1002/2017JG004140

Appling, A. P., J. S. Read, L. A. Winslow, and others. 2018b. The metabolic regimes of 356 rivers in the United States. Sci. Data 5: 180292. doi:10.1038/sdata.2018.292

Arroita, M., A. Elosegi, and R. O. Hall. 2018. Twenty years of daily metabolism show riverine recovery following sewage abatement. Limnol. Oceanogr. 1–16. doi:10.1002/lno.11053

Barnett, T. P., J. C. Adam, and D. P. Lettenmaier. 2005. Potential impacts of a warming climate on water availability in snow-dominated regions. Nature 438: 303–309. doi:10.1038/nature04141

Battin, T. J., K. Besemer, M. M. Bengtsson, A. M. Romani, and A. I. Packmann. 2016. The ecology and biogeochemistry of stream biofilms. Nat. Rev. Microbiol. 14: 251–263. doi:10.1038/nrmicro.2016.15

Battin, T. J., S. Luyssaert, L. a. Kaplan, A. K. Aufdenkampe, A. Richter, and L. J. Tranvik. 2009. The boundless carbon cycle. Nat. Geosci. 2: 598–600. doi:10.1038/ngeo618

Battin, T. J., A. Wille, R. Psenner, and A. Richter. 2004. Large-scale environmental controls on microbial biofilms in high-alpine streams. Biogeosciences 1: 159–171. doi:10.5194/bg-1-159-2004

Beniston, M. 2005. Mountain Climates and Climatic Change: An Overview of Processes Focusing on the European Alps. Pure Appl. Geophys. 162: 1587–1606. doi:10.1007/s00024-005-2684-9

Beniston, M., D. Farinotti, M. Stoffel, and others. 2018. The European mountain cryosphere: a review of its current state, trends, and future challenges. Cryosph. 12: 759–794. doi:10.5194/tc-12-759-2018

Berggren, M., and P. A. del Giorgio. 2015. Distinct patterns of microbial metabolism associated to riverine dissolved organic carbon of different source and quality. J. Geophys. Res. Biogeosciences 120: 989–999. doi:10.1002/2015JG002963

Berggren, M., H. Laudon, and M. Jansson. 2009. Hydrological control of organic carbon support for bacterial growth in boreal headwater streams. Microb. Ecol. 57: 170–178. doi:10.1007/s00248-008-9423-6

Berghuijs, W. R., R. A. Woods, and M. Hrachowitz. 2014. A precipitation shift from snow towards rain leads to a decrease in streamflow. Nat. Clim. Chang. 4: 583–586. doi:10.1038/NCLIMATE2246

Beria, H., J. R. Larsen, N. C. Ceperley, A. Michelon, T. Vennemann, and B. Schaefli. 2018. Understanding snow hydrological processes through the lens of stable water isotopes. Wiley Interdiscip. Rev. Water 5: e1311. doi:10.1002/wat2.1311

Bernhardt, E. S., J. B. Heffernan, N. B. Grimm, and others. 2018. The metabolic regimes of flowing waters. Limnol. Oceanogr. 63: S99–S118. doi:10.1002/lno.10726

Bernot, M. J., D. J. Sobota R. O. Hall, and others. 2010. Inter-regional comparison of land-use effects on stream metabolism. Freshw. Biol. 55: 1874–1890. doi:10.1111/j.1365-2427.2010.02422.x

Bianchi, T. S., P. Natl, and A. Sci. 2012. Correction for Bianchi, The role of terrestrially derived organic carbon in the coastal ocean: A changing paradigm and the priming effect. Proc. Natl. Acad. Sci. 109: 5134–5134. doi:10.1073/pnas.1202757109

Biggs B. J. F., M. J. Duncan, A. M. Suren, and J.R. Holomuzki. 2001. The importance of bed sediment stability to benthic eco-systems of streams. GRAVEL-BED RIVERS V edited by M. Paul Mosley, New Zealand Hydrological Society Inc., Wellington. Page 423 – 449. ISBN 0 473 07486 9

Biggs, B. J. F., R. A. Smith, and M. J. Duncan. 1999. Velocity and Sediment Disturbance of Periphyton in Headwater Streams: Biomass and Metabolism. J. North Am. Benthol. Soc. 18: 222–241. doi:10.2307/1468462

Biggs B.J.F., and H.A. Thomsen. 1995. Disturbance of stream periphyton by perturbations in shear stress: time to structural failure and differences in community resistance. Journal of Phycology 31, 233–241.

Bond, N. R., and B. J. Downes. 2003. The independent and interactive effects of fine sediment and flow on benthic invertebrate communities characteristic of small upland streams. Freshw. Biol. 48: 455–465. doi:10.1046/j.1365-2427.2003.01016.x

Boyer, E. W., G. M. Hornberger, K. E. Bencala, and D. M. McKnight. 1997. Response characteristics of DOC flushing in an alpine catchment. Hydrol. Process. 11: 1635–1647. doi:10.1002/(SICI)1099-1085(19971015)11:12<1635::AID-HYP494>3.0.CO;2-H

Brighenti, S., M. Tolotti, M. C. Bruno, G. Wharton, M. T. Pusch, and W. Bertoldi. 2019. Ecosystem shifts in Alpine streams under glacier retreat and rock glacier thaw: A review. Sci. Total Environ. 675: 542–559. doi:10.1016/j.scitotenv.2019.04.221

Brooks, P. D., D. M. Mcknight, and K. E. Bencala. 1999. The relationship between soil heterotrophic activity , soil dissolved organic carbon ( DOC ) leachate , and catchment-scale DOC export in headwater catchments. Water Resour. Res. 35: 1895–1902. doi:10.102

Brown, L. E., D. M. Hannah, and A. M. Milner. 2003. Alpine Stream Habitat Classification: An Alternative Approach Incorporating the Role of Dynamic Water Source Contributions. Arctic, Antarct. Alp. Res. 35: 313–322. doi:10.1657/1523-0430(2003)035[0313:ASHCAA]2.0.CO;2

Brown, L. E., A. M. Milner, and D. M. Hannah. 2007. Groundwater influence on alpine stream ecosystems. Freshw. Biol. 52: 878–890. doi:10.1111/j.1365-2427.2007.01739.x

Camarero, L., and J. Catalan. 2012. Atmospheric phosphorus deposition may cause lakes to revert from phosphorus limitation back to nitrogen limitation. Nat. Commun. 3: 1118. doi:10.1038/ncomms2125

Cauvy-Fraunié, S., P. Andino, R. Espinosa, R. Calvez, D. Jacobsen, and O. Dangles. 2016. Ecological responses to experimental glacier-runoff reduction in alpine rivers. Nat. Commun. 7: 1–7. doi:10.1038/ncomms12025

Cayan, D. R., M. D. Dettinger, S. A. Kammerdiener, J. M. Caprio, and D. H. Peterson. 2001. Changes in the Onset of Spring in the Western United States. Bull. Am. Meteorol. Soc. 82: 399–415. doi:10.1175/1520-0477(2001)082<0399:CITOOS>2.3.CO;2

CH2018 (2018), CH2018 – Climate Scenarios for Switzerland, Technical Report, National Centre for Climate Services, Zurich, 271 pp. ISBN: 978-3-9525031-4-0

Choi, G., D. A. Robinson, and S. Kang. 2010. Changing Northern Hemisphere Snow Seasons. J. Clim. 23: 5305–5310. doi:10.1175/2010JCLI3644.1

Clifford, N. J., K. S. Richards, R. A. Brown, and S. N. Lane. 1995. Scales of Variation of Suspended Sediment Concentration and Turbidity in a Glacial Meltwater Stream. Geogr. Ann. Ser. A, Phys. Geogr. 77: 45–65. doi:10.2307/521277

Clitherow, L. R., J. L. Carrivick, and L. E. Brown. 2013. Food Web Structure in a Harsh Glacier-Fed River. PLoS One 8. doi:10.1371/journal.pone.0060899

Cole, J. J., Y. T. Prairie, N. F. Caraco, and others. 2007. Plumbing the global carbon cycle: Integrating inland waters into the terrestrial carbon budget. Ecosystems 10: 171–184. doi:10.1007/s10021-006-9013-8

Connolly, R., M. Connolly, W. Soon, D. R. Legates, R. G. Cionco, and V. M. V. Herrera. 2019. Northern Hemisphere Snow-Cover Trends (1967–2018): A Comparison between Climate Models and Observations. Geosciences 9: 135. doi:10.3390/geosciences9030135

Cronin, G., J. H. McCutchan, J. Pitlick, and W. M. Lewis. 2007. Use of Shields stress to reconstruct and forecast changes in river metabolism. Freshw. Biol. 52: 1587–1601. doi:10.1111/j.1365-2427.2007.01790.x

Dawson, J. J. C., C. Soulsby, D. Tetzlaff, M. Hrachowitz, S. M. Dunn, and I. A. Malcolm. 2008. Influence of hydrology and seasonality on DOC exports from three contrasting upland catchments. Biogeochemistry 90: 93–113. doi:10.1007/s10533-008-9234-3

Demars, B. O. L., J. Russell Manson, J. S. Ólafsson, and others. 2011. Temperature and the metabolic balance of streams. Freshw. Biol. 56: 1106–1121. doi:10.1111/j.1365-2427.2010.02554.x

Durand, Y., G. Giraud, M. Laternser, P. Etchevers, L. Mérindol, and B. Lesaffre. 2009. Reanalysis of 47 Years of Climate in the French Alps (1958–2005): Climatology and Trends for Snow Cover. J. Appl. Meteorol. Climatol. 48: 2487–2512. doi:10.1175/2009JAMC1810.1

Enquist, B. J., E. P. Economo, T. E. Huxman, A. P. Allen, D. D. Ignace, and J. F. Gillooly. 2003. Scaling metabolism from organisms to ecosystems. Nature 423: 639–42. doi:10.1038/nature01671

Fell, S. C., J. L. Carrivick, M. G. Kelly, L. Füreder, and L. E. Brown. 2018. Declining glacier cover threatens the biodiversity of alpine river diatom assemblages. Glob. Chang. Biol. 24: 5828–5840. doi:10.1111/gcb.14454

Fellman, J. B., E. Hood, P. A. Raymond, J. Hudson, M. Bozeman, and M. Arimitsu. 2015. Evidence for the assimilation of ancient glacier organic carbon in a proglacial stream food web. Limnol. Oceanogr. 60: 1118–1128. doi:10.1002/lno.10088

Finger, D., G. Heinrich, A. Gobiet, and A. Bauder. 2012. Projections of future water resources and their uncertainty in a glacierized catchment in the Swiss Alps and the subsequent effects on hydropower production during the 21st century. Water Resour. Res. 48: 1–20. doi:10.1029/2011WR010733

Finn, D. S., K. Räsänen, and C. T. Robinson. 2010. Physical and biological changes to a lengthening stream gradient following a decade of rapid glacial recession. Glob. Chang. Biol. 16: 3314–3326. doi:10.1111/j.1365-2486.2009.02160.x

Fleming, S. W., and G. K. Clarke. 2005. Attenuation of High-Frequency Interannual Streamflow Variability by Watershed Glacial Cover. J. Hydraul. Eng. 131: 615–618. doi:10.1061/(ASCE)0733-9429(2005)131:7(615)

Frei, P., S. Kotlarski, M. A. Liniger, and C. Schär. 2017. Snowfall in the Alps: Evaluation and projections based on the EURO-CORDEX regional climate models. Cryosph. Discuss. 1–38. doi:10.5194/tc-2017-7

Freimann, R., H. Bürgmann, S. E. G. Findlay, and C. T. Robinson. 2014. Spatio-Temporal Patterns of Major Bacterial Groups in Alpine Waters J.A. Gilbert [ed.]. PLoS One 9: e113524. doi:10.1371/journal.pone.0113524

Freimann, R., H. Bürgmann, S. E. Findlay, and C. T. Robinson. 2013. Bacterial structures and ecosystem functions in glaciated floodplains: contemporary states and potential future shifts. ISME J. 7: 2361–2373. doi:10.1038/ismej.2013.114

Füreder, L., C. Schütz, M. Wallinger, and R. Burger. 2001. Physico-chemistry and aquatic insects of a glacier-fed and a spring-fed alpine stream. Freshw. Biol. 46: 1673–1690. doi:10.1046/j.1365-2427.2001.00862.x

Gabbud, C., M. Bakker, M. Clémençon, and S. N. Lane. 2020. Hydropower flushing events cause severe loss of macrozoobenthos in Alpine streams. Water Resour. Res. n/a. doi:10.1029/2019WR024758

Gardner, A. S., G. Moholdt, J.G., B. Wouters, and others. 2013. A Reconciled Estimate of Glacier Contributions to Sea Level Rise: 2003 to 2009. Science (80-. ). 340: 852–857.

Gurnell, A., P. Edwards, G. Petts, and J. Ward. 2000. A conceptual model for alpine proglacial river channel evolution under changing climatic conditions. CATENA 38: 223–242. doi:10.1016/S0341-8162(99)00069-7

Hall, R. O. 2016. Metabolism of Streams and Rivers, p. 151–180. In J.B. Jones and E.H. Stanley [eds.], Stream Ecosystems in a Changing Environment. Elsevier.

Hall, R. O., and J. L. Tank. 2005. Correcting whole-stream estimates of metabolism for groundwater input. Limnol. Oceanogr. Methods 3: 222–229. doi:10.4319/lom.2005.3.222

Hall, R. O., J. L. Tank, M. A. Baker, E. J. Rosi-Marshall, and E. R. Hotchkiss. 2016. Metabolism, Gas Exchange, and Carbon Spiraling in Rivers. Ecosystems 19: 73–86. doi:10.1007/s10021-015-9918-1

Hall, R. O., C. B. Yackulic, T. A. Kennedy, M. D. Yard, E. J. Rosi-Marshall, N. Voichick, and K. E. Behn. 2015. Turbidity, light, temperature, and hydropeaking control primary productivity in the Colorado River, Grand Canyon. Limnol. Oceanogr. 60: 512–526. doi:10.1002/lno.10031

Hannah, D. M., B. P. G. Smith, A. M. Gurnell, and G. R. McGregor. 2000. An approach to hydrograph classification. Hydrol. Process. 14: 317–338. doi:10.1002/(SICI)1099-1085(20000215)14:2<317::AID-HYP929>3.0.CO;2-T

Hanson, P. C., S. R. Carpenter, N. Kimura, C. Wu, S. P. Cornelius, and T. K. Kratz. 2008. Evaluation of metabolism models for free-water dissolved oxygen methods in lakes. Limnol. Oceanogr. Methods 6: 454–465. doi:10.4319/lom.2008.6.454

Hieber, M., C. T. Robinson, S. R. Rushforth, and U. Uehlinger. 2001. Algal Communities Associated with Different Alpine Stream Types. Arctic, Antarct. Alp. Res. 33: 447. doi:10.2307/1552555

Hieber, M., C. T. Robinson, U. Uehlinger, and J. V. Ward. 2005. A comparison of benthic macroinvertebrate assemblages among different types of alpine streams. Freshw. Biol. 50: 2087–2100. doi:10.1111/j.1365-2427.2005.01460.x

Hock, R. 2005. Glacier melt: a review of processes and their modelling. Prog. Phys. Geogr. Earth Environ. 29: 362–391. doi:10.1191/0309133305pp453ra

Hodson, A. 2007. Phosphorus in Glacial Meltwaters, p. 81–82. In Glacier Science and Environmental Change. Blackwell Publishing.

Hodson, A., P. Mumford, and D. Lister. 2004. Suspended sediment and phosphorus in proglacial rivers: bioavailability and potential impacts upon the P status of ice-marginal receiving waters. Hydrol. Process. 18: 2409–2422. doi:10.1002/hyp.1471

Holmes, R. M., J. W. McClelland, P. A. Raymond, B. B. Frazer, B. J. Peterson, and M. Stieglitz. 2008. Lability of DOC transported by Alaskan rivers to the Arctic Ocean. Geophys. Res. Lett. 35: n/a--n/a. doi:10.1029/2007GL032837

Holtgrieve, G. W., D. E. Schindler, T. A. Branch, and Z. T. A'mar. 2010. Simultaneous quantification of aquatic ecosystem metabolism and reaeration using a Bayesian statistical model of oxygen dynamics. Limnol. Oceanogr. 55: 1047–1063. doi:10.4319/lo.2010.55.3.1047

Hood, E., T. J. Battin, J. Fellman, S. O'Neel, and R. G. M. Spencer. 2015. Storage and release of organic carbon from glaciers and ice sheets. Nat. Geosci. 8: 1–6. doi:10.1038/ngeo2331

Hood, E., M. N. Gooseff, and S. L. Johnson. 2006. Changes in the character of stream water dissolved organic carbon during flushing in three small watersheds, Oregon. J. Geophys. Res. 111: G01007. doi:10.1029/2005JG000082

Hope, D., M. F. Billett, and M. S. Cresser. 1994. A review of the export of carbon in river water: Fluxes and processes. Environ. Pollut. 84: 301–324. doi:10.1016/0269-7491(94)90142-2

Hornberger, G. M., K. E. Bencala, and D. M. McKnight. 1994. Hydrological controls on dissolved organic carbon during snow-melt in the Snake River near Montezuma, Colorado. Biogeochemistry 25: 147–165. doi:10.1007/BF00024390

Horton, P., B. Schaefli, A. Mezghani, B. Hingray, and A. Musy. 2006. Assessment of climate-change impacts on alpine discharge regimes with climate model uncertainty. Hydrol. Process. 20: 2091–2109. doi:10.1002/hyp.6197

Hotaling, S., D. S. Finn, J. Joseph Giersch, D. W. Weisrock, and D. Jacobsen. 2017. Climate change and alpine stream biology: progress, challenges, and opportunities for the future. Biol. Rev. 92: 2024–2045. doi:10.1111/brv.12319

Huryn, A. D., J. P. Benstead, and S. M. Parker. 2014. Seasonal changes in light availability modify the temperature dependence of ecosystem metabolism in an arctic stream. Ecology 95: 2840–2850. doi:10.1890/13-1963.1

Huss, M. 2011. Present and future contribution of glacier storage change to runoff from macroscale drainage basins in Europe. Water Resour. Res. 47: 1–14. doi:10.1029/2010WR010299

Huss, M. 2012. Extrapolating glacier mass balance to the mountain-range scale: the European Alps 1900–2100. Cryosph. 6: 713–727. doi:10.5194/tc-6-713-2012

Huss, M., B. Bookhagen, C. Huggel, and others. 2017. Toward mountains without permanent snow and ice. Earth's Futur. 5: 418–435. doi:10.1002/2016EF000514

Huss, M., and M. Fischer. 2016. Sensitivity of Very Small Glaciers in the Swiss Alps to Future Climate Change. Front. Earth Sci. 4: 1–17. doi:10.3389/feart.2016.00034

Huss, M., and R. Hock. 2018. Global-scale hydrological response to future glacier mass loss. Nat. Clim. Chang. 8: 135–140. doi:10.1038/s41558-017-0049-x

IPCC, 2014: Climate Change 2014: Synthesis Report. Contribution of Working Groups I, II and III to the Fifth Assessment Report of the Intergovernmental Panel on Climate Change [Core Writing Team, R.K. Pachauri and L.A. Meyer (eds.)]. IPCC, Geneva, Switzerland, 151 pp

IPCC, 2018: Summary for Policymakers. In: Global Warming of 1.5°C. An IPCC Special Report on the impacts of global warming of 1.5°C above pre-industrial levels and related global greenhouse gas emission pathways, in the context of strengthening the global response to the threat of climate change, sustainable development, and efforts to eradicate poverty [Masson-Delmotte, V., P. Zhai, H.-O. Pörtner, D. Roberts, J. Skea, P.R. Shukla, A. Pirani, W. Moufouma-Okia, C. Péan, R. Pidcock, S. Connors, J.B.R. Matthews, Y. Chen, X. Zhou, M.I. Gomis, E. Lonnoy, T. Maycock, M. Tignor, and T. Waterfield (eds.)]. In Press

IPCC, 2019: Summary for Policymakers. In: IPCC Special Report on the Ocean and Cryosphere in a Changing Climate [H.-O. Pörtner, D.C. Roberts, V. Masson-Delmotte, P. Zhai, M. Tignor, E. Poloczanska, K. Mintenbeck, M. Nicolai, A. Okem, J. Petzold, B. Rama, N. Weyer (eds.)]. In press.

Izagirre, O., U. Agirre, M. Bermejo, J. Pozo, and A. Elosegi. 2008. Environmental controls of whole-stream metabolism identified from continuous monitoring of Basque streams. J. North Am. Benthol. Soc. 27: 252–268. doi:10.1899/07-022.1

Izagirre, O., M. Bermejo, J. Pozo, and A. Elosegi. 2007. RIVERMET©: An Excel-based tool to calculate river metabolism from diel oxygen-concentration curves. Environ. Model. Softw. 22: 24–32. doi:10.1016/j.envsoft.2005.10.001

Jacobsen, D., S. Cauvy-Fraunie, P. Andino, R. Espinosa, D. Cueva, and O. Dangles. 2014. Runoff and the longitudinal distribution of macroinvertebrates in a glacier-fed stream: Implications for the effects of global warming. Freshw. Biol. 59: 2038–2050. doi:10.1111/fwb.12405

Jacobsen, D., A. M. Milner, L. E. Brown, and O. Dangles. 2012. Biodiversity under threat in glacier-fed river systems. Nat. Clim. Chang. 2: 361–364. doi:10.1038/nclimate1435

Kaser, G., M. Grosshauser, and B. Marzeion. 2010. Contribution potential of glaciers to water availability in different climate regimes. Proc. Natl. Acad. Sci. 107: 20223–20227. doi:10.1073/pnas.1008162107

Khamis, K., L. E. Brown, D. M. Hannah, and A. M. Milner. 2016. Glacier-groundwater stress gradients control alpine river bio-diversity. Ecohydrology 9: 1263–1275. doi:10.1002/eco.1724

Klein, G., Y. Vitasse, C. Rixen, C. Marty, and M. Rebetez. 2016. Shorter snow cover duration since 1970 in the Swiss Alps due to earlier snowmelt more than to later snow onset. Clim. Change 139: 637–649. doi:10.1007/s10584-016-1806-y

Kuhn, M. 2001. The nutrient cycle through snow and ice, a review. Aquat. Sci. 63: 150–167. doi:10.1007/PL00001348

Lancaster, J., and A. G. Hildrew. 1993. Flow Refugia and the Microdistribution of Lotic Macroinvertebrates. J. North Am. Benthol. Soc. 12: 385–393. doi:10.2307/1467619

Lane, S. N., M. Bakker, C. Gabbud, N. Micheletti, and J.-N. Saugy. 2017. Sediment export, transient landscape response and catchment-scale connectivity following rapid climate warming and Alpine glacier recession. Geomorphology 277: 210–227. doi:10.1016/j.geomorph.2016.02.015

Lane, S. N., and P. W. Nienow. 2019. Decadal-Scale Climate Forcing of Alpine Glacial Hydrological Systems. Water Resour. Res. 55: 2478–2492. doi:10.1029/2018WR024206

Lapierre, J.-F., F. Guillemette, M. Berggren, and P. a del Giorgio. 2013. Increases in terrestrially derived carbon stimulate organic carbon processing and $CO_2$ emissions in boreal aquatic ecosystems. Nat. Commun. 4: 2972. doi:10.1038/ncomms3972

Li, X., Y. Ding, J. Xu, and others. 2018. Importance of Mountain Glaciers as a Source of Dissolved Organic Carbon. J. Geophys. Res. Earth Surf. 123: 2123–2134. doi:10.1029/2017JF004333

Lovett, G. M., J. J. Cole, and M. L. Pace. 2006. Is net ecosystem production equal to ecosystem carbon accumulation? Ecosystems 9: 152–155. doi:10.1007/s10021-005-0036-3

Marty, C., S. Schlögl, M. Bavay, and M. Lehning. 2017a. How much can we save? Impact of different emission scenarios on future snow cover in the Alps. Cryosphere 11: 517–529. doi:10.5194/tc-11-517-2017

Marty, C., A-M. Tilg, and T. Jonas. 2017b. Recent Evidence of Large-Scale Receding Snow Water Equivalents in the European Alps. J. Hydrometeorol. 18: 1021–1031. doi:10.1175/JHM-D-16-0188.1

Marzolf, E. R., P. J. Mulholland, and A. D. Steinman. 1994. Improvements to the Diurnal Upstream–Downstream Dissolved Oxygen Change Technique for Determining Whole-Stream Metabolism in Small Streams. Can. J. Fish. Aquat. Sci. 51: 1591–1599. doi:10.1139/f94-158

Meyer J.L. and Wallace J.B. 1998. Leaf Litter as a Source of Dissolved Organic Carbon in Streams. Ecosystems 1, 240–249.

Milner, A. M., L. E. Brown, and D. M. Hannah. 2009. Hydroecological response of river systems to shrinking glaciers. Hydrol. Process. 23: 62–77. doi:10.1002/hyp.7197

Milner, A. M., K. Khamis, T. J. Battin, and others. 2017. Glacier shrinkage driving global changes in downstream systems. Proc. Natl. Acad. Sci. 201619807. doi:10.1073/pnas.1619807114

Milner, A. M., and G. E. Petts. 1994. Glacial rivers: physical habitat and ecology. Freshw. Biol. 32: 295–307. doi:10.1111/j.1365-2427.1994.tb01127.x

Mote, P. W., S. Li, D. P. Lettenmaier, M. Xiao, and R. Engel. 2018. Dramatic declines in snowpack in the western US. npj Clim. Atmos. Sci. 1: 2. doi:10.1038/s41612-018-0012-1

Mulholland, P. J., C. S. Fellows, J. L. Tank, and others. 2001. Inter-biome comparison of factors controlling stream metabolism. Freshw. Biol. 46: 1503–1517. doi:10.1046/j.1365-2427.2001.00773.x

Niedrist, G. H., M. Cantonati, and L. Füreder. 2018. Environmental harshness mediates the quality of periphyton and chirono-mid body mass in alpine streams. Freshw. Sci. 37: 519–533. doi:10.1086/699480

Odum, H. T. 1956. Primary Production in Flowing Waters. Limnol. Oceanogr. 1: 102–117. doi:10.4319/lo.1956.1.2.0102

Pellerin, B. A., J. F. Saraceno, J. B. Shanley, S. D. Sebestyen, G. R. Aiken, W. M. Wollheim, and B. A. Bergamaschi. 2012. Taking the pulse of snowmelt: In situ sensors reveal seasonal, event and diurnal patterns of nitrate and dissolved organic matter variability in an upland forest stream. Biogeochemistry 108: 183–198. doi:10.1007/s10533-011-9589-8

Peterson C. G. 1996. Response of benthic algal communities to natural physical disturbance. In: Stevenson RJ, Bothwell ML, Lowe RLe editors. Algal Ecology: freshwater benthic ecosystems. San Diego (CA): Academic Press. p. 375–402

Rabatel, A., B. Francou, A. Soruco, and others. 2013. Current state of glaciers in the tropical Andes: a multi-century perspective on glacier evolution and climate change. Cryosph. 7: 81–102. doi:10.5194/tc-7-81-2013

Rasmussen, J. J., A. Baattrup-Pedersen, T. Riis, and N. Friberg. 2011. Stream ecosystem properties and processes along a tem-perature gradient. Aquat. Ecol. 45: 231–242. doi:10.1007/s10452-010-9349-1

Ren, Z., N. Martyniuk, I. A. Oleksy, A. Swain, and S. Hotaling. 2019. Ecological Stoichiometry of the Mountain Cryosphere. Front. Ecol. Evol. 7: 1–16. doi:10.3389/fevo.2019.00360

Resh, V. H., A. V Brown, A. P. Covich, and others. 1988. The Role of Disturbance in Stream Ecology. J. North Am. Benthol. Soc. 7: 433–455. doi:10.2307/1467300

Rhim, R. 1996. Critical loads of nitrogen and their exceedances. Environmental Series No. 275, Swiss Agency for the Environ-ment, Forests and Landscape, Berne

Riley, A. J., and W. K. Dodds. 2013. Whole-stream metabolism: strategies for measuring and modeling diel trends of dissolved oxygen. Freshw. Sci. 32: 56–69. doi:10.1899/12-058.1

Rinke, K., C. T. Robinson, and U. Uehlinger. 2001. A Note on Abiotic Factors that Constrain Periphyton Growth in Alpine Glacier Streams. Int. Rev. Hydrobiol. 86: 361–366. doi:10.1002/1522-2632(200106)86:3<361::AID-IROH361>3.0.CO;2-Z

Roberts, B. J., and P. J. Mulholland. 2007. In-stream biotic control on nutrient biogeochemistry in a forested stream, West Fork of Walker Branch. J. Geophys. Res. Biogeosciences 112: 1–11. doi:10.1029/2007JG000422

Roberts, B. J., P. J. Mulholland, and W. R. Hill. 2007. Multiple Scales of Temporal Variability in Ecosystem Metabolism Rates: Results from 2 Years of Continuous Monitoring in a Forested Headwater Stream. Ecosystems 10: 588–606. doi:10.1007/s10021-007-9059-2

Robinson, C. T., U. Uehlinger, F. Guidon, P. Schenkel, and R. Skvarc. 2002. Limitation and retention of nutrients in alpine streams of Switzerland. SIL Proceedings, 1922-2010 28: 263–272. doi:10.1080/03680770.2001.11902585

Rosa, J., V. Ferreira, C. Canhoto, and M. A. S. Graça. 2013. Combined effects of water temperature and nutrients concentration on periphyton respiration - implications of global change. Int. Rev. Hydrobiol. 98: 14–23. doi:10.1002/iroh.201201510

Rott, E., M. Cantonati, L. Füreder, and P. Pfister. 2006. Benthic Algae in High Altitude Streams of the Alps -- a Neglected Com-ponent of the Aquatic Biota. Hydrobiologia 562: 195–216. doi:10.1007/s10750-005-1811-z

Savoy, P., A. P. Appling, J. B. Heffernan, E. G. Stets, J. S. Read, J. W. Harvey, and E. S. Bernhardt. 2019. Metabolic rhythms in flowing waters: An approach for classifying river productivity regimes. Limnol. Oceanogr. 1–17. doi:10.1002/lno.11154

Sawyer, A. H., L. A. Kaplan, O. Lazareva, and H. A. Michael. 2014. Hydrologic dynamics and geochemical responses within a floodplain aquifer and hyporheic zone during Hurricane Sandy. Water Resour. Res. 50: 4877–4892. doi:10.1002/2013WR015101

Schaner, N., N. Voisin, B. Nijssen, and D. P. Lettenmaier. 2012. The contribution of glacier melt to streamflow. Environ. Res. Lett. 7: 034029. doi:10.1088/1748-9326/7/3/034029

Sebestyen, S. D., E. W. Boyer, J. B. Shanley, C. Kendall, D. H. Doctor, G. R. Aiken, and N. Ohte. 2008. Sources, transformations, and hydrological processes that control stream nitrate and dissolved organic matter concentrations during snowmelt in an upland forest. Water Resour. Res. 44: 1–14. doi:10.1029/2008WR006983

Segura, C., J. H. McCutchan, W. M. Lewis, and J. Pitlick. 2011. The influence of channel bed disturbance on algal biomass in a Colorado mountain stream. Ecohydrology 4: 411–421. doi:10.1002/eco.142

Serquet, G., C. Marty, J. P. Dulex, and M. Rebetez. 2011. Seasonal trends and temperature dependence of the snowfall/pre-cipitation- day ratio in Switzerland. Geophys. Res. Lett. 38: 14–18. doi:10.1029/2011GL046976

Sertić Perić, M., C. Jolidon, U. Uehlinger, and C. T. Robinson. 2015. Long-term ecological patterns of alpine streams: An imprint of glacial legacies. Limnol. Oceanogr. 60: 992–1007. doi:10.1002/lno.10069

Singer, G. A., C. Fasching, L. Wilhelm, J. Niggemann, P. Steier, T. Dittmar, and T. J. Battin. 2012. Biogeochemically diverse organic matter in Alpine glaciers and its downstream fate. Nat. Geosci. 5: 710–714. doi:10.1038/ngeo1581

Slemmons, K. E. H., J. E. Saros, and K. Simon. 2013. The influence of glacial meltwater on alpine aquatic ecosystems: a review. Environ. Sci. Process. Impacts 15: 1794–806. doi:10.1039/c3em00243h

Smith, H. J., A. Schmit, R. Foster, S. Littman, M. M. Kuypers, and C. M. Foreman. 2016. Biofilms on glacial surfaces: hotspots for biological activity. npj Biofilms Microbiomes 2: 16008. doi:10.1038/npjbiofilms.2016.8

Smith, T., and B. Bookhagen. 2018. Changes in seasonal snow water equivalent distribution in High Mountain Asia (1987 to 2009). Sci. Adv. 4: e1701550. doi:10.1126/sciadv.1701550

Staehr, P. A., J. M. Testa, W. M. Kemp, J. J. Cole, K. Sand-Jensen, and S. V. Smith. 2012. The metabolism of aquatic ecosystems: History, applications, and future challenges. Aquat. Sci. 74: 15–29. doi:10.1007/s00027-011-0199-2

Stewart, I. T., D. R. Cayan, and M. D. Dettinger. 2004. Changes in Snowmelt Runoff Timing in Western North America under a `Business as Usual' Climate Change Scenario. Clim. Change 62: 217–232. doi:10.1023/B:CLIM.0000013702.22656.e8

Tank, S. E., J. B. Fellman, E. Hood, and E. S. Kritzberg. 2018. Beyond Respiration: Controls on lateral carbon fluxes across the terrestrial-aquatic interface. Limnol. Oceanogr. Lett. doi:10.1002/lol2.10065

Uehlinger, U. 2000. Resistance and resilience of ecosystem metabolism in a flood-prone river system. Freshw. Biol. 45: 319–332. doi:10.1046/j.1365-2427.2000.00620.x

Uehlinger, U. 2006. Annual cycle and inter-annual variability of gross primary production and ecosystem respiration in a flood-prone river during a 15-year period. Freshw. Biol. 51: 938–950. doi:10.1111/j.1365-2427.2006.01551.x

Uehlinger, U., H. Bührer, and P. Reichert. 1996. Periphyton dynamics in a floodprone prealpine river: evaluation of significant processes by modelling. Freshw. Biol. 36: 249–263. doi:10.1046/j.1365-2427.1996.00082.x

Uehlinger, U., and M. W. Naegeli. 1998. Ecosystem Metabolism, Disturbance, and Stability in a Prealpine Gravel Bed River. J. North Am. Benthol. Soc. 17: 165–178. doi:10.2307/1467960

Uehlinger, U., C. T. Robinson, M. Hieber, and R. Zah. 2010. The physico-chemical habitat template for periphyton in alpine glacial streams under a changing climate. Hydrobiologia 657: 107–121. doi:10.1007/s10750-009-9963-x

Uehlinger, U., R. Zah, and H. Bürgi. 1998. The Val Roseg project: Temporal and spatial patterns of benthic algae in an Alpine stream ecosystem influenced by glacier runoff. IAHS-AISH Publ. 248: 419–424.

Ulseth, A. J., E. Bertuzzo, G. A. Singer, J. Schelker, and T. J. Battin. 2018. Climate-Induced Changes in Spring Snowmelt Impact Ecosystem Metabolism and Carbon Fluxes in an Alpine Stream Network. Ecosystems 21: 373–390. doi:10.1007/s10021-017-0155-7

Val, J., R. Pino, E. Navarro, and D. Chinarro. 2016. Addressing the local aspects of global change impacts on stream metabolism using frequency analysis tools. Sci. Total Environ. 569–570: 798–814. doi:10.1016/j.scitotenv.2016.06.178

Van de Bogert, M. C., S. R. Carpenter, J. J. Cole, and M. L. Pace. 2007. Assessing pelagic and benthic metabolism using free water measurements. Limnol. Oceanogr. Methods 5: 145–155. doi:10.4319/lom.2007.5.145

Vidon, P., L. E. Wagner, and E. Soyeux. 2008. Changes in the character of DOC in streams during storms in two Midwestern watersheds with contrasting land uses. Biogeochemistry 88: 257–270. doi:10.1007/s10533-008-9207-6

Vuille, M., B. Francou, P. Wagnon, I. Juen, G. Kaser, B. G. Mark, and R. S. Bradley. 2008. Climate change and tropical Andean glaciers: Past, present and future. Earth-Science Rev. 89: 79–96. doi:10.1016/j.earscirev.2008.04.002

Walther, G.-R., E. Post, P. Convey, and others. 2002. Ecological responses to recent climate change. Nature 416: 389–395. doi:10.1038/416389a

Ward, J. V. 1994. Ecology of alpine streams. Freshw. Biol. 32: 277–294. doi:10.1111/j.1365-2427.1994.tb01126.x

Ward, N. D., R. G. Keil, P. M. Medeiros, and others. 2013. Degradation of terrestrially derived macromolecules in the Amazon River. Nat. Geosci. 6: 530–533. doi:10.1038/ngeo1817

Wellnitz, T. A., and J. V. Ward. 2000. Herbivory and irradiance shape periphytic architecture in a Swiss alpine stream. Limnol. Oceanogr. 45: 64–75. doi:10.4319/lo.2000.45.1.0064

Wiegner, T. N., L. A. Kaplan, J. D. Newbold, P. H. Ostrom, and P. E. H. O. Strom. 2005. Contribution of dissolved organic C to stream metabolism : a mesocosm study using 13 C-enriched tree-tissue leachate. J. North Am. Benthol. Soc. 24: 48–67. doi:10.1899/0887-3593(2005)024<0048:CODOCT>2.0.CO;2

Wilhelm, L., G. A. Singer, C. Fasching, T. J. Battin, and K. Besemer. 2013. Microbial biodiversity in glacier-fed streams. ISME J. 7: 1651–60. doi:10.1038/ismej.2013.44

Willmott, C. J., C. M. Rowe, and Y. Mintz. 1985. Climatology of the terrestrial seasonal water cycle. J. Climatol. 5: 589–606. doi:10.1002/joc.3370050602

Wohl, E. 2010. Mountain Rivers Revisited, American Geophysical Union.

Woods, R. A. 2009. Analytical model of seasonal climate impacts on snow hydrology: Continuous snowpacks. Adv. Water Resour. 32: 1465–1481. doi:10.1016/j.advwatres.2009.06.011

Yvon-Durocher, G., J. M. Caffrey, A. Cescatti, and others. 2012. Reconciling the temperature dependence of respiration across timescales and ecosystem types. Nature 487: 472–476.

Zah, R., P. Burgherr, S. M. Bernasconi, and U. Uehlinger. 2001. Stable isotope analysis of macroinvertebrates and their food sources in a glacier stream. Freshw. Biol. 46: 871–882. doi:10.1046/j.1365-2427.2001.00720.x

Zarnetske, J. P., M. Bouda, B. W. Abbott, J. Saiers, and P. A. Raymond. 2018. Generality of Hydrologic Transport Limitation of Watershed Organic Carbon Flux Across Ecoregions of the United States. Geophys. Res. Lett. 45: 11,702-11,711. doi:10.1029/2018GL080005

Zemp, M., H. Frey, I. Gärtner-Roer, and others. 2015. Historically unprecedented global glacier decline in the early 21st century. J. Glaciol. 61: 745–762. doi:10.3189/2015JoG15J017

Zemp, M., W. Haeberli, M. Hoelzle, and F. Paul. 2006. Alpine glaciers to disappear within decades? Geophys. Res. Lett. 33: L13504. doi:10.1029/2006GL026319

# Chapter 2   Alpine glacier shrinkage drives shift in dissolved organic carbon export from quasi-chemostasis to transport limitation

## 2.1    Abstract

The export of dissolved organic carbon (DOC) from catchments is considered as an important energy flux through streams and a major connection between terrestrial and aquatic systems. However, the impact that predicted hydrological changes due to glacier retreat and reduction in snow cover changes will have on DOC export from high-mountain streams remains unclear. In this study, we measured daily runoff and DOC yield during one year in Alpine streams draining catchments with different levels of glacier coverage. DOC yield showed a varied response to runoff across the catchments and varied seasonally as a function of the degree of glaciation and vegetation cover. Using space-for-time substitution, our results indicate that the controls on DOC yield from Alpine catchments change from chemostasis to transport-limitation as glaciers shrink.

## 2.2    Introduction

Mountain glaciers are shrinking worldwide owing to global warming. As glaciers shrink, runoff generated from ice melt initially increases until a peak is reached, beyond which it diminishes until the ice mass has disappeared (Huss and Hock 2018). The potential effects of glacier shrinkage on glacier-fed streams have been studied focusing on alterations in hydrological regimes, water availability, geomorphology and biodiversity (Lane et al. 2017; Milner et al. 2017; Bakker et al. 2018; Lane and Nienow 2019). Glacier runoff carries sediments and solutes, including inorganic nutrients and organic carbon, and its change is also anticipated to affect the biogeochemistry of glacier-fed streams (Milner et al. 2017).

Dissolved organic carbon (DOC) is a significant component of the land-to-ocean carbon flux (Regnier et al. 2013) and constitutes a large source of energy to stream ecosystem metabolism (Battin et al. 2009). Within streams, DOC can be metabolized leading to respiratory $CO_2$ release to the atmosphere, transiently stored or exported downstream and ultimately to the ocean. Below the tree line, terrestrial vegetation and soils

constitute a major source of DOC that enters streams via various hydrological flow paths, often during rainfall or snowmelt (e.g., Boyer et al. 1997; Lafrenière and Sharp 2004). In high-mountain catchments above the tree line, alternative sources of DOC may gain importance because of poorly developed soils. For instance, mountain glaciers can release significant amounts of organic carbon to downstream ecosystems (Hood et al. 2015; Li et al. 2018), where it can even partially sustain stream food webs (Fellman et al. 2015).

The transport of DOC across the terrestrial-aquatic interface is thus relevant for stream ecosystem functioning and its export from the catchment is critical for the carbon balance at catchment scale (Tank et al. 2018). Despite this, our ability to predict the impact of climate change on DOC export is relatively limited at present (Zarnetske et al. 2018). DOC export from catchments can be expressed as the load (Mass/Time) or yield (Mass/Area/Time). While both quantities are relevant for stream carbon budgets, the comparison of DOC yields between different streams can identify the effects of catchment properties (e.g., drainage area, land use) upon DOC export. Furthermore, the relationship between DOC yield and discharge indicates if the DOC flux is limited by hydrological transport or by sources of DOC within the catchment, or if it is in chemostasis (Creed et al. 2015; Vaughan et al. 2017; Zarnetske et al. 2018). Elucidating these potential drivers is relevant given the expected climate-induced alterations of the hydrological regime of streams and changing land cover.

Despite the understanding that glacier shrinkage may affect the functioning of glacier-fed streams and even downstream biogeochemistry, the drivers of DOC export from glacierized catchments have been rarely studied (e.g., Hood and Scott 2008; Tockner et al. 2002). Most of our current understanding of DOC export from high-altitude catchments rests on studies of snow-covered catchments and snowmelt, where the latter was reported as a major contributor to annual DOC export (Ågren et al. 2010; Boyer et al. 1997; Hood et al. 2003; Lafrenière and Sharp 2004). Both ice melt and snowmelt shape the hydrological regime of glacier-fed streams, but the relevance of these periods for annual DOC fluxes is poorly understood. This is also because the ice melt itself can be a DOC source to the stream (Hood et al. 2015; Li et al. 2018) .

The aim of this study was to elucidate how runoff, particularly as mediated by snowmelt and glacier ice melt, affects the DOC yield from non-glacierized and glacierized catchments. We used high-frequency (every 10 minutes) measurements of discharge, streamwater temperature, turbidity and FDOM over one year to infer DOC concentrations and yields from twelve streams distributed over four catchments in the Swiss Alps. This allowed us to use a space-for-time substitution approach to show that the drivers of DOC yield may shift from quasi-chemostasis to hydrological transport limitation in alpine catchments as glaciers shrink.

## 2.3    Methods

### 2.3.1   Study sites

We selected six streams that are not fed by glaciers (that is, draining non-glacierized catchments) (La Vièze, Z1, Z2 and Z3; Torrent de la Peule, P1; Tributary of Torrent du Valsorey, T1; Ruisseau du Richard, R1) and six glacier-fed streams under the influence of glacier ice melt dynamics (Avançon de Nant, N1 and N2; Dranse de Ferret, F1 and F2; Torrent du Valsorey, V1 and V2) in the Swiss Alps (Figure SI 2.1; Text S1). With this sampling design, we covered non-glacierized and glacierized catchments where the latter had glacier coverage ranging from 2% to 28%. Across these glacierized catchments, glacier coverage has decreased by 35 to 100% since the little ice age in 1850 (Table 2.1). This selection allowed a space-for-time substitution approach as often done to assess downstream implications of glacier shrinkage (Heckman et al. 2016). The catchments (1778 to 2893 m a.s.l.) are dominated by steep slopes and sparsely vegetated (grassland and shrubs) rocky terrain (Table 2.1; Table SI 2.1).  Coniferous forest is present at the Avançon de Nant and the

Ruisseau du Richard with less than 16% coverage. Mixed forest is present at the downstream site of La Vièze (Z1, 15% coverage). Spring runoff is dominated by snowmelt in non-glacierized catchments and the combination of both snow and ice melt in glacierized catchments, peaking in spring and summer respectively. Land cover was assessed based on CORINE© Land Cover Inventory 2012 of the European Union, Copernicus Land Monitoring Service.

## 2.3.2 Sensor network and in situ measurements

We equipped all twelve streams with sensors measuring streamwater chromophoric DOC (Cyclops-7 CDOM/FDOM, Turner Designs), turbidity (Cyclops-7 Turbidity, Turner Designs), water depth (Odyssey Capacitance Logger, Dataflow Systems Ltd), and temperature. Optical sensors were calibrated in the laboratory before deployment following the manufacturers' specifications. Turbidity sensors were calibrated to nephelometric turbidity units (NTU) using sensor-specific Turbidity 4000 NTU Calibration Standard – Formazin (Sigma-Aldrich®) up to 2000 NTU. Excitation and emission wavelengths of the FDOM fluorometers were centred at 325 (band pass: 120) nm and 470 (band pass: 60) nm, respectively. Such sensors are now being increasingly used to study FDOM, and by conversion DOC concentration, at high temporal resolution in various freshwater ecosystems (e.g., Pellerin et al. 2012, Koenig et al. 2017; Tissier et al. 2013; Tunaley et al. 2016; Wilson et al. 2013) (Text S3). FDOM measurements were converted from signal voltage to parts per billion (ppb) of quinine sulfate equivalents (QSE) (fluorescence of 1 ppb quinine sulfate monohydrate (Sigma-Aldrich®) in 0.05 M $H_2SO_4$) using a two-point calibration curve (0 to 1000 ppb QSE).

Streamwater FDOM, temperature, turbidity and depth were measured at 10 min intervals from 1 October 2016 to the 30 September 2017. We visited all sites at least monthly for sensor maintenance, data downloading and grab sampling for DOC analysis. Streamwater samples were filtered (pre-combusted GF/F filters, Whatman) into acid-washed, pre-combusted glass vials and analysed using a Sievers M5310c TOC Analyzer (GE Analytical Instruments) (accuracy: ± 2 %, precision: < 1 %, detection limit: 22 μg C/L).

Discharge was determined using slug-injections of sodium chloride as a conservative tracer (Gordon et al. 2004) and rating curves between streamwater depth and discharge were established for each site (Text S2). Where streamwater depth data were missing because of sensor malfunctioning, we inferred data from gauging stations within the respective catchments (Text S2). We derived instantaneous daily discharge ($m^3$/s) from the 10-min frequency time series averaged to daily means. We filled data gaps in daily discharge data using linear interpolation and estimated daily runoff (mm/d).

## 2.3.3 Relationships between streamwater FDOM and DOC concentrations

We corrected sensor FDOM values for streamwater temperature ($FDOM_{temp}$) and turbidity ($FDOM_{corr}$) as:

$$FDOM_{temp} = \frac{FDOM_{raw}}{1 - 0.016(Temp_m - Temp_{ref})}$$

Equation 2.1 FDOM temperature correction

$$FDOM_{corr} = \frac{FDOM_{temp}}{0.95e^{(-0.002\,Turb_m)}+0.03}$$

Equation 2.2 FDOM$_{temp}$ turbidity correction

where *FDOM$_{raw}$* is the uncorrected FDOM, *Temp$_m$* is streamwater temperature, *Temp$_{ref}$* is the reference temperature at 10°C and *Turb$_m$* is streamwater turbidity (Watras et al. 2011; Lee et al. 2015). We derived the coefficients from laboratory experiments on the sensor-specific effect of a range of temperatures and turbidity on the FDOM signal. Coefficients were comparable with those previously reported (Watras et al. 2011; Downing et al. 2012; Lee et al. 2015; Saraceno et al. 2017). Time series of streamwater DOC concentrations were computed from least-squared linear regressions between *FDOM$_{corr}$* sensor data and DOC concentrations measured from grab samples (Text S3).

## 2.3.4 Calculations of DOC loads and yields

We modelled the daily load of DOC (kg C/d) in each stream using LOADEST (Runkel et al. 2004), normalized to catchment area to derive daily DOC yield (kg C km$^{-2}$ d$^{-1}$). LOADEST uses time series of daily constituent concentration data and the corresponding measurement of stream discharge to build a calibration regression, which is then applied to a complete data series of daily discharge to obtain daily constituent loads (mass/d) (Runkel et al. 2004). We created twelve site-specific calibration input files with the available pairs of daily DOC concentration and discharge (Text S4). We derived DOC concentration data from the 10-min frequency time series averaged to daily means. Site-specific regressions were validated using an Adjusted Maximum Likelihood Estimator (AMLE). We selected the best fit of the predefined regression models available based on Akaike's Information Criterion (AIC).

We provide the 95% confidence interval on the predicted DOC yield as provided by LOADEST as a measure of the uncertainty associated with the DOC yields. However, LOADEST does not propagate the error related to discharge rating curves and FDOM/DOC relationships. Therefore, we also calculated DOC yield using the 'conservative' approach (i.e., Load = [DOC] * Q) for those days where DOC concentration ([DOC]) and discharge (Q) were available (Text S5). We estimated the uncertainty in DOC yield using a Gaussian error propagation. Calculating these uncertainties makes particular sense for the streams with almost complete time series of both discharge and DOC.

## 2.3.5 Data analysis

We approximated hydrologic periods (i.e., winter baseflow, spring snowmelt, summer ice melt, fall baseflow) typical for alpine streams by partitioning discharge into baseflow and high flows using a recursive digital filter approach and the *EcoHydRology* package in *R* (Fuka et al. 2018). The value of the filter parameter (or the hydrograph recession constant) was set at 0.925 (Nathan and McMahon 1990). This step was followed by manual adjustment of the periods because the onset of the winter baseflow and snowmelt, for instance, vary with altitude.

We quantified the relationships between runoff and DOC yield, rather than DOC concentration, as these are well suited to evaluate the carbon balance at catchment level (Zarnetske et al. 2018). We used a power function to describe the relationship between runoff and DOC yield for each stream throughout the study period of one year, where the slope coefficient (*b*) refers to chemostasis, source or transport limitation of DOC. Chemostasis (*b*=1) occurs when the mass of DOC delivered to the stream can keep up with rising discharge; source limitation (*b*<1) occurs when DOC in the stream is being diluted due to an inability of the catchment to produce more DOC as discharge rises; transport limitation (*b*>1) occurs when new DOC

sources are mobilized as discharge increases (e.g., Creed et al. 2015; Zarnetske et al. 2018). The intercept, *a*, is a DOC concentration normalization coefficient (Zarnetske et al. 2018). We transformed (natural log) the power model and calculated least-squares linear regression models on the data to retain the intercept (*a*) and slope coefficient (*b*). The goodness of fit and the parameter estimation significance were assessed based on the coefficient of determination ($R^2$) and the *P* value. As in other studies (e.g., Vaughan et al. 2017; Zarnetske et al. 2018), our models did not account for potential temporal autocorrelation of the data.

We evaluated the effect of runoff on DOC yield across all streams at a daily basis using a linear mixed-effect model with random-effect terms. The linear mixed-effect model was fitted using the *lme* function (Pinheiro et al. 2018) and included runoff and streamwater temperature as fixed effects and site as random effect (with random intercept and slope). Here we used the temporal correlation structure defined by the residuals (autoregressive process of order 1, or AR(1)). We evaluated the goodness of fit of the model by calculating marginal and conditional $R^2$ using the *r.squaredGLMM* function (Barton 2018). All statistical analyses were conducted in *R* (version 3.5.1, R Development Core Team, 2018) and on DOC yield estimates from LOADEST.

## 2.4 Results and discussion

### 2.4.1 Runoff dynamics

Runoff in high-alpine streams is influenced by altitude and latitude, glacier mass balance and snowpack (Milner et al. 2017), and can vary from seasonal (e.g., snow melt in spring) to daily (e.g., ice melt in summer) scales. Because runoff is a master variable for stream biogeochemistry, we first describe its temporal patterns in our study catchments.

Annual runoff was generally higher in the glacierized (1304±218 mm; median: 1280 mm) than in the non-glacierized catchments (992±581 mm; median: 888 mm) (Table 2.1). Runoff dynamics in all study streams exhibited seasonal patterns with extended baseflow in winter, snowmelt in spring, ice melt in summer (in glacier-fed streams) and baseflow in autumn (Figure 2.1; Table SI 2.3). Average baseflow runoff in winter (glacierized: 61±23 mm, median: 60 mm; non-glacierized: 36±32 mm, median: 30 mm) and autumn (glacierized: 157±61 mm, median: 136 mm; non-glacierized: 180±142 mm, median: 147 mm) contributed on average 5% (winter) and 12% (autumn) and 3% (winter) and 16% (autumn) for glacierized and non-glacierized streams respectively.

Peak runoff started with snowmelt in spring (glacierized: 748±118 mm, median: 733 mm; non-glacierized: 539±249 mm; median: 512 mm) and contributed on average 58±2 % and 58±10 % to the annual runoff from glacierized and non-glacierized catchments, respectively. The continuation of peak runoff into summer was particularly pronounced in glacierized catchments where summer runoff (338±83 mm; median: 320 mm) contributed on average 26±5 % to the annual runoff compared to 22±8 % in non-glacierized (237±199 mm; median: 209 mm) catchments. Summer runoff increased significantly ($R^2$=0.74, *P*<0.05) with glacier coverage across the six glacier-fed streams. These differences are likely due to the combined effects of the larger snowpack in glacierized catchments owing to their higher elevations and glacier runoff itself. In fact, it is well established that annual runoff in glacierized catchments can increase due to elevated rates of glacier volume loss (Hood and Scott 2008; Milner et al. 2017).

### 2.4.2 Streamwater DOC concentration

Streamwater DOC concentrations were consistently low in all streams (Table 2.1). They were closely bracketed by those reported from similar systems (Barker et al. 2013; Li et al. 2018) but lower than those

in headwater streams draining forested catchments (Mulholland 1997; Creed et al. 2015). Average annual DOC concentrations were significantly higher (Mann-Whitney U-test; $P$<0.01) in streams draining non-glacierized (344.5 ± 106.8 µg C/L) than glacierized (144.8 ± 26.4 µg C/L) catchments. Annual average DOC concentration in glacier-fed streams was not related to glacier coverage ($R^2$=0.05, $P$>0.05) but to vegetation coverage ($R^2$=0.59, $P$<0.01).

| Site Code | Altitude Site (m a.s.l.) | Catchment Area (km²) | % Glacier coverage loss 2012/1850 | % Vegetated | %Glaciers and perpetual snow | % Bare Rocks | Mean daily runoff (mm/d) | Annual runoff (mm/y) | Mean DOC (µg C/L) | Mean daily DOC yield (kg C km⁻² d⁻¹) | Annual DOC yield LOADEST (kg C km⁻² y⁻¹) (2.5%, 97.5% CI) | Conservative DOC yield estimation (kg C/km²) (± SD, days) |
|---|---|---|---|---|---|---|---|---|---|---|---|---|
| | | | | | Glacierized sites | | | | | | | |
| V1 | 1937 | 23.2 | 38 | 28 (13) | 22 | 50 | 3.8 ± 4.4 | 1406 | 182.5 ± 65.7 | 0.7 ± 0.73 | 256 (245, 267) | 199 ± 38 (314) |
| V2 | 2148 | 18.1 | 35 | 25 (8) | 27 | 48 | 3.8 ± 4.1 | 1380 | 152.7 ± 57.2 | 0.6 ± 0.65 | 218 (207, 229) | 223 ± 38 (365) |
| F1 | 1774 | 20.2 | 73 | 57 (5) | 2 | 41 | 2.9 ± 3.4 | 1092 | 159.9 ± 55 | 0.43 ± 0.46 | 158 (152, 165) | 156 ± 20 (362) |
| F2 | 1995 | 9.3 | 73 | 40 (0) | 4 | 56 | 3.1 ± 3 | 1110 | 111.4 ± 16.7 | 0.35 ± 0.39 | 129 (126, 132) | 61 ± 6 (252) |
| N1 | 1201 | 13.4 | 42 | 50 (19) | 5 | 45 | 3.2 ± 2.8 | 1180 | 142.9 ± 34.7 | 0.46 ± 0.46 | 168 (153, 184) | 48 ± 3 (170) |
| N2 | 1465 | 9.0 | 42 | 43 (9) | 7 | 50 | 4.5 ± 3.8 | 1655 | 119.3 ± 32.9 | 0.56 ± 0.58 | 204 (196, 213) | 179 ± 43 (290) |
| | | | | | Non-glacierized sites | | | | | | | |
| T1 | 2161 | 3.1 | 100 | 65 (32) | 0 | 35 | 1.2 ± 1.7 | 427 | 262.6 ± 161.4 | 0.46 ± 0.81 | 179 (166, 192) | 146 ± 40 (306) |
| Z1 | 1415 | 3.6 | NA | 100 (32) | 0 | 0 | 3.9 ± 3.3 | 1413 | 411.9 ± 116.2 | 1.66 ± 1.53 | 605 (555, 660) | 197 ± 16 (116) |
| Z2 | 1630 | 0.7 | NA | 100 (45) | 0 | 0 | 5.2 ± 3.9 | 1899 | 447.5 ± 173.8 | 2.57 ± 2.23 | 937 (875, 998) | 509 ± 55 (197) |
| Z3 | 1689 | 0.3 | NA | 100 (24) | 0 | 0 | 1.9 ± 3.2 | 744 | 359.2 ± 148.7 | 0.84 ± 1.54 | 308 (288, 329) | 233 ± 20 (236) |
| P1 | 2027 | 4.0 | NA | 61 (2) | 0 | 39 | 2.8 ± 3.2 | 1032 | 171.1 ± 106.6 | 0.54 ± 0.7 | 198 (177, 220) | 108 ± 23 (258) |
| R1 | 1200 | 14.3 | 53 | 51 (8) | 6 | 43 | 1.2 ± 1.6 | 438 | 414.5 ± 124.3 | 0.5 ± 0.66 | 184 (169, 199) | 49 ± 22 (168) |

Table 2.1 Summary of catchment and streamflow characteristics, DOC concentration and DOC yield estimates. Bare rocks, glaciers and perpetual snow and vegetated cover percentage are based on CORINE Land Cover Inventory 2012. Percent vegetation cover in brackets refers to mixed and coniferous forest, moors and heathlands. Remaining vegetation types include pastures, sparsely vegetated areas and natural grassland. Glacier coverage in 1850 is from Maisch et al. (2000). Shown are means ± standard deviation. Conservative estimates of DOC yields include in brackets the number of days for which the yield was determined
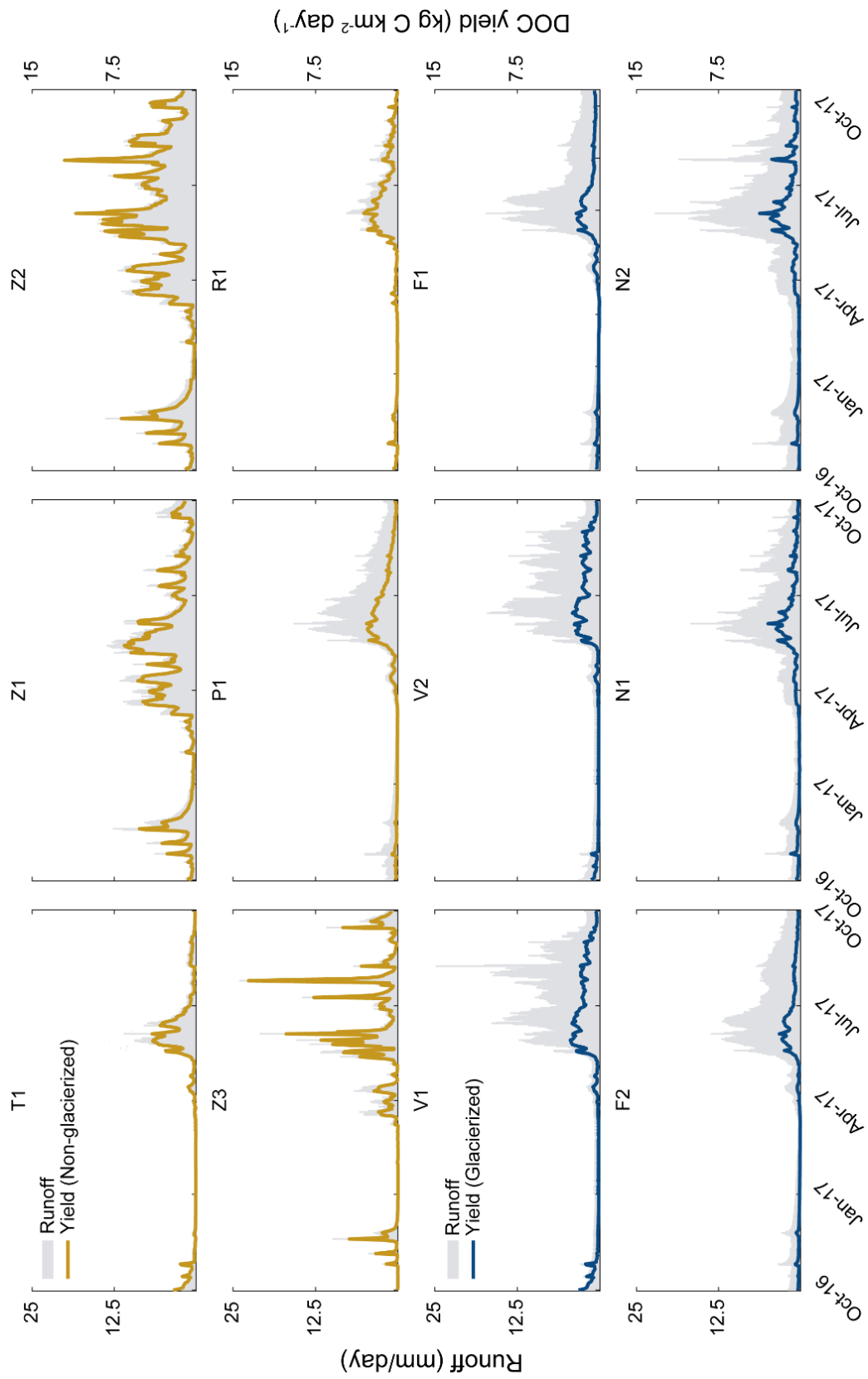
Figure 2.1 Time series of daily runoff and daily yield during the year of study.

## 2.4.3 Temporal and spatial patterns of DOC yields

First, we explored the partitioning of the annual DOC yield over the hydrological periods. The average contribution of the DOC yield during snowmelt to the total annual yield was 62±3 % and 62±13 % for streams in glacierized and non-glacierized catchments, respectively (Table SI 2.3). This shows that more than half of the total annual DOC export occurred during spring in these high-alpine catchments. Spring contributions to DOC yield tended to be higher (61.7±9.1 %) than the equivalent contribution to runoff (57.8±7 %), which would imply that reservoirs of organic carbon are being mobilized during snowmelt across all sites. This is in line with the DOC flushing from near-surface soil horizons observed in an alpine catchment in Colorado (Boyer et al. 1997). Snowmelt was also reported to be critical for the DOC export from high-latitude catchments suggesting that carbon production during the cold season is important for regulating arctic DOC transport (Finlay et al. 2006). We evoke a similar relevance of DOC production during winter for high-alpine streams, most likely originating from the sparse vegetation from the antecedent summer degrading underneath the snowpack as reported from high-elevation catchments in the Rocky Mountains (Brooks et al. 1999). Furthermore, direct leaching of DOC from terrestrial plant material contained within the snowpack (Lafrenière and Sharp 2004) or atmospheric deposition (Mladenov et al. 2012) may also contribute to the streamwater DOC..

DOC yield during summer contributed on average 21±3 % and 22±11 % to the annual DOC yield from glacierized and non-glacierized catchments, respectively. In the glacier-fed streams, DOC yield increased with the degree of glacier coverage ($R^2$=0.92, $P$<0.01) during summer, which is likely attributable to elevated glacier runoff. DOC yield during autumn and winter contributed on average 8±5 % and 9±8 % to the annual DOC yield from glacierized and non-glacierized catchments. We suggest that this is attributable to the DOC poor groundwater predominantly feeding high-alpine streams during these periods (e.g., Milner et al. 2017).

## 2.4.4 Drivers of DOC yields

For most of our study streams, the power function describing the relationship between runoff and DOC yield resulted in a slope coefficient (*b*) higher than 1. Interestingly, *b* values in non-glacierized streams (0.99±0.05 to 1.51±0.03) were significantly (t-test: $P$<0.05) greater than 1, whereas *b* values in glacier-fed streams (0.92±0.02 to 1.13±0.03) were not significantly (t-test: $P$>0.05) greater than 1 (Figure 2.2; Figure SI 2.4). These results indicate that DOC yield in non-glacierized catchments was largely controlled by transport limitation. Peak runoff in these streams occurred during snowmelt and sometimes in summer during storm events (i.e., in Z2 and Z3) (Figure 2.1). Overall values of *b* in non-glacierized catchments show that the hydrological mobilization of DOC and its supply to the stream was guaranteed and likely enhanced by the activation of terrestrial DOC reservoirs as runoff increases during these events. On the other hand, *b* values closer to 1 for glacier-fed streams suggest chemostasis where DOC production and mobilization are nearly proportional to changes in runoff (Godsey et al. 2009). Additionally, ice melt from glaciers in summer contributes directly to stream runoff, and concomitantly and proportionally to the DOC yield in glacier-fed streams. In fact, upon melting, ice-locked DOC can contribute to the downstream DOC pool (Hood et al. 2015; Li et al. 2018; Singer et al. 2012). We argue that ice melt as a common source of water and DOC underlies the quasi-chemostasis of the DOC yield in glacier-fed streams.

The slope coefficient, *b,* was positively related to vegetation coverage, including mixed or coniferous forest, moors and heathlands, typically indicative of later successional stages following glacier recession in alpine catchments (Figure 2.2). In addition, the intercept, *a*, was positively related to vegetation coverage including all types (e.g., grass land) of vegetation ($R^2$=0.42; $P$<0.05), further supporting the notion of DOC source availability but transport limitation. We found the highest *b* (1.51±0.03) associated with the spring-

fed stream T1  where sources of DOC may be contained within fringing wetlands. This is in agreement with the observation that wetland coverage increases the likelihood of transport limitation in a wide range of catchments (Zarneskte et al. 2018).
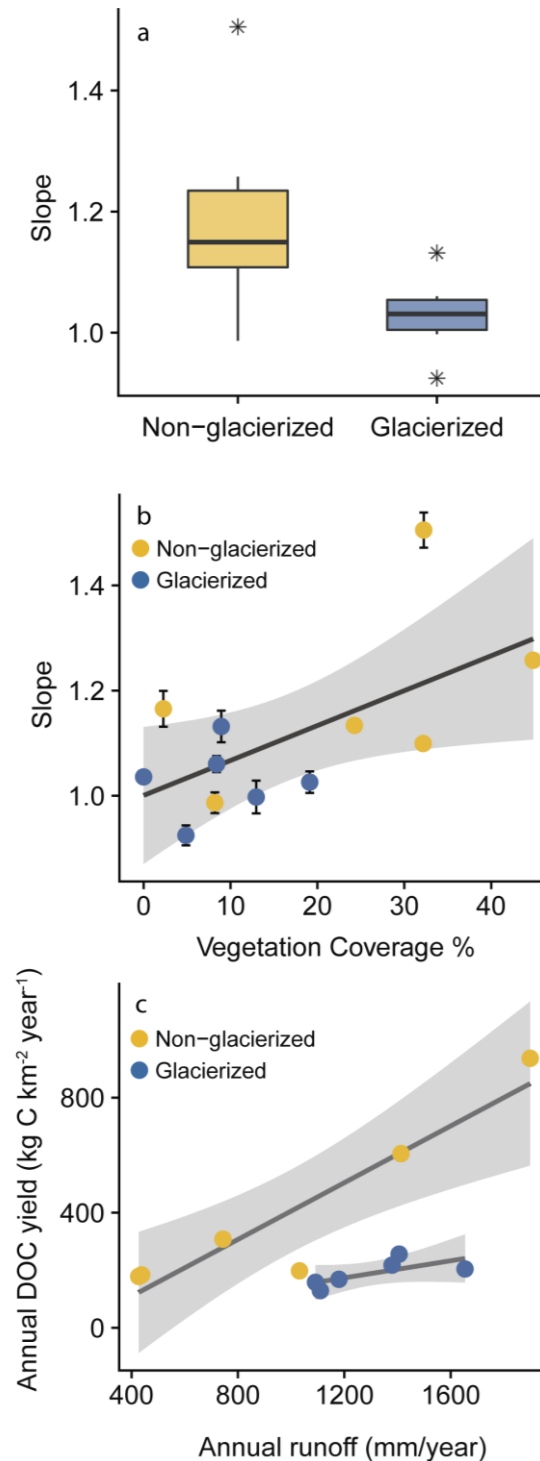


Figure 2.2 (a) Box and whisker plot of twelve slope coefficients grouped by glacier presence (line within the box is the median, the box defines 25th and 75th percentiles, and the whiskers extend to the largest and lowest value no further than 1.5 times the box length) and (b) relationship of slope coefficients b against vegetation cover including mixed or coniferous forest, moors and heathlands. Line is least-square linear regression: y = 0.007x + 1; $R^2$ = 0.37; *P*<0.05. (c) Annual DOC yield increased with annual runoff across sites, where the relationship for yield versus runoff for glacierized sites (least-square linear regression: y = 0.148x - 4.64; $R^2$=0.49; P>0.05) differs from that of non-glacierized sites (least-square linear regression: y = 0.492x − 86.89; $R^2$=0.86; *P*<0.01).

Vegetation coverage was highest in the catchments that experienced highest glacier loss by area since 1850 ($R^2$=0.57; $P$<0.05 ; Figure SI 2.5) and we assume, therefore, that the build-up of soils as a source of DOC to the streams was higher in these catchments. It is reasonable to assume that glacierized catchments are out of equilibrium in terms of the relationships between climate and soil development as they have undergone ice retreat over the last 120 years at least. Because soil development on deglaciated terrain is a complex function of temperature, and hence altitude, moisture limitation and weathering (Miller and Lane 2019), for instance, we argue that our observed patterns of DOC yield between glacierized and non-glacierized catchments may not be exclusively linked to the degree of glacier coverage. Rather they could be linked to the extent to which the surface regolith has weathered to allow soil and associated organic matter stocks to develop as glaciers recede.

The streams (Z1, Z2 and Z3) draining the Champéry catchment had highest annual DOC yields and, along with T1, the highest slope coefficient *b* as well. The Champéry catchment has not been glacierized since the little ice age at least and could be considered as an end-member towards which the presently glacierized catchments may evolve in terms of DOC yield.

This assumes that the increase in streamwater DOC concentration with the encroachment of vegetation has a stronger positive effect on DOC yields than the decrease in runoff associated with glacier shrinkage. We acknowledge that the local climate, changing with altitude and exposure, may interfere with this relationship as indicated by the DOC yield in P1, also glacier-free since the little ice age at least. In fact, the difference between the P1 and the streams in the Champéry catchment may be attributable to the differences in altitude between these systems and its impact on climate and hence on the development of vegetation and soils.

In overall agreement with the power function analyses, the mixed effect model, including a temporal autocorrelation structure, revealed higher slopes for DOC yield and runoff relationships for streams draining non-glacierized than glacierized catchments (Table SI 2.4 and Table SI 2.5). We recognize that the results from the power function analyses and the linear mixed effect model are not directly comparable. Nevertheless, we interpret the similar results from both analyses as evidence of different drivers of DOC yield in glacierized and non-glacierized catchments.

## 2.4.5  Contextualizing annual DOC yields from high-alpine catchments

LOADEST and our 'conservative' approach yielded reasonably close estimates of annual DOC yields, at least for the sites with rather complete time series (Table 2.1). Uncertainty associated with the second approach was relatively high for some streams, which we attribute to the error related to discharge measurements. This is not unexpected though as it is inherently difficult to get proper measurements of high discharge in steep mountain channels with high roughness. Nevertheless, our estimates are closely bracketed by those from similar systems or lower than those from more productive systems (Figure SI 2.6).

The annual DOC yield averaged 189±46 kg C $km^{-2}$ $y^{-1}$ (median: 186 kg C $km^{-2}$ $y^{-1}$) in glacierized and 401±308 kg C $km^{-2}$ $y^{-1}$ (median: 253 kg C $km^{-2}$ $y^{-1}$) in non-glacierized catchments (Table 2.1). As expected from our analysis of DOC yield at the daily scale, the response of annual DOC yields to runoff also differed between glacierized and non-glacierized catchments (Figure 2.2). In fact, per unit annual runoff, the annual DOC yield from non-glacierized catchments was on average 3.32 times larger than the DOC yield from glacierized catchments. These differing relationships are comparable to those reported from catchments with and without wetlands (Mulholland 1997), for instance. They emphasize the various sources (e.g., soils, glacier ice) of organic carbon and their relative extent in glacierized and non-glacierized catchments. Annual DOC yields estimated in this study are lower than those reported from catchments with wetlands and forests

but comparable to those from temperate grasslands (Hope et al. 1994). For instance, the DOC yield for Z2 (937 kg C km$^{-2}$ y$^{-1}$) in the La Vièze catchment with its high vegetation cover is close to the yield reported from a high-altitude stream in the Rocky Mountains (960 kg C km$^{-2}$ y$^{-1}$) (Pacific et al. 2010). On the other hand, the annual DOC yields from our glacierized catchments are not comparable to the high DOC yields from Alaskan catchments, likely attributable to the very high runoff from Alaskan glaciers (Hood and Scott 2008).

## 2.5    Conclusions

Mountain glaciers are shrinking rapidly worldwide, but impacts on downstream biogeochemistry, such as on the DOC export fluxes, remain poorly understood (Milner et al. 2017). Using a space-for-time substitution approach, we found that a quasi-chemostasis of DOC yield in glacier-fed streams may shift to a limitation by hydrologic transport as glaciers shrink. Underlying processes are complex and likely entail shifts at the level of catchment hydrology, soil development and weathering. For instance, we propose that as glaciers shrink, runoff production from ice melt directly feeding into the stream channel will diminish, whereas hydrological flow paths through catchments may diversify potentially delivering DOC from various sources to the streams. At the same time, soil organic carbon and its spatial distribution within catchments will be impacted by changes in plant communities and soil properties due to warmer temperatures (Mayor et al. 2017). Shifts in the seasonal patterns of runoff and DOC yield will impact the timing and magnitude of the lateral DOC fluxes from terrestrial to aquatic ecosystems, and further to downstream ecosystems.

## 2.6    Supporting information

**Text S1 Catchment delimitation and land use analysis**

We identified and delineated the catchments using high-resolution (2 x 2 m) Swiss digital elevation data (swissALTI3D; Source: Geodata © swisstopo). We used the hydrology toolbox in ArcGIS 10.3 (Environmental Systems Research Institute (ESRI)) to determine flow direction, flow accumulation and catchment boundaries. Land use coverage including glacier coverage within each catchment was determined from the digital version of CORINE Land Cover inventory 2012 (© European Union, Copernicus Land Monitoring Service 2018, European Environment Agency (EEA)) and the catchment boundaries previously delineated from the DEM. Digital version of Swiss glacier coverage in 1850 was obtained from Swiss Glacier Inventory 1850 (Maisch et al. 2000).

**Text S2 Streamwater FROMcorr and DOC concentrations relationships**

The FDOM sensor used in this study uses a single excitation/emission (ex325nm/em470nm) pair to estimate the quantity of fluorescent, humic-like DOM similar to Peak C as reported by Coble (1996). Its EX/EM wavelengths are suited for determining terrestrial DOM that often dominates in headwaters (Aiken et al. 1985). Glacial runoff is typically low in DOC concentration and includes besides humic-like compounds also protein-like compounds (e.g., Barker et al. 2006, Singer et al. 2012). The latter contribute little by mass to glacier DOM (Singer et al. 2012) and are poorly captured with the regular FDOM sensors as used in our study.

When the magnitude of fluorescence emission is proportional to the DOC concentration, FDOM sensors can be used as a proxy of DOC concentration during snowmelt (Pellerin et al. 2010) and storms events (Saraceno et al. 2009) episodes that can account for up to 86% of the annual DOC export from catchments (Raymond and Saiers 2010). In our study, the use of FDOM sensor as a proxy of DOC concentration is supported by the relationships between DOC concentrations determined from discrete grab samples and

their FDOM readings (Figure SI 2.2). Furthermore, predicted DOC concentrations during glacier melt are within the same range of those reported from previous studies (i.e. Singer et al. 2012; Li et al. 2018) (Figure SI 2.3). Therefore, we are convinced that we captured DOC concentrations at a 10-min resolution sufficiently well enough to infer DOC yields at the seasonal and annual level.

In order to use *in situ* FDOM sensor values as a proxy of DOC concentration, we related DOC concentrations from discrete streamwater samples with the concurrent $FDOM_{corr}$ values at the time of the sampling (Figure SI 2.2). In situ $FDOM_{corr}$ versus grab sample DOC was site-specific for V1 (n = 11; sampled from 27.10.2016 to 11.10.2017), T1 (n = 9; from 27.10.2016 to 12.09.2017), V2 (n = 11; from 27.10.2016 to 11.10.2017) and P1 (n = 9; from 06.10.2016 to 17.10.2017). For the rest of the sites, we obtained $FDOM_{corr}$ − DOC concentrations relationships combining data for the sites of the same study area in order to increase the strength of the linear regression by adding more measurements into the model: N1, N2 and R1 (n = 39; from 21.07.2016 to 26.10.2017), Z1, Z2 and Z3 (n = 24; from 02.08.2016 to 02.11.2017) and F1 and F2 (n = 25; from 01.08.2016 to 17.10.2017). Sensor sensitivity and range of DOC concentration values measured within each valley were considered when integrating the measurements.

**Text S3 Rating curves and time series of discharge gap filling**

Rating curves between water depth and discharge were stablished for each site using a power-law model: V1 ($R^2$=0.97; n=5; *P*=0.002), V2 ($R^2$=0.95; n=7; *P*<0.001), T1 ($R^2$=0.85; n=10; *P*<0.001), Z1 ($R^2$=0.96; n=12; *P*<0.001), Z2 ($R^2$=0.97; n=6; *P*<0.001), Z3 ($R^2$=0.99; n=6; *P*<0.001), F1 ($R^2$=0.85; n=29; *P*<0.001), F2 ($R^2$=0.97; n=8; *P*<0.001), P1 ($R^2$=0.93; n=8; *P*<0.001), N2 ($R^2$=0.89; n=6; *P*=0.004) and R1 ($R^2$=0.91; n=0.91; *P*=0.01). We reconstructed incomplete time series of discharge due to depth sensor malfunction by filling in the gaps using linear correlated discharge data available from the nearest site (always from the same common study area) and from the same period. Using this approach, we reconstructed discharge data at 10 min frequency of F2 (from 1 October 2016 to 26 July 2017), P1 (from 10 November 2016 to 7 June 2017), N2 (from 1 October 2016 to 10 July 2017) and R1 (from 6 July 2017 to 30 October 2017), Z3 (from 1 October 2016 to 18 July 2017) and Z2 (from 27 October 2016 to 23 April 2017 and from 2 September 2017 to 20 September 2017). For N2, we obtained discharge data and a stage-discharge curve for N1 ($R^2$=0.90; n=55; *P*<0.001) from the stream gauging station maintained by the Mountain Hydrology and Mass Movements research unit of the Swiss Federal Institute for Forest, Snow and Landscape (WSL) and by the Institute of Earth Surface Dynamics of University of Lausanne. For both sites of Torrent du Valsorey (i.e. V1 and V2) sites and its tributary (i.e. T1), depth data were not recorded from December 2016 to mid-May 2017 (winter baseflow and beginning of snowmelt) and, in the two Valsorey sites, from 10 August 2017 to end of the period of study. In order to fill in these gaps, we used mean daily discharge data (L/s) provided by DransEnergie SA, a society in charge of the management of the hydro-electric power station located 600 m (Lat: 45.935, Long: 7.226) downstream V1 station. We extrapolated daily discharge data for those periods using linear correlated discharge relationships between DransEnergie discharge data and discharge data from sensor for the same period. As a consequence, for the period missing in these three sites, only daily discharge data was available. We filled data gaps in daily discharge data using linear interpolation to finally obtain twelve complete time series of daily discharge for the 365 days of study. Maximum consecutive days to interpolate were 8 across all sites.

**Text S4 LOADEST calibration files**

To build the calibration regression, the model requires a minimum of 12 measurements of the constituent concentration over a range of discharge conditions (Runkel et al. 2004). Due to data gaps in the $FDOM_{corr}$ time series, the smaller data set with paired DOC concentration-discharge records was for the downstream

site in La Vièze (Z1) (n = 116) and the more complete was for the upstream site of Torrent du Valsorey (V2) (n = 365).

**Text S5 DOC yield estimation uncertainty**

Due to data gaps in our FDOM time series, we used LOADEST software (Runkle et al. 2004) to obtain complete times series of daily load for the 365 days of study in each stream. According to LOADEST documentation, the uncertainty associated with each estimate is expressed in terms of the standard error that incorporates parameter uncertainty and random error and provides a description of how closely estimated loads correspond to actual loads. Also, the standard error is used within the program to develop 95% confidence intervals for each estimate of mean load. In Table 2.1, we report 95% confidence intervals for the total annual DOC yield estimated from LOADEST.

However, we acknowledge that the use of LOADEST for daily load estimations instead of the 'conservative' approach (i.e., Load = [DOC] * Q; where [DOC] and Q corresponds respectively to DOC concentration (g C/L) and discharge (L/d)) does not allow an estimate of load uncertainty associated with the error derived from DOC/ FDOM relationships and from streamwater depth/discharge regressions.

As an exercise to quantify the error in DOC yield estimates derived from those two regressions, a simple uncertainty estimation was performed using a Gaussian error propagation for the period of the year where both DOC concentration ([DOC]) and discharge (Q) were available. The error (δLoad) associated with each daily individual DOC load was estimated as:

$$Daily\ \delta Load = Daily\ Load * \sqrt{\left(\frac{\delta[DOC]}{[DOC]}\right)^2 + \left(\frac{\delta Q}{Q}\right)^2}\ [kg\ C\ d^{-1}]$$

Equation 2.3 Daily load error calculation

The error (δ[DOC]) associated with DOC concentration was the standard deviation (i.e,. ± 68% confidence interval) linked with each DOC concentration value estimated from FDOM/DOC regressions for each site individually or for several sites pooled within the same catchment (Figure SI 2.2). The error (δQ) associated with discharge was the standard deviation (i.e., ± 68% confidence interval) linked with each of the discharge values estimated from the rating curves between streamwater depth and discharge for each site (Text S3). We obtained total load (kg C) and total δLoad (kg C) for the period estimated by adding daily loads and δLoad. We derived total DOC yield (kg C/km$^2$) and total δYield (kg C/km$^2$) (Table 2.1) normalizing total load (kg C) and total δLoad (kg C) by catchment area. We compared these manual calculations of DOC yields with the LOADEST estimates for those sites where times series of DOC concentration were relatively complete (i.e., V2 (n=365), F1 (n=362) or V1 (n=314)).

# 2.6.1   Figures supporting information
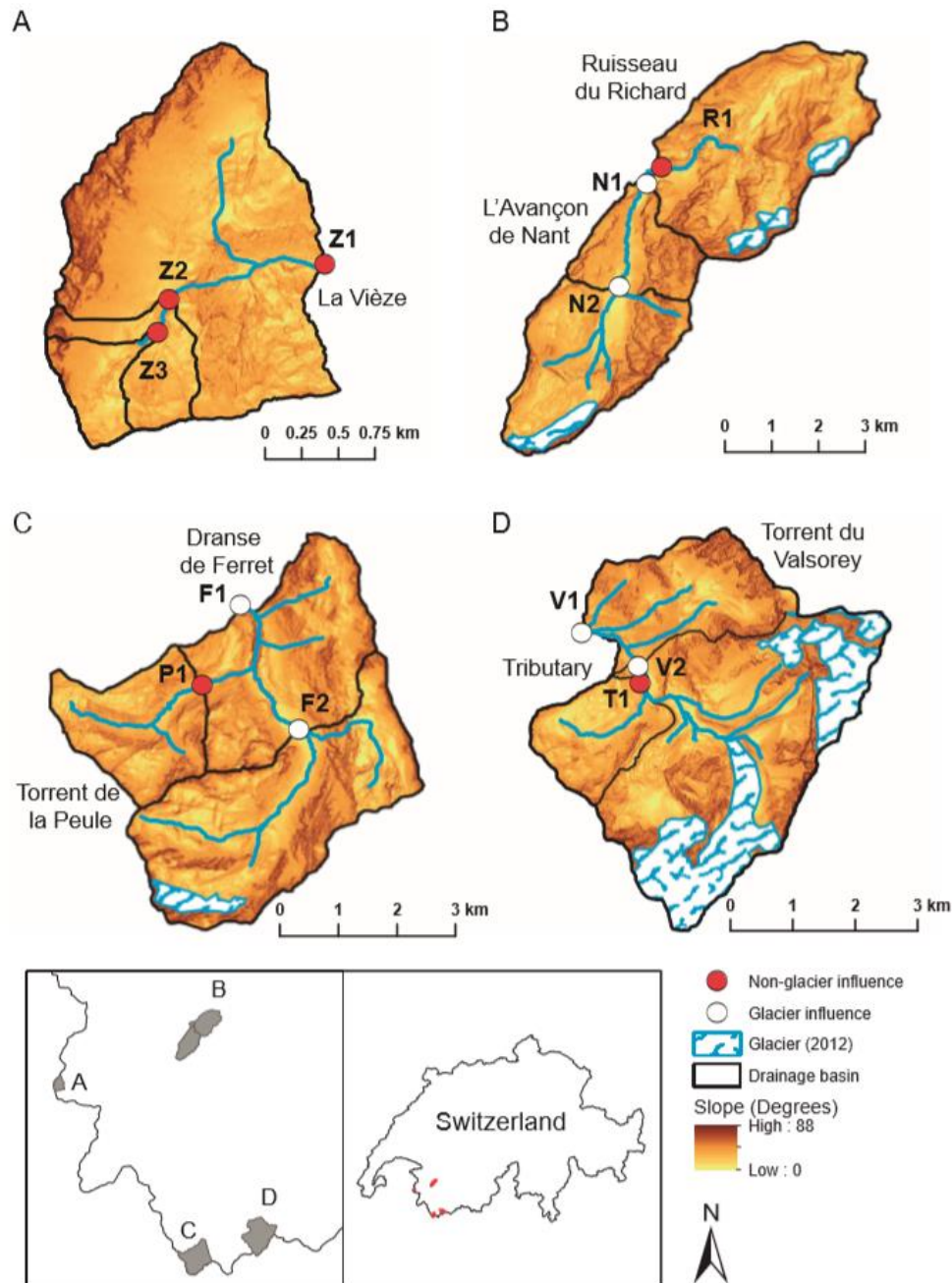


Figure SI 2.1 Map showing the location, catchment boundaries and glacier coverage of the twelve alpine study sites located in the southwestern part of the Swiss Alps. Acronyms correspond to the codes of the study sites. Glacier cover extracted from CORINE Land Cover Inventory 2012, EEA.
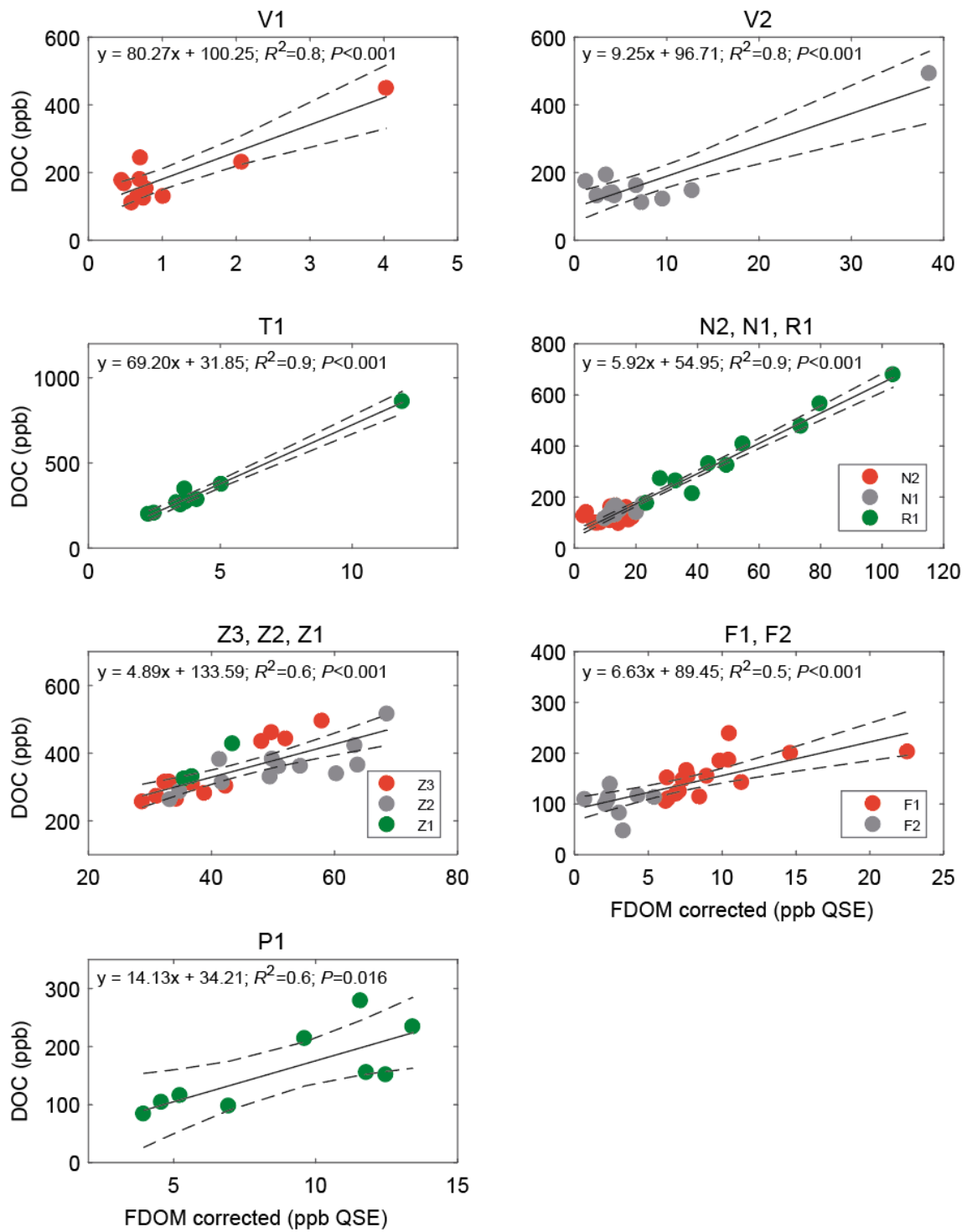
Figure SI 2.2 Linear regressions (solid line) between FDOMcorr and DOC concentration for each site or study area. Dashed lines are 95% confidence interval. Equation and statistical parameters are included in the figure.
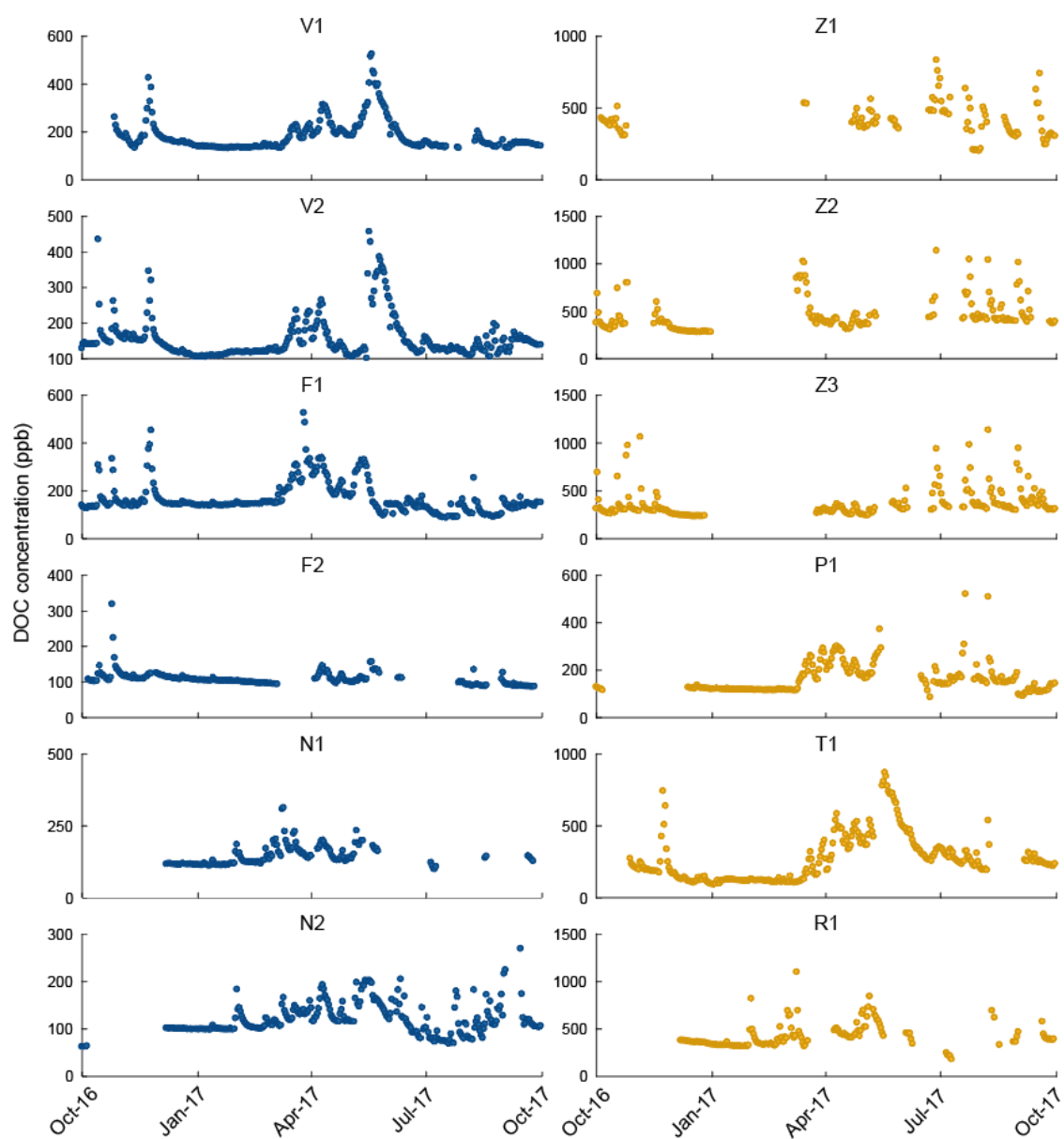
Figure SI 2.3 Times series of daily DOC concentrations estimated for the twelve study sites.
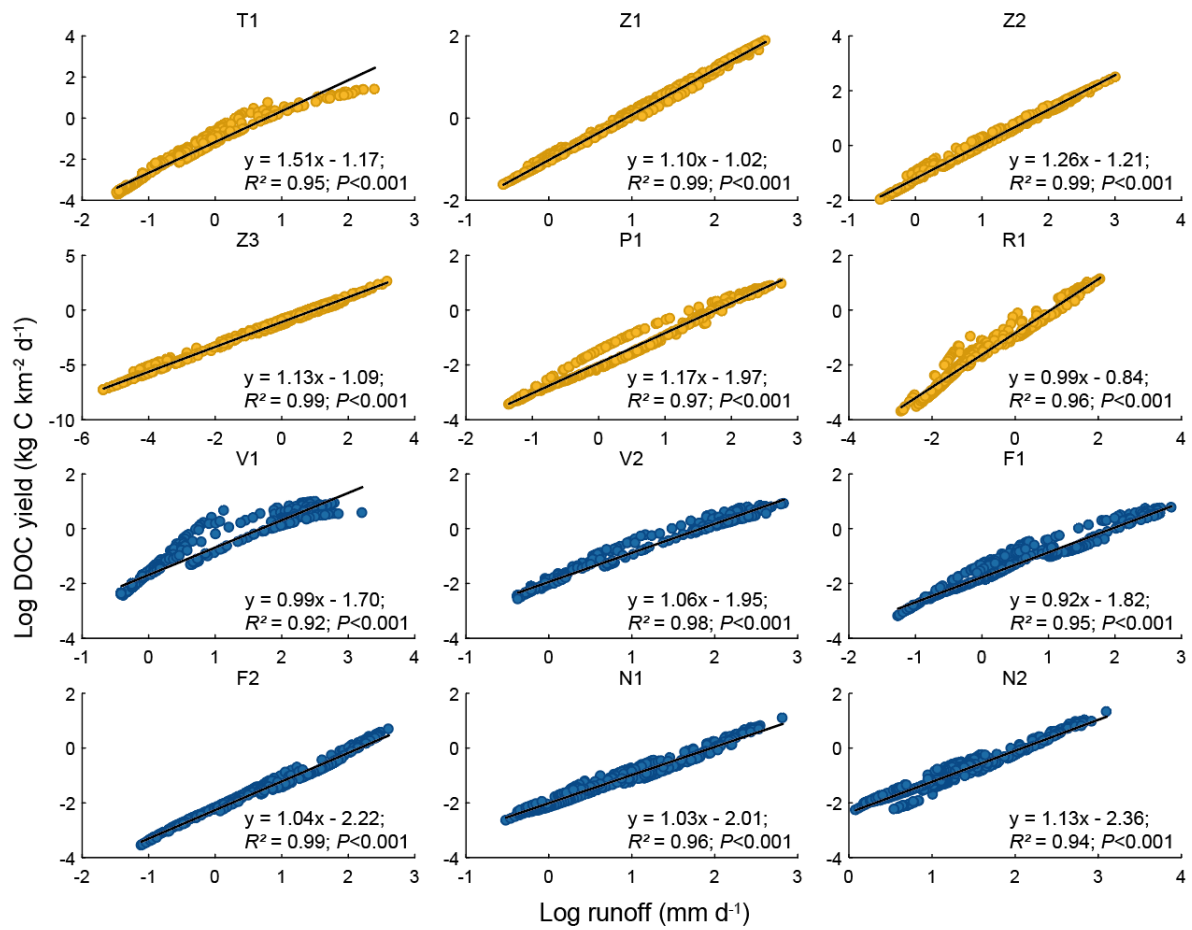
Figure SI 2.4 Natural log-linear relationships between daily runoff and daily yield across twelve study sites. Points represent data points and black line represents fitted line (least-squared linear regression).
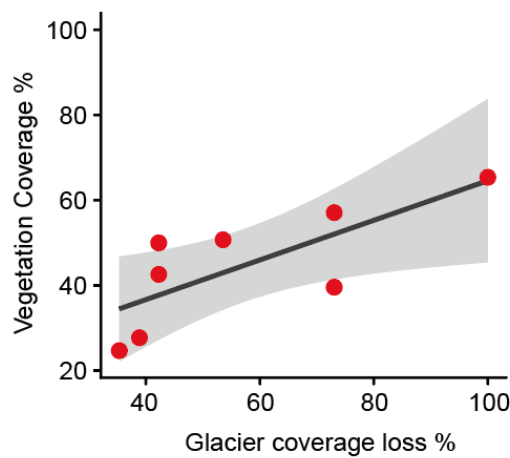


Figure SI 2.5 Relationship between glacier coverage loss between 1850 and 2012 and percentage of vegetation coverage in 2012. Line is least-square linear regression: y = 18.05+46.53x, $R^2$=0.57; $P$<0.05.
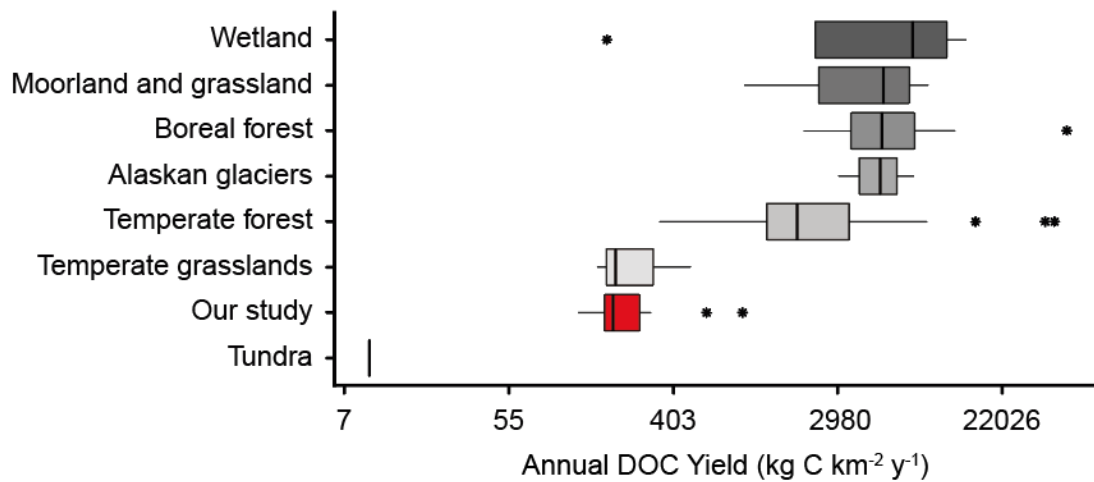
Figure SI 2.6 Box and whisker plot summarizing DOC export rates from different ecosystem types. Line within the box is the median, the box defines 25th and 75th percentiles, and the whiskers extend to the largest and lowest value no further than 1.5 times the box length. Data from: Algerich et al. (2016), Fasching et al. (2016), Fraser et al. (2001), Hood and Scott (2008), Hope et al. (1994), Laudon et al. (2004), Pacific et al. (2010), Sebestyen et al. (2009) and Strohmeier et al. (2013). Classification follows ecosystem types defined by Hope et al. (1994). Export rates from other studies were classified accordingly. New levels were created for export rates data from Hood and Scott (2008) (Alaskan glaciers). Export rates were transformed to kg C km$^{-2}$ y$^{-1}$.

## 2.6.2   Tables supporting information

| Site Code | Lat. | Long. | Average altitude catchment (m a.s.l.) | Average slope catchment (degrees) |
|---|---|---|---|---|
| V1 | 45.934 | 7.233 | 2868 ± 399 | 32.2 ± 15.5 |
| V2 | 45.930 | 7.245 | 2893 ± 399 | 31.4 ± 15.7 |
| F1 | 45.905 | 7.116 | 2421 ± 249 | 30.6 ± 13.4 |
| F2 | 45.887 | 7.128 | 2528 ± 218 | 30.1 ± 14.9 |
| N1 | 46.253 | 7.110 | 2010 ± 382 | 35.6 ± 16.7 |
| N2 | 46.232 | 7.102 | 2112 ± 329 | 34.1 ± 17.1 |
| T1 | 45.928 | 7.246 | 2548 ± 182 | 26.2 ± 12.6 |
| Z1 | 46.159 | 6.815 | 1778 ± 399 | 29.7 ± 12.6 |
| Z2 | 46.157 | 6.801 | 1832 ± 95 | 26.8 ± 11.5 |
| Z3 | 46.155 | 6.800 | 1870 ± 76 | 27.1 ± 11.7 |
| P1 | 45.894 | 7.108 | 2384 ± 157 | 29.5 ± 11.1 |
| R1 | 46.254 | 7.110 | 2081 ± 362 | 34.7 ± 16.1 |

Table SI 2.1 Study sites location and additional characteristics of catchments. Means reported as mean ± standard deviation.

| Site Code | Winter (mm) (% of annual) Days in season | Spring (mm) (% of annual) Days in season | Summer (mm) (% of annual) Days in season | Autumn (mm) (% of annual) Days in season |
|---|---|---|---|---|
| **Glacierized Sites** | | | | |
| V1 | 79 (5 %) 104 | 760 (54 %) 133 | 459 (33 %) 56 | 108 (8 %) 72 |
| V2 | 91 (7 %) 115 | 768 (56 %) 122 | 408 (29 %) 56 | 113 (8 %) 72 |
| F1 | 36 (3 %) 76 | 660 (60 %) 129 | 267 (25 %) 69 | 129 (12 %) 91 |
| F2 | 42 (4 %) 76 | 632 (57 %) 129 | 292 (26 %) 68 | 144 (13 %) 92 |
| N1 | 44 (4 %) 53 | 707 (60 %) 151 | 252 (21 %) 62 | 177 (15 %) 99 |
| N2 | 76 (5 %) 55 | 962 (58 %) 148 | 347 (21 %) 63 | 270 (16 %) 99 |
| **Non-Glacierized Sites** | | | | |
| T1 | 27 (6 %) 104 | 286 (67 %) 123 | 59 (14 %) 66 | 55 (13 %) 72 |
| Z1 | 74 (5 %) 72 | 802 (57 %) 111 | 219 (15 %) 75 | 318 (23 %) 107 |
| Z2 | 77 (4 %) 72 | 819 (43 %) 103 | 619 (33 %) 82 | 384 (20 %) 108 |
| Z3 | 2 (0.3 %) 72 | 372 (50 %) 103 | 223 (30 %) 73 | 147 (19.7 %) 117 |
| P1 | 33 (3 %) 76 | 652 (63 %) 134 | 200 (20 %) 58 | 147 (14 %) 97 |
| R1 | 6 (1 %) 48 | 301 (69 %) 156 | 100 (23 %) 62 | 31 (7 %) 99 |

Table SI 2.2 Runoff values across study sites and seasonal periods delimitated.

| Site Code | Winter (kg C/km²) (% of annual) Days in season | Spring (kg C/ km²) (% of annual) Days in season | Summer (kg C/ km²) (% of annual) Days in season | Autumn (kg C/ km²) (% of annual) Days in season |
|---|---|---|---|---|
| **Glacierized Sites** | | | | |
| V1 | 12 (5 %) 104 | 150 (58 %) 133 | 61 (24 %) 56 | 33 (13 %) 72 |
| V2 | 13 (6 %) 115 | 128 (59 %) 122 | 58 (26 %) 56 | 19 (9 %) 72 |
| F1 | 6 (4 %) 76 | 100 (63 %) 129 | 32 (20 %) 69 | 20 (13 %) 91 |
| F2 | 4 (3 %) 76 | 79 (62 %) 129 | 29 (22 %) 68 | 17 (13 %) 92 |
| N1 | 5 (3 %) 53 | 110 (66 %) 151 | 29 (17 %) 62 | 24 (14 %) 99 |
| N2 | 8 (4 %) 55 | 131 (64 %) 148 | 38 (19 %) 63 | 27 (13 %) 99 |
| **Non-Glacierized Sites** | | | | |
| T1 | 4 (2 %) 104 | 128 (72 %) 123 | 18 (10 %) 66 | 29 (16 %) 72 |
| Z1 | 27 (4 %) 72 | 366 (61 %) 111 | 91 (15 %) 75 | 121 (20 %) 107 |
| Z2 | 22 (2 %) 72 | 420 (45 %) 103 | 324 (35 %) 82 | 171 (18 %) 108 |
| Z3 | 0.35 (0.11 %) 72 | 142 (46 %) 103 | 107 (35%) 73 | 58.65 (18.89 %) 117 |
| P1 | 4 (2 %) 76 | 148 (75 %) 134 | 30 (15 %) 58 | 16 (8 %) 97 |
| R1 | 2 (1 %) 48 | 129 (70 %) 156 | 35 (19 %) 62 | 18 (10 %) 99 |

Table SI 2.3 DOC yield values across study sites and seasonal periods delimitated.

| Site Code | Intercept | Slope | Coefficient temperature |
|---|---|---|---|
| **Glacierized Sites** | | | |
| V1 | 0.63 | 0.07 | -0.00196 |
| V2 | 0.54 | 0.14 | -0.00196 |
| F1 | 0.47 | 0.11 | -0.00196 |
| F2 | 0.45 | 0.16 | -0.00196 |
| N1 | 0.53 | 0.17 | -0.00196 |
| N2 | 0.44 | 0.18 | -0.00196 |
| **Non-glacierized Sites** | | | |
| T1 | 1.06 | 0.33 | -0.00196 |
| Z1 | 1.29 | 0.45 | -0.00196 |
| Z2 | 1.45 | 0.60 | -0.00196 |
| Z3 | 1.40 | 0.51 | -0.00196 |
| P1 | 0.55 | 0.13 | -0.00196 |
| R1 | 1.22 | 0.39 | -0.00196 |

Table SI 2.4 Study site specific coefficients from linear mixed-effect model.

| Independent Variables (fixed factors): | |
|---|---|
| Runoff | 0.268*** |
| | (0.052) |
| Water Temperature | -0.002 |
| | (0.002) |
| Intercept | 0.835*** |
| | (0.125) |
| Observations | 4354 |
| LogLik | 5917.618 |
| AICc | -11819.240 |
| $R^2{}_{fixed}$ | 0.58 |
| $R^2{}_{cond.}$ | 0.95 |

Table SI 2.5 Linear mixed model statistics. Note: ***$P<0.001$, ( ) = Std. error, LogLik = negative log likelihood estimate, AICc = AIC value corrected for the number of predictors within the model, $R^2$ *fixed* indicate the variance explained by fixed effects and $R^2$ *cond.* indicates the variance explained by both random and fixed effects.

# 2.7     References

Ågren, A., M. Haei, S. J. Köhler, K. Bishop, and H. Laudon. 2010. Regulation of stream water dissolved organic carbon (DOC) concentrations during snowmelt; the role of discharge, winter climate and memory effects. Biogeosciences 7: 2901–2913. doi:10.5194/bg-7-2901-2010

Aiken, G. R., D. M. McKnight, R. L. Wershaw, and P. Mac- Carthy. 1985. Humic substances in soil, sediment and water. New York: Wiley and Sons

Argerich, A., R. Haggerty, S. L. Johnson, and others. 2016. Comprehensive multiyear carbon budget of a temperate headwater stream. J. Geophys. Res. Biogeosciences 121: 1306–1315. doi:10.1002/2015JG003050

Bakker, M., A. Costa, T. A. Silva, and others. 2018. Combined Flow Abstraction and Climate Change Impacts on an Aggrading Alpine River. Water Resour. Res. 54: 223–242. doi:10.1002/2017WR021775

Barker, J. D., M. J. Sharp, S. J. Fitzsimons, and R. J. Turner. 2006. Abundance and Dynamics of Dissolved Organic Carbon in Glacier Systems. Arctic, Antarct. Alp. Res. 38: 163–172. doi: 10.1657/1523-0430(2006)38[163:AADODO]2.0.CO;2

Barker, J. D., A. Dubnick, W. B. Lyons, and Y.-P. Chin. 2013. Changes in Dissolved Organic Matter (DOM) Fluorescence in Proglacial Antarctic Streams. Arctic, Antarct. Alp. Res. 45: 305–317. doi:10.1657/1938-4246-45.3.305

Barton, K. (2018). MuMIn: Multi-Model Inference. R package version 1.42.1. https://CRAN.R-project.org/package=MuMIn

Battin, T. J., S. Luyssaert, L. a. Kaplan, A. K. Aufdenkampe, A. Richter, and L. J. Tranvik. 2009. The boundless carbon cycle. Nat. Geosci. 2: 598–600. doi:10.1038/ngeo618

Boyer, E. W., G. M. Hornberger, K. E. Bencala, and D. M. McKnight. 1997. Response characteristics of DOC flushing in an alpine catchment. Hydrol. Process. 11: 1635–1647. doi:10.1002/(SICI)1099-1085(19971015)11:12<1635::AID-HYP494>3.0.CO;2-H

Brooks, P. D., D. M. Mcknight, and K. E. Bencala. 1999. The relationship between soil heterotrophic activity , soil dissolved organic carbon ( DOC ) leachate , and catchment-scale DOC export in headwater catchments. Water Resour. Res. 35: 1895–1902. doi:10.102

Coble, P. G. 1996. Characterisation of marine and terrestrial DOM in seawater using excitation–emission matrix spectroscopy. Mar. Chem. 51: 325–346, doi:10.1016/0304- 4203(95)00062-3

Creed, I. I. F., D. D. M. Mcknight, B. A. Pellerin, and others. 2015. The river as a chemostat : fresh perspectives on dissolved organic matter flowing down the river continuum. Can. J. Fish. Aquat. Sci. 14: 1–14. doi:10.1139/cjfas-2014-0400

Downing, B. D., B. A. Pellerin, B. A. Bergamaschi, J. F. Saraceno, and T. E. C. Kraus. 2012. Seeing the light: The effects of particles, dissolved materials, and temperature on in situ measurements of DOM fluorescence in rivers and streams. Limnol. Oceanogr. Methods 10: 767–775. doi:10.4319/lom.2012.10.767

Fasching, C., A. J. Ulseth, J. Schelker, G. Steniczka, and T. J. Battin. 2016. Hydrology controls dissolved organic matter export and composition in an Alpine stream and its hyporheic zone. Limnol. Oceanogr. 61: 558–571. doi:10.1002/lno.10232

Fellman, J. B., E. Hood, P. A. Raymond, J. Hudson, M. Bozeman, and M. Arimitsu. 2015. Evidence for the assimilation of ancient glacier organic carbon in a proglacial stream food web. Limnol. Oceanogr. 60: 1118–1128. doi:10.1002/lno.10088

Finlay, J., J. Neff, S. Zimov, A. Davydova, and S. Davydov. 2006. Snowmelt dominance of dissolved organic carbon in high-latitute watersheds: Implications for characterization and flux of river DOC. Geophys. Res. Lett. 33: 2–6. doi:10.1029/2006GL025754

Fraser, C. J. D., N. T. Roulet, and T. R. Moore. 2001. Hydrology and dissolved organic carbon biogeochemistry in an ombrotrophic bog. Hydrol. Process. 15: 3151–3166. doi:10.1002/hyp.322

Fuka, D.R., M.T. Walter, J.A. Archibald, T.S. Steenhuis, and Z. M. Easton. 2018. EcoHydRology: A community modeling foundation for Eco-Hydrology. R package version 0.4.12.1. https://CRAN.R-project.org/package=EcoHydRology

Godsey, S. E., J. W. Kirchner, and D. W. Clow. 2009. Concentration-discharge relationships reflect chemostatic characteristics of US catchments. Hydrol. Process. 23: 1844–1864. doi:10.1002/hyp.7315

Gordon, N. D., T.A. McMahon, B. L. Finlayson, C. J. Gippel, and R. J. Nathan. 2004. Stream hydrology: An introduction for ecologists. Chichester: John Wiley

Heckmann, T., S. McColl, and D. Morche. 2016. Retreating ice: research in pro-glacial areas matters. Earth Surf. Process. Landforms 41: 271–276. doi:10.1002/esp.3858

Hood, E., T. J. Battin, J. Fellman, S. O'Neel, and R. G. M. Spencer. 2015. Storage and release of organic carbon from glaciers and ice sheets. Nat. Geosci. 8: 1–6. doi:10.1038/ngeo2331

Hood, E., D. M. McKnight, and M. W. Williams. 2003. Sources and chemical character of dissolved organic carbon across an alpine/subalpine ecotone, Green Lakes Valley, Colorado Front Range, United States. Water Resour. Res. 39: 1–12. doi:10.1029/2002WR001738

Hood, E., and D. Scott. 2008. Riverine organic matter and nutrients in southeast Alaska affected by glacial coverage. Nat. Geosci. 1: 583–587. doi:10.1038/ngeo280

Hope, D., M. F. Billett, and M. S. Cresser. 1994. A review of the export of carbon in river water: Fluxes and processes. Environ. Pollut. 84: 301–324. doi:10.1016/0269-7491(94)90142-2

Huss, M., and R. Hock. 2018. Global-scale hydrological response to future glacier mass loss. Nat. Clim. Chang. 8: 135–140. doi:s41558-017-0049-x

Koenig, L. E., M. D. Shattuck, L. E. Snyder, J. D. Potter, and W. H. McDowell. 2017. Deconstructing the Effects of Flow on DOC, Nitrate, and Major Ion Interactions Using a High-Frequency Aquatic Sensor Network. Water Resour. Res. 53: 10655–10673. doi:10.1002/2017WR020739

Lafreniere, M. J., and M. J. Sharp. 2004. The Concentration and Fluorescence of Dissolved Organic Carbon (DOC) in Glacial and Nonglacial Catchment. Artic, Antarct. Alp. Res. 36: 156–165. doi:https://doi.org/10.1657/1523-0430(2004)036[0156:TCAFOD]2.0.CO;2

Lane, S. N., and P. W. Nienow. 2019. Decadal-Scale Climate Forcing of Alpine Glacial Hydrological Systems. Water Resour. Res. 55: 2478–2492. doi:10.1029/2018WR024206

Laudon, H., S. Köhler, and I. Buffam. 2004. Seasonal TOC export from seven boreal catchments in northern Sweden. Aquat. Sci. - Res. Across Boundaries 66: 223–230. doi:10.1007/s00027-004-0700-2

Lee, E. J., G. Y. Yoo, Y. Jeong, K. U. Kim, J. H. Park, and N. H. Oh. 2015. Comparison of UV-VIS and FDOM sensors for in situ monitoring of stream DOC concentrations. Biogeosciences 12: 3109–3118. doi:10.5194/bg-12-3109-2015

Li, X., Y. Ding, J. Xu, and others. 2018. Importance of Mountain Glaciers as a Source of Dissolved Organic Carbon. J. Geophys. Res. Earth Surf. 123: 2123–2134. doi:10.1029/2017JF004333

Maisch, M., A. Wipf, B. Denneler, J, Battaglia, C. Benz. 2000. Die Gletscher der Schweizer Alpen: Gletscherhochstand 1850, Aktuelle Vergletscherung, Gletscherschwund-Szenarien. (Schlussbericht NFP 31). 2. Auflage. vdf Hochschul-verlag an der ETH Zürich, 373 pp. & Paul, F. 2004, The new Swiss glacier inventory 2000 – application of remote sensing and GIS. PhD Thesis, Department of Geography, University of Zurich, Schriftenreihe Physische Geographie, 52, 210 pp.

Mayor, J. R., N. J. Sanders, A. T. Classen, and others. 2017. Elevation alters ecosystem properties across temperate treelines globally. Nature 542: 91–95. doi:10.1038/nature21027

Miller, H. R., and S. N. Lane. 2019. Biogeomorphic feedbacks and the ecosystem engineering of recently deglaciated terrain. Prog. Phys. Geogr. 43: 24–45. doi:10.1177/0309133318816536

Milner, A. M., K. Khamis, T. J. Battin, and others. 2017. Glacier shrinkage driving global changes in downstream systems. Proc. Natl. Acad. Sci. 201619807. doi:10.1073/pnas.1619807114

Mladenov, N., M. W. Williams, S. K. Schmidt, and K. Cawley. 2012. Atmospheric deposition as a source of carbon and nutrients to an alpine catchment of the Colorado Rocky Mountains, *Biogeosciences*, 9, 3337-3355, https://doi.org/10.5194/bg-9-3337-2012

Mulholland, P. J. 1997. Dissolved Organic Matter Concentration and Flux in Streams. J. North Am. Benthol. Soc. 16: 131–141. doi:10.2307/1468246

Nathan, R. J., and T. A. McMahon. 1990. Evaluation of automated techniques for base flow and recession analyses. Water Resour. Res. 26: 1465–1473. doi:10.1029/WR026i007p01465

Pacific, V. J., K. G. Jencso, and B. L. McGlynn. 2010. Variable flushing mechanisms and landscape structure control stream DOC export during snowmelt in a set of nested catchments. Biogeochemistry 99: 193–211. doi:10.1007/s10533-009-9401-1

Pellerin, B. A., J. F. Saraceno, J. B. Shanley, S. D. Sebestyen, G. R. Aiken, W. M. Wollheim, and B. A. Bergamaschi. 2012. Taking the pulse of snowmelt: In situ sensors reveal seasonal, event and diurnal patterns of nitrate and dissolved organic matter variability in an upland forest stream. Biogeochemistry 108: 183–198. doi:10.1007/s10533-011-9589-8

Pinheiro, J., D. Bates, S. DebRoy, D. Sarkar, and R Core Team. 2018. nlme: linear and nonlinear mixed effects models. R package version 3.1-137, https://CRAN.R-project.org/package=nlme

Raymond, P. A., and J. E. Saiers. 2010. Event controlled DOC export from forested watersheds. Biogeochemistry 100: 197–209. doi:10.1007/s10533-010-9416-7

Regnier, P., P. Friedlingstein, P. Ciais, and others. 2013. Anthropogenic perturbation of the carbon fluxes from land to ocean. Nat. Geosci. 6: 597–607. doi:10.1038/ngeo1830

Runkel, R. L., C. G. Crawford, and T.A. Cohn. 2004. Load Estimator (LOADEST): A FORTRAN program for estimating constituent loads in streams and rivers, Tech. Meth., 4, chap. A5, 69 pp., U. S. Geol. Surv., Denver, Colorado

Saraceno, J. F., B. A. Pellerin, B. D. Downing, E. Boss, P. A. M. Bachand, and B. A. Bergamaschi. 2009. High-frequency in situ optical measurements during a storm event: Assessing relationships between dissolved organic matter, sediment concentrations, and hydrologic processes. J. Geophys. Res. Biogeosciences 114: 1–11. doi:10.1029/2009JG000989

Saraceno, J. F., J. B. Shanley, B. D. Downing, and B. A. Pellerin. 2017. Clearing the waters: Evaluating the need for site-specific field fluorescence corrections based on turbidity measurements. Limnol. Oceanogr. Methods 15: 408–416. doi:10.1002/lom3.10175

Sebestyen, S. D., E. W. Boyer, and J. B. Shanley. 2009. Responses of stream nitrate and DOC loadings to hydrological forcing and climate change in an upland forest of the northeastern United States. J. Geophys. Res. Biogeosciences 114: 1–11. doi:10.1029/2008JG000778

Singer, G. a., C. Fasching, L. Wilhelm, J. Niggemann, P. Steier, T. Dittmar, and T. J. Battin. 2012. Biogeochemically diverse organic matter in Alpine glaciers and its downstream fate. Nat. Geosci. 5: 710–714. doi:10.1038/ngeo1581

Strohmeier, S., K. H. Knorr, M. Reichert, S. Frei, J. H. Fleckenstein, S. Peiffer, and E. Matzner. 2013. Concentrations and fluxes of dissolved organic carbon in runoff from a forested catchment: Insights from high frequency measurements. Biogeosciences 10: 905–916. doi:10.5194/bg-10-905-2013

Tank, S. E., J. B. Fellman, E. Hood, and E. S. Kritzberg. 2018. Beyond Respiration: Controls on lateral carbon fluxes across the terrestrial-aquatic interface. Limnol. Oceanogr. Lett. doi:10.1002/lol2.10065

Tissier, G., Y. Perrette, M. Dzikowski, J. Poulenard, F. Hobléa, E. Malet, and B. Fanget. 2013. Seasonal changes of organic matter quality and quantity at the outlet of a forested karst system (La Roche Saint Alban, French Alps). J. Hydrol. 482: 139–148. doi:10.1016/j.jhydrol.2012.12.045

Tockner, K., F. Malard, U. Uehlinger, and J. V. Ward. 2002. Nutrients and organic matter in a glacial river-floodplain system (Val Roseg, Switzerland). Limnol. Oceanogr. 47: 266–277. doi:10.4319/lo.2002.47.1.0266

Tunaley, C., D. Tetzlaff, J. Lessels, and C. Soulsby. 2016. Linking high-frequency DOC dynamics to the age of connected water sources. Water Resour. Res. 52: 5232–5247. doi:10.1002/2015WR018419

Vaughan, M. C. H., W. B. Bowden, J. B. Shanley, and others. 2017. High-frequency dissolved organic carbon and nitrate measurements reveal differences in storm hysteresis and loading in relation to land cover and seasonality. Water Resour. Res. 53: 5345–5363. doi:10.1002/2017WR020491

Watras, C. J., P. C. Hanson, T. L. Stacy, K. M. Morrison, J. Mather, Y.-H. Hu, and P. Milewski. 2011. A temperature compensation method for CDOM fluorescence sensors in freshwater. Limnol. Oceanogr. Methods 9: 296–301. doi:10.4319/lom.2011.9.296

Wilson, H. F., J. E. Saiers, P. A. Raymond, and W. V. Sobczak. 2013. Hydrologic Drivers and Seasonality of Dissolved Organic Carbon Concentration, Nitrogen Content, Bioavailability, and Export in a Forested New England Stream. Ecosystems 16: 604–616. doi:10.1007/s10021-013-9635-6

Zarnetske, J. P., M. Bouda, B. W. Abbott, J. Saiers, and P. A. Raymond. 2018. Generality of Hydrologic Transport Limitation of Watershed Organic Carbon Flux Across Ecoregions of the United States. Geophys. Res. Lett. 45: 11,702-11,711. doi:10.1029/2018GL080005

# Chapter 3 Temporal dynamics and drivers of dissolved oxygen differ among high-alpine stream types

An edited version of this chapter was sent to the journal *Limnology and Oceanography,* John Wiley & Sons publications. Currently is under review.

Authors of this manuscrip are the following: Marta Boix Canadell, Lluís Gómez-Gener, Mélanie Clémençon, Stuart N. Lane, Tom J. Battin.

M. B. C was involved in the fieldwork, conceived the study, analysed data and results and wrote the manuscript.

## 3.1    Abstract

High-resolution time series of dissolved oxygen (DO) have recently revealed different ecosystem energetics regimes across various stream types. This is relevant to better understand the transformation and retention of nutrients and carbon in stream ecosystems. However, the patterns and controls of stream energetics in high-mountain landscapes remain largely unknown. Here we monitored DO saturation (every 10 minutes) over two years in a glacier-fed, krenal (groundwater-fed) and a nival (snowmelt-fed) stream as they are typical for the high mountains. We used daily Shannon entropy to explore the temporal dynamics of streamwater DO and to infer information on the ecosystem energetics and on the potential drivers. We found discharge as a major modulator of drivers, such as light availability at the stream bottom, gas exchange rate or streambed stability, on the seasonal and daily DO variations. Elevated bed movement along with high turbidity and very high gas exchange rates drove the daily DO patterns in the glacier-fed stream during snow and ice melt, whereas light seemed to be the major driver of the DO dynamics in the krenal and nival streams. We found a window of favourable conditions for potential gross primary production (GPP) during the freshet in the glacier-fed stream, whereas GPP seemed to extend over longer periods in the krenal and nival streams. Our findings suggest how the energetic regimes of these high-mountain streams may change in the future as their biological and physical drivers change owing to climate warming.

## 3.2    Introduction

Time-series of streamwater dissolved oxygen (DO) can reveal patterns and processes of stream ecosystem energetics (Bernhardt et al. 2018). The temporal variation of streamwater DO concentrations at diurnal and seasonal scales arises from the balance between biological and physical processes. In terms of physical processes, turbulence increases DO availability across a range of time-scales (Moog and Jirka 1999), and this is generally a function of shear at the air-water interface boundary (Tamburrino and Gulliver 2002). In shallow streams, this interface is strongly impacted upon by channel slope and bed roughness (Raymond et al. 2012; Ulseth et al. 2019). Steeper slopes increase water velocity which, in combination with bed roughness, can increase shear at the air-water interface, and hence turbulence, which is directly related to

oxygen exchange (Zappa et al. 2007). There is a positive effect of temperature on the gas transfer velocity, which, however, becomes negligible as turbulence increases (Demars and Manson 2013). In terms of biological processes, DO can be both produced, notably by gross primary production (GPP), and removed, notably by ecosystem respiration (ER). In high-alpine streams, most of the GPP is confined to benthic sediments, colonized by cyanobacteria, diatoms, Hydrurus and bryophytes, for instance (Rott et al. 2016). ER involves both the respiration from the autotrophic and heterotrophic component of the benthic communities but also from the heterotrophic communities within the hyporheic zone (Naegeli and Uehlinger 1997; Battin et al. 2016).

Light availability, flow-induced disturbance and temperature count among the primary determinants of GPP and ER (Uehlinger and Naegeli 1998; Roberts et al. 2007; Acuña et al. 2008). Variations in light regimes can come from shading by the riparian vegetation, streamwater turbidity owing to suspended sediment, catchment topography and related variation in exposure to solar radiation. Besides light availability, streambed movement and scouring resulting from hydraulic forces acting on the sediments can constrain the accumulation of algal biomass with implications for GPP (e.g., Biggs et al. 1999; Uehlinger et al. 2002). Furthermore, the positive effect of temperature on GPP and ER is well established (e.g., Demars et al. 2011; Rasmussen et al. 2011), with ER being more sensitive to changes in temperature than GPP (Enquist et al. 2003; Allen et al. 2005). Seasonal loadings of inorganic forms of nutrients (e.g., nitrate, phosphate) and organic carbon can also fuel ER (Berggren and del Giorgio 2015; Rosa et al. 2013). When light and disturbance are not limiting, such pulsed nutrient supplies can also accelerate GPP (e.g., Mulholland et al. 2001).

The availability of reliable and affordable sensors now allows the study of the temporal dynamics of DO concentration and related environmental parameters at fine temporal scales and this over prolonged periods (Rode et al. 2016). In the last decade, time series of stream DO have been collected across different stream types with the purpose of understanding the temporal patterns of stream ecosystem metabolism and its drivers (e.g., Bernhardt et al. 2018; Appling et al. 2018; Savoy et al. 2019). Processes that dominate streamwater DO concentration are ultimately responsible of the DO regime typical for each stream or river, much as its energetic fingerprint (Bernhardt et al. 2018; Savoy et al. 2019). In large rivers in temperate zones, DO time series exhibit large daily DO variations resulting from enhanced GPP in summer (Dodds et al. 2015). In contrast, closed canopy reaches in headwater streams may impact DO dynamics such that peaks in DO concentration often mismatch the timing of potential light availability (Bernhardt et al. 2018). Furthermore, DO dynamics may also reflect the impact of stochastic flow-induced disturbance in low-order streams compared, for example, to the strong seasonality in larger and less frequently disturbed rivers.

In high-mountain streams, the melting of snow and glacial ice imparts a unique signature on the physicochemical properties of the streamwater, including temperature, turbidity and related light attenuation, solute composition and concentration, as well as streambed stability (Ward 1994; Robinson et al. 2002; Uehlinger et al. 2010; Gabbud et al. 2020). The interactions between these parameters over daily and seasonal scales create scenarios in which biological and physical processes play roles of alternating relevance in shaping stream ecosystem functioning. Thus far, despite the ubiquitous presence of high-mountain streams and their relevance for global biogeochemical fluxes (e.g., Horgby et al. 2019), we have limited understanding of the processes that regulate DO dynamics across temporal scales in these ecosystems. This is remarkable given the profound climate-driven hydrological and physicochemical changes that these streams are facing. As the climate becomes warmer, depending on altitude, precipitation in spring and autumn will increasingly shift from snow fall to rain with major consequences on snow pack and runoff dynamics (e.g., Berghuijs et al. 2014, Beniston et al. 2018). At the same time, mountain glaciers are shrinking (IPCC, 2019), which further changes the magnitude and within-year

distribution of runoff (Lane and Nienow 2019) and related physical and chemical parameters in glacier-fed streams (e.g., Milner et al. 2017). Implications of this unprecedented environmental change for ecosystem energetics in high-mountain streams remain largely elusive at present (Milner et al. 2017).

In this study, we aim to evaluate the effect of drivers, including light availability, streambed stability and gas exchange rate, to determine the interactions between physical and biological processes that shape DO dynamics in high-mountain streams: one glacier-fed (glacial), one groundwater-fed (krenal) and one snowmelt-fed (nival), in the Swiss Alps. To asses this, we collect time series of DO saturation (%) measured every 10 minutes over 24 months. We derive Shannon entropy index to quantify daily patterns of streamwater DO as it was recently done for the temporal dynamics of discharge in a glacier-fed stream (Lane and Nienow 2019). Estimating GPP in highly turbulent streams with very high gas exchange rates is inherently difficult (e.g., Hall et al. 2015), and we therefore use DO entropy as an indicator for stream ecosystem energetics at daily and seasonal scales. We posit that the relative importance of potential drivers, such as light and streambed stability, changes among the three stream types, and that this comparison provides insights into the consequences of climate warming for stream ecosystem development in the high mountains.

## 3.3     Materials and methods

### 3.3.1   Study sites

Using the classification of Alpine streams types (*sensu* Brown et al. 2003), we study a glacial (Torrent du Valsorey, 28 % glacier coverage), a krenal (Valsorey Spring) and a nival (Torrent de la Peule) stream in the Swiss Alps (Figure 3.1; Table 3.1). All three streams drain catchments above the tree line where vegetation, is predominantly primary colonisers, including grasses and shrubs. Stream channel slopes are elevated (6.5 ± 1.1 %) and the streambed primarily composed of poorly sorted, coarse gravel and cobbles in the glacier-fed and nival stream. The streambed of the krenal stream was composed of finer sediments and was partially covered by large patches of bryophytes. Discharge follows temporal trends typical for high-alpine streams with extended baseflow in winter when the streams are completely or partially snow covered, and with a marked snowmelt peak in spring followed by ice melt in the glaciated catchment in summer. All streams are also subject to the effects of summer rainfall.

### 3.3.2   Baseline catchment characteristics

We identified and delineated the catchments using high-resolution (2 x 2 m) Swiss digital elevation model (DEM: swissALTI3D; Source: Geodata © swisstopo). We used the hydrology tool box in ArcGIS 10.3 (Environmental Systems Research Institute (ESRI)) to determine flow direction, flow accumulation and eventually catchment boundaries. Land use coverage including glacier coverage within each catchment was based on the digital version of CORINE Land Cover inventory 2012 (© European Union, Copernicus Land Monitoring Service 2018, European Environment Agency (EEA)) and the catchment boundaries previously delimited from the DEM.

### 3.3.3   Monitoring environmental parameters with sensors

At each stream, we deployed sensors to monitor streamwater DO concentration (mg $O_2$/L), temperature (ºC; miniDOT, Precision Measurement Engineering, Vista, California, USA), turbidity (NTU; Cyclops-7 Turbidity, Turner Designs), and water depth (mm; Odyssey Capacitance Logger, Dataflow Systems Ltd). At each site we also monitored atmospheric pressure (mbar; Track-It™ Monarch Instrument) and photosynthetic active radiation (PAR) (Lux; Onset HOBO® Pendant) at the banks (1 m above ground). In

order to measure PAR that reaches the streambed, we placed additional PAR sensors at the stream bottom. All parameters were continuously recorded at 10 min interval from 15 October 2016 to 15 October 2018. We visited each stream approximately monthly for sensor maintenance and data downloading. During these visits, we measured streamwater temperature and DO concentration with daily calibrated WTW multiparameter probes (Xylem Inc., USA). During winter, visits were less frequent because of the harsh conditions inherent of these environments (e.g., avalanche risk).

Spot gauging to determine discharge for calibration of water level records was determined using slug-injections of sodium chloride as a conservative racer (Gordon et al. 2004). Rating curves between streamwater depth and discharge were established for each site using a power-law model by fitting a linear regression on natural log transformed data (glacier-fed stream: $R^2$=0.95; n=7; $P$<0.001; groundwater-fed stream: $R^2$=0.85; n=10; $P$<0.001; nival stream: $R^2$=0.93; n=8; $P$<0.001). When data were missing because of sensor malfunctioning (166 days in krenal stream, 217 days in glacier-fed streams and 210 days in La Peule), we extrapolated gaps, if possible, using discharge data from the nearest gauging station within the catchment (Boix Canadell et al. 2019). When this was not possible, variables derived from discharge (e.g., gas exchange rate, streambed movement) are missing as well.
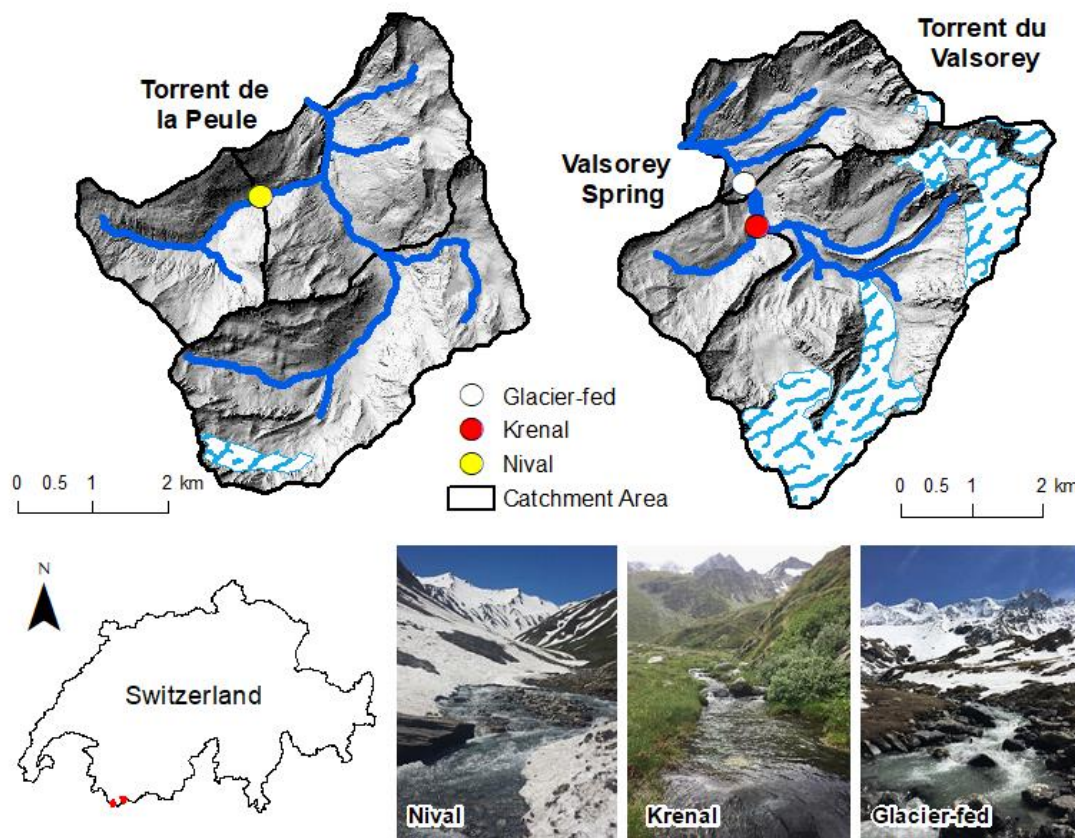


Figure 3.1 Location of study streams and sensor stations in the Swiss Alps.

### 3.3.4 Daily oxygen entropy

We estimated DO saturation concentration (i.e., the theoretical concentration of DO if the air and water temperature were at equilibrium) as a function of water temperature and atmospheric pressure and we converted our measured DO concentration to a percentage of atmospheric saturation (DO percent saturation). Next, daily entropy of DO saturation (%) was calculated using:

$$E_d = \frac{1}{n}\sum_{i=1}^{n}\frac{S_i}{\overline{S_i}}log\frac{S_i}{\overline{S_i}}$$

Equation 3.1

where $s_i$ is the DO saturation for time step $i$ for $n$ time steps within each day $d$. Equation 3.1 measures the extent of deviation within each day from the mean DO saturation for that day. A higher value of $E_d$ indicates a greater range of diurnal variability of DO saturation as compared to the daily mean value. Essentially daily DO entropy informs on the departure of DO saturation from its baseline and is thus assumed to reflect biological (e.g., GPP) and physical (e.g., gas exchange) processes.

### 3.3.5 Gas exchange rate

For each stream, we estimated gas exchange rates K600 (d$^{-1}$) from argon tracer gas injections (Ulseth et al. 2019). Argon releases were conducted through the year to capture variability of the gas exchange coefficient during different flow conditions (i.e. baseflow, snow and glacier melt). K600 for the entire study period were computed from stream specific log-log least-squared linear regressions between discharge data and K600 measured in the field. Discharge ($Q$, m$^3$/s) and velocity ($v$, m/s) were calculated from slug releases during the day of the gas injection. We measured stream channel width (n = 10) of the upstream reach and estimated mean stream depth assuming hydraulic continuity, that is, $\overline{z_{i,d}} = Q/wv$. Further details on the estimation of K600 and hydraulic geometry are provided in Ulseth et al. (2019).

### 3.3.6 PAR attenuation

For the periods where measurements of water depth data, turbidity and PAR at the stream bottom were available, we calculated coefficient of extinction of PAR ($K_d$, m$^{-1}$) using the light attenuation function:

$$I_z = I_o exp^{-K_d \times z}$$

Equation 3.2

where $I_z$ is the PAR reaching the stream bottom, $I_o$ is the PAR reaching the stream surface and $z$ is the water depth (m) at the sensor location. We used the water depth data recorded from the water depth sensor which was deployed next to the PAR sensor. Next, we related $K_d$ with of the corresponding value of the streamwater turbidity to obtain a $K_d$ for each time step as a function of turbidity. Finally, we applied the light attenuation function with the turbidity-specific $K_d$ to obtain the PAR at the stream bottom as a function of streamwater depth at each time point. We converted measured lux (lumens/m$^2$) to photosynthetic photon flux density (µmol m$^{-2}$ s$^{-1}$) for the 400-700 nm band diving lux by constant value of 54 given by Thimijan and Heins (1983).

### 3.3.7 Modelling streambed stability

We used a 2D hydrodynamic model to predict shear stresses and combined them with sediment size distribution data to infer the relative proportion of the streambed with sediments moving owing to increases in discharge. We consider this as a proxy for streambed stability. Streambed topography and grain size characterization from the reach upstream of our sensors was obtained from digital elevation models (DEMs) and high-resolution orthoimaginery using structure-from-motion photogrammetry (SfM-MvS) and bathymetric correction due to the effects of refraction in the water column (Dietrich 2017). Aerial photographs were taken during low flow (nival stream: 12 October 2017; krenal and glacier-fed streams: 13 October 2017) with a drone (SZ DJI Technology Co. Ltd) equipped with a 12.4 megapixel camera. Image overlap was approximately 80% along the flight path, the drone was flown at two altitudes and the camera was set as off-nadir, so as to minimise the systematic error in acquired data (Carbonneau and Dietrich 2017). Before each flight, we marked ground control points spaced throughout the reach for posterior image georeferencing and determined their position to within a few centimetres using a Trimble real-time kinematic (RTK) GPS unit. All images were processed using Pix4D software (Pix4D SA). The resulting orthomosaics and DEMs had spatial resolutions between 1.24 and 1.28 cm/px and were georeferenced to the Swiss grid system (x, y) and mean annual sea level. Finally, we delimited and corrected wetted areas of generated DEMs for refractive effects as in Dietrich (2017).

Median sediment sizes were estimated with digital image processing of the high-resolution orthophoto (Carbonneau et al. 2004). Using ArcGIS 10.3, for each of the three rivers, 20 grids of 1m x 1m with 16 line intersections were evenly superimposed onto the image covering both wet and dry areas of the active channel. Within each grid, the intermediate $b$ axis of pebbles which were at the line intersection was manually draw and its length (mm) automatically measured. This gave an estimate of median grain size ($D_{50}$) for each grid. We then apply a 1m x 1m moving window to the orthoimagery and calculate the semi-variance for different sub windows from 3 x 3 pixels to the n x n pixels corresponding to the size of the moving window. Tests suggested that the maximum semi-variance measured was strongly correlated with $D_{50}$. Thus the $D_{50}$ measures were divided randomly into training and validating datasets. The training dataset was used to parameterise the relationship between grain size and semi-variance. This relationship was then applied to the orthoimagery for the river concerned to produce a map of $D_{50}$. These were validated using the second dataset.

In order to obtain estimates of bed shear stress we used a method similar to that adopted for a similar type of stream (Gabbud et al. 2020) and a summary is provided here. We used the BASEMENT v2.7 hydraulic model (ETHZ, VAW, 2017), which solves the depth-averaged form of the Navier-Stokes equations for mass and momentum conservation using a finite element mesh (Vetsch et al. 2018). Turbulence was represented using a Reynolds decomposition with a zero-order eddy viscosity turbulence model. Bed shear stresses were represented using a quadratic friction law with a Manning roughness coefficient. Model solution used an exact Riemann solver and time steps were set automatically using the Courant-Friedrichs-Lewy condition. The downstream boundary used a depth-discharge relationship based upon the Manning equation and in all cases it was set downstream of the zone of interest in this study. In all model runs a steady discharge was applied at the upstream section and the model run to steady state, with the mass balance error (the difference between mass inflow rate and mass outflow rate) less than 0.5%.

The DEM of the channel bathymetry was resampled to 0.1 m resolution for the hydraulic modelling, a resolution that reflected a compromise between representation of topographic detail and computational efficiency. These data were converted into an unstructured triangular mesh using BASEmesh in the Quantum GIS software.

In all cases, the model was parameterised using Manning's n by comparing inundated zones measured in the orthophoto with model predictions of inundation (see Gabbud et al. (2020) for the detailed method). Once the model was optimized, discharges were simulated every 0.1 m$^3$/s, 0.06 m$^3$/s and 0.04 m$^3$/s for the glacier-fed stream (n = 62), groundwater-fed stream (n = 46) and nival stream (n = 23) between the minimum and the maximum values of the range of discharge measured in each stream. All other parameter values were left constant. The bottom shear stress ($\tau_b$) values predicted for each model run were then compared with a critical shear stress required for entrainment, using a Shields stress:

$$\tau_{oc} = 0.06(\rho_s - \rho)gD_{50}$$

Equation 3.3

where $g$ the gravitational constant, $\rho_s$ is the sediment particle density (km/m$^3$), $\rho$ is the water density (km/m$^3$), and $D_{50}$ is the median of the particle size distribution extracted from the D50 map of the reach corresponding to the same hydraulic model grid cell. Application of this rule is supported by qualitative observations that the streambeds were poorly armoured. For each reach, it was possible to calculate the percentage of the streambed that was mobile for each simulated discharge and the provided a look up table. By applying the look up table to the calibrated discharge record, we were able to transform the time series of discharge into a time series of streambed stability. This approach needed only one modification for the krenal stream. The moss cover was estimated by the texture based *D$_{50}$* mapping to be sand and easily movable. Field observations suggested that these zones of moss cover were extremely stable. Thus, for the krenal reach, moss was mapped on the orthoimage and associated zones were labelled as permanently stable in the application of the look up table.

## 3.3.8  Data analysis

For each stream we identified the snow-free periods for both years by combining satellite images with field observations and by inspecting time series of DO saturation and its deviation from the winter baseline. In 2018, there was a delay in the loss of the snow cover, the latter extending into summer in the catchment drained by the nival stream, that clearly reduced PAR at the stream bottom until July.

For the snow-free periods in 2017 and 2018, we conducted quantile regression analyses using the *quantreg* package in R (Koenker 2019) to determine if the 90$^{th}$ percentile of the frequency distribution of DO changed as a function of average of PAR, turbidity, K600, bed stability and discharge. The *quantreg* package requires a sample size of at least 1000 to calculate *P* values but can calculate the slope and intercept of regressions with smaller samples sizes. We were not able to determine significance for the different relationships but report the slope and intercept results to show the general trends. Streambed movement (%) was arcsine-square-root transformed for quantile regression analyses.

Additionally, we applied for each stream individually a partial least squares regression (PLS) analysis to explore how daily average of PAR, turbidity, K600, bed stability and discharge predict daily DO entropy during the 2017 snow-free period (glacier-fed stream: n = 277 days; krenal stream:  n =  251 days; nival stream: n = 124 days). PLS identifies the relationship between independent (X) and dependent (Y) data matrices through a linear, multivariate model and produces latent variables (PLS components) representing the combination of X variables that best describe the distribution of observations in "Y space" (Eriksson et al. 2006). We determined the goodness of fit (R$^2$Y) and the predictive ability (Q$^2$Y) of the model by comparing modelled and actual Y observations through a cross validation process. We identified the importance of each X variable by using variable importance on the projection (VIP) scores, calculated as the

sum of square of the PLS weights across all components. VIP values > 1 indicate variables that are most important to the overall model (Eriksson et al. 2006). The PLS was fitted using the *plsr* function from the R package *pls* (Mevik et al. 2019). We dealt with temporal autocorrelation of the data by detrending and differencing the time series of both dependent and independent variables using the R package *forecast* (Hyndman et al. 2019). Data pre-processing for PLS analysis also included the arcsine of the square root of % of streambed movement and the data standardization of all variables. All statistical analyses were conducted in *R* (version 3.6.1, R Development Core Team, 2019) except entropy calculations that were conducted using MATLAB (The Mathworks Inc., Natik, Massachussets).

## 3.4    Results

### 3.4.1   Physical template of alpine streams

The annual dynamics of the physical template potentially relevant to ecosystem metabolism differed markedly among our three study streams (Figure 3.2). The hydrological regime of the glacier-fed stream was characterized by distinct snowmelt in spring and glacial melt in summer with a median discharge of 0.28 $m^3$/s during the study period. Obviously, the groundwater-fed and the nival streams had slightly differing hydrological regimes different from the glacier-fed stream and with lower median discharge (0.01 $m^3$/s and 0.08 $m^3$/s, respectively). Snowmelt discharge in the krenal stream differed between years, an observation consistent with the greater snow pack during the 2017/2018 winter across western Alps (Stoffel and Corona 2018).

Streamwater turbidity was often high in the glacier-fed stream during summer (values of 1712 and 2500 NTU in July 2017 and 2018, respectively) and related to discharge ($R^2$=0.54; $P$<0.001). Turbidity was generally low in the krenal (median: 1.5 NTU) and nival (median: 1.2 NTU) streams and occasionally peaked with increases in discharge; however, on an annual basis, turbidity and discharge were not significantly related in these streams (krenal: $R^2$=0.01; $P$<0.01; nival: $R^2$=0.02; $P$<0.01). Both water depth and turbidity affected PAR attenuation within the streamwater. In the glacier-fed stream, daily mean of radiation (median: 44 µmol $m^{-2}$ $s^{-1}$) reaching the stream bottom was as low as 0.18 µmol $m^{-2}$ $s^{-1}$ and 0.27 µmol $m^{-2}$ $s^{-1}$ in August 2017 and 2018, respectively. Owing to reduced turbidity and shallower streamwater, daily mean of radiation near the stream bottom was generally higher in the krenal (median: 204 µmol $m^{-2}$ $s^{-1}$) and nival (median: 400 µmol $m^{-2}$ $s^{-1}$) streams during the two snow-free periods.

On an annual basis, streambed movement was generally higher in the glacier-fed stream (median: 0.2 %; range: 0.12 – 8.9 %) than in the krenal (median: 0 %; range: 0 – 1.3 %) and nival (median: 0 %; range: 0 – 4.3 %) streams. Not unexpectedly, elevated streambed movement was clearly related to increased runoff from snowmelt and ice melt. The relationship between relative streambed movement and discharge was described by a simple power-law model, of which the coefficient (*b*) varied among streams. The coefficient was lowest (0.61; 95% CI: 0.60, 0.62) in the glacier-fed stream despite its high streambed movement; it was 0.86 (95% CI: 0.83, 0.89) in the krenal and 1.52 (95% CI: 1.48, 1.56) in the nival stream.

Owing to the highly turbulent character of the glacier-fed stream, we found very high gas exchange rates in this stream (median: 841 $d^{-1}$), with potential maxima as high as 6,273 $d^{-1}$. Over the year, median gas exchange rates were lower in the krenal (median: 133 $d^{-1}$) and nival (median: 363 $d^{-1}$) streams and, as expected, clearly driven by changes in discharge.

### 3.4.2 Dynamics and entropy of dissolved oxygen saturation

The continuous monitoring of streamwater dissolved oxygen revealed distinct temporal trends in oxygen saturation in all three study streams (Figure 3.3). During snow cover, median oxygen saturation was generally low (glacier-fed: 96 %; krenal: 92 %; nival: 95 %) and its diel variation (as the coefficient of variation, CV) is low as well (glacier-fed: 0.7 %; krenal: 1.5 %; nival: 1.3 %). With the onset of the freshet and the following snowmelt peak, streamwater oxygen saturation markedly increased (above 100% saturation) in the glacier-fed and nival streams. During that same period, the diel variations in oxygen saturation increased as well in the glacier-fed (median: 98 %; CV: 2.8 %) and nival (median: 97 %; CV: 3.5 %) streams, particularly in that former. These dynamics differed in the krenal stream. Here streamwater oxygen consistently remained below saturation (median: 94 %) and yet it depicted clear diel swings (CV: 2 %).

Our entropy approach, which essentially describes the departure from the baseline over 24 hours periods, captured the diel variation in oxygen saturation well, and this even on an annual scale (Figure 3.3). Low baseline oxygen saturation combined with reduced diel departures translates into low daily entropy values during snow cover (median for glacier-fed stream: $4.7 \times 10^{-6}$; (log: -12.2), krenal stream: $3.2 \times 10^{-6}$; (log: -12.6), and nival stream: $6.4 \times 10^{-7}$; (log: -14.3)). Daily entropy increased with the freshet and remained elevated throughout spring and early summer in all three streams. The nival stream (median: 0.0002; (log: -8.1)) had highest daily entropy, followed by the krenal (median: $5.5 \times 10^{-5}$; (log: -9.8) and the glacier-fed (median: $1.7 \times 10^{-5}$; (log: -10.9) stream.

### 3.4.3 Potential drivers of the daily oxygen entropy

Quantile regressions allowed us to identify potential drivers of the daily oxygen entropy during the snow-free period and this for both years individually (Figure 3.4). In the glacier-fed stream, daily oxygen entropy positively and consistently related to discharge and related variables (i.e., turbidity, bed movement and gas exchange rate). Despite the heavily skewed distribution of the data (e.g., turbidity, gas exchange rate), these relationships were inverse in both the krenal and nival streams. The relationship between daily oxygen entropy and PAR at the stream bottom differed among streams. It was negative in the glacier-fed stream, positive in the snow-fed stream, and this for both years, while no real trend was detected for the krenal stream. We found it remarkable that the observed trends were generally reproducible between both years, despite smaller sample sizes in 2018.

The PLS model identified turbidity, bed activity, gas exchange rate and discharge as predictors (VIP>1) of daily oxygen entropy in the glacier-fed stream ($R^2Y = 0.20$; $Q^2Y = 0.17$) (Figure 3.5). The regression coefficients show a positive effect of these four variables and a negative but non-significant effect of PAR on daily oxygen entropy. Conversely, PAR explained most of the observed variation in daily oxygen entropy in the two non-glacier fed streams (Figure 3.5)., with elevated daily oxygen entropy primarily positively related to PAR (coef = 0.26; VIP=1.96) in the krenal stream. Furthermore, the PLS model ($R^2Y = 0.26$; $Q^2Y = 0.24$) also revealed bed movement as a control (with a negative effect) on the daily oxygen entropy (coef = -0.11; VIP = 0.83) in the krenal stream. In the nival stream, PAR (coef = 0.30; VIP = 1.97) was positively related to daily oxygen entropy whereas turbidity (coef = -0.14; VIP = 0.9) was inversely related to daily oxygen entropy ($R^2Y = 0.30$; $Q^2Y = 0.24$).

| Stream | Lat./Long. | Altitude (m a.s.l.) | Catchment Area (km²) | Average altitude catchment (m a.s.l.) | Average slope catchment (Degrees) | % Vegetated | % Bare Rocks | %Glaciers and perpetual snow |
|---|---|---|---|---|---|---|---|---|
| Glacier-fed | 45.930; 7.245 | 2148 | 18.1 | 2893 ± 399 | 31.4 ± 15.7 | 25 | 48 | 28 |
| Nival | 45.894; 7.108 | 2027 | 4.0 | 2384 ± 157 | 29.5 ± 11.1 | 61 | 39 | 0 |
| Krenal | 45.928; 7.246 | 2161 | 3.1 | 2548 ± 182 | 26.2 ± 12.6 | 65 | 35 | 0 |

Table 3.1 Summary of catchment characteristics of the three studied streams.
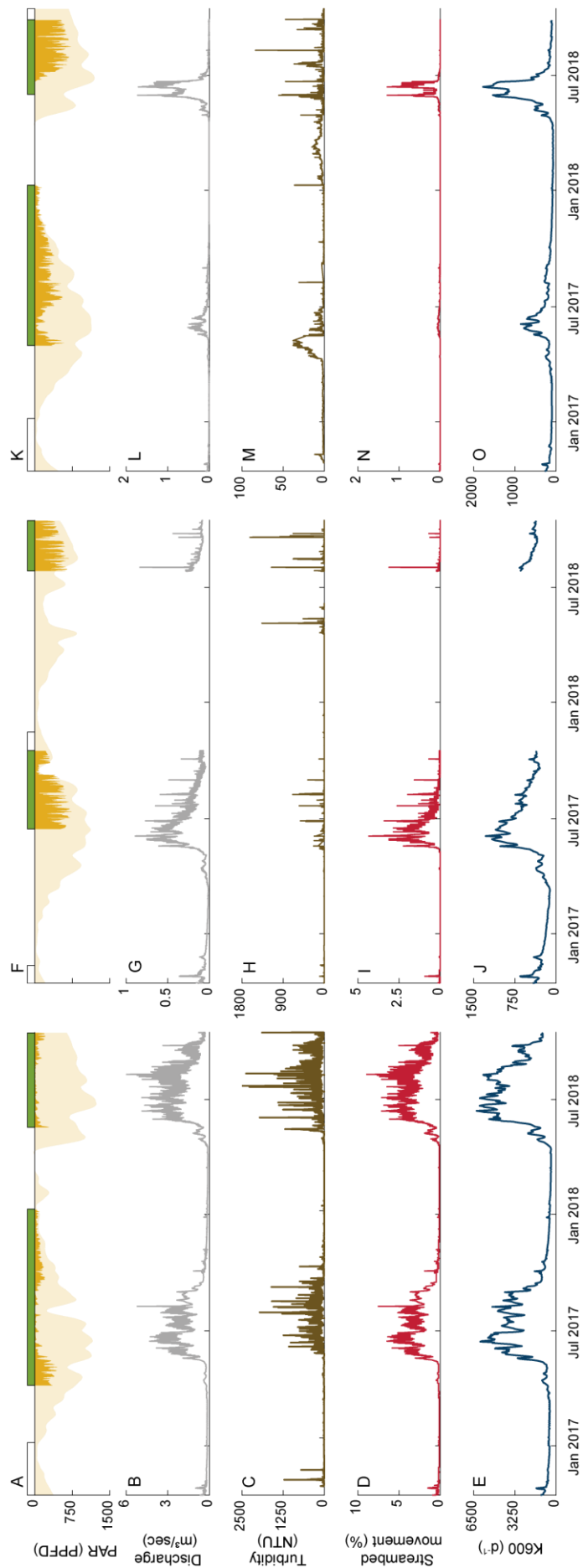
Figure 3.2 Time series of environmental data in A-E: glacier-fed, F-J: nival and K-O: krenal streams. Bars above plots A, F and K represent snow-free periods. Green bars represent periods analysed with quantile regression (2017 and 2018) and PLS analysis (2017). No bars represent snow-covered periods. PAR reaching the stream surface is shown in light yellow. PAR reaching the streambed for the studied periods is shown in dark yellow. Discharge, turbidity and % streambed movement represented at 10 min frequency. PAR and K600 data represented by daily means
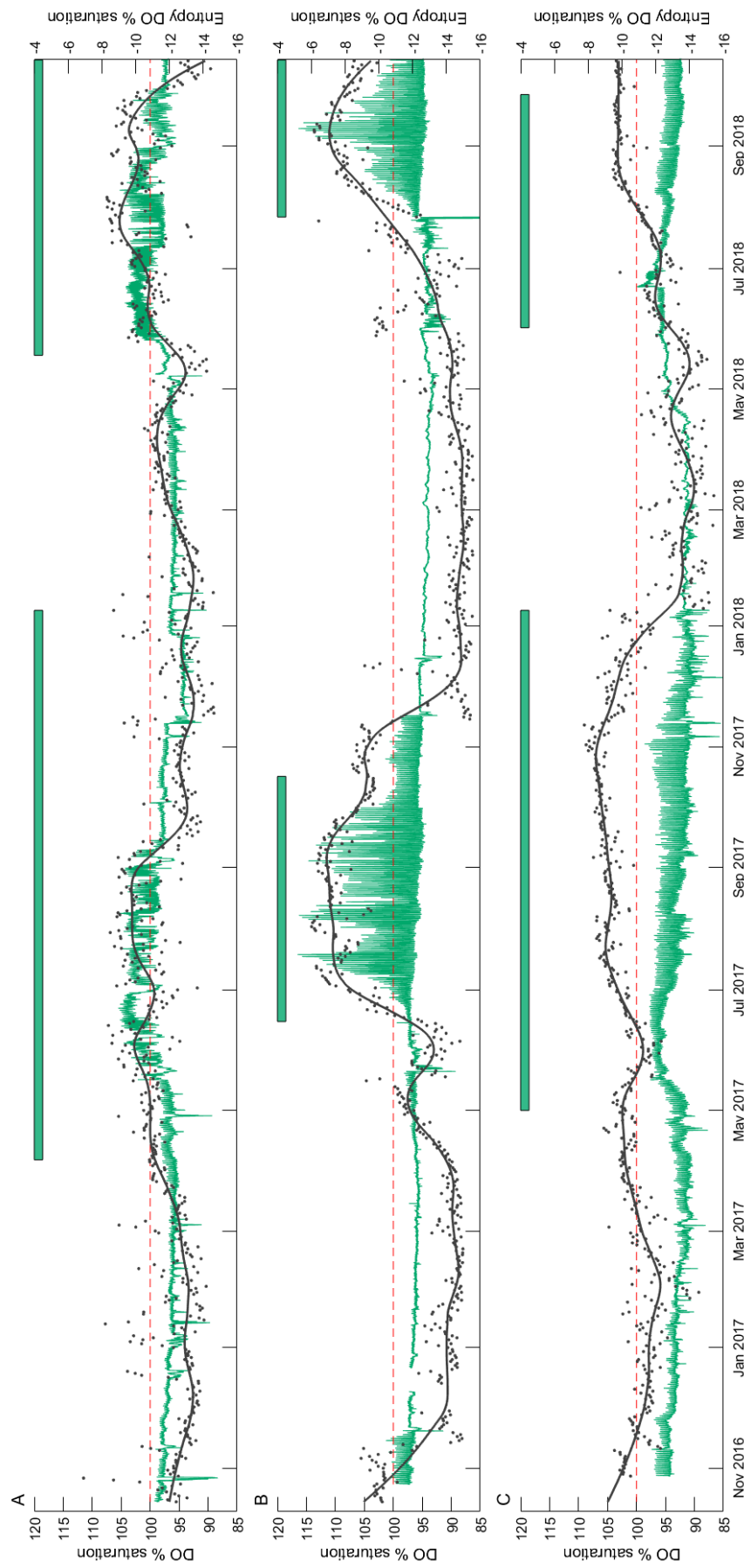
Figure 3.3 Time series of dissolved oxygen (DO) % saturation (dots) and smoothing filter applied on oxygen entropy data (line). A: glacier-fed, B: nival, C: krenal. Oxygen entropy is natural log transformed for representation purposes. Dashed red line shows 100% saturation limit. See caption Figure 3.2 for explanation of the bars above each plot.
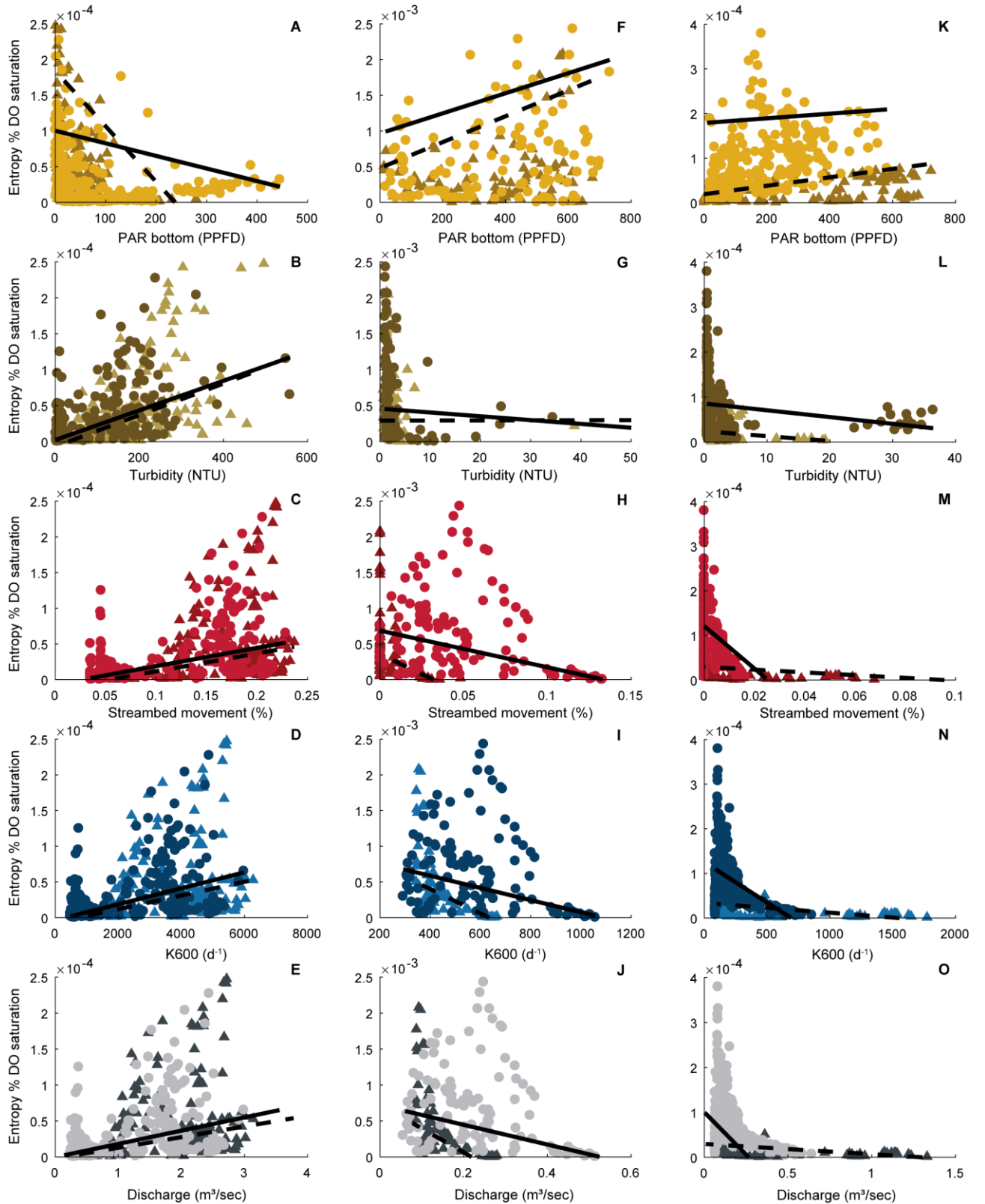
Figure 3.4 Scatter plots with relationship between daily entropy and different variables for both 2017 (circles) and 2018 (triangles). Lines represent 90th percentile regression for 2017 (continuous) and 2018 (dashed). A-E: glacier-fed stream, F-J: nival stream, K-O: krenal stream.
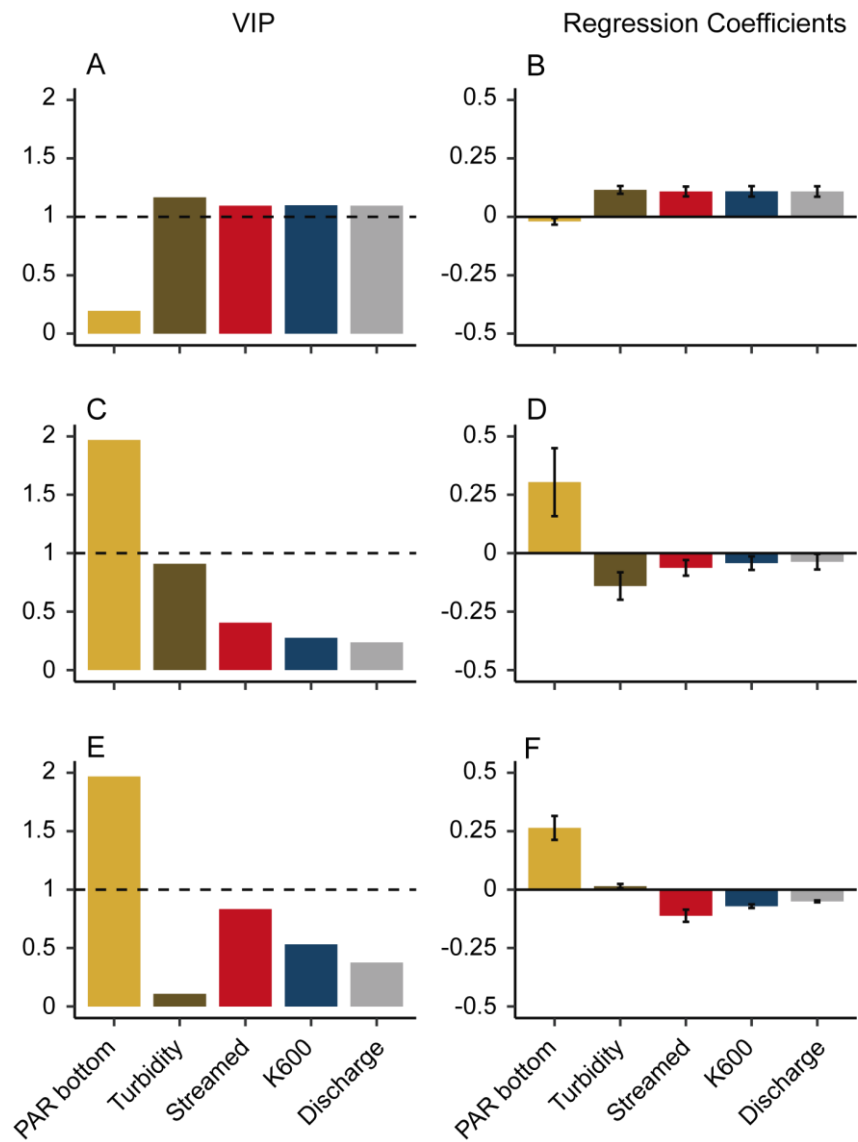
Figure 3.5 Results from PLS analysis. A-B: glacier-fed, C-D: nival, E-F: krenal.

## 3.5 Discussion

The acquisition of high-frequency time series of streamwater DO is increasingly improving our ability to understand stream energetics across temporal scales and biomes (Bernhardt et al. 2018). While climate and associated light and hydrologic regimes are understood as first-order controls on metabolic regimes, the combined effects of these physical controls (and their derivatives) with biological processes on stream metabolism are poorly understood to date. Our findings highlight the differing DO fingerprints and their potential drivers in three typical alpine stream types.

### 3.5.1 Timing and magnitude of streamwater DO

The discharge of alpine streams is typically very low from the end of autumn to the beginning of the freshet in spring, when channels are partially or completely covered by snow, or even frozen (Ward 1994). Consistent with this, our study streams remained snow-covered throughout winter when we registered the lowest DO saturation values. This observation may relate to major infiltration of groundwater, typically low in DO, sustaining baseflow during this period (Riley and Dodds 2013; Horgby et al. 2019). Also, as suggested by the lower daily DO entropy during this period, snow-covered streams seemed to enter a 'dormant period' during which no major biophysical processes deviate oxygen saturation from the groundwater-imposed baseline. Groundwater discharge domination is supported by the high median electrical conductivity of the streamwater during these periods (glacier-fed stream: 289 µS/cm; krenal: 241 µS/cm; nival stream: 599 µS/cm; unpublished data) and comparable to other studies (Brown et al. 2007; Horgby et al. 2019). Streamwater DO started to show different dynamics when stream flow became relieved from dominant groundwater inputs and snowmelt, for instance, started to contribute to the rising discharge during the freshet. The response of DO varied in accordance with the physical template encountered within each stream and determined, for the most part, by the hydrological regime. Elevated discharge as sustained by snow and ice melt increases PAR attenuation and physical disturbance which are both unfavourable for the benthic algae in the glacier-fed stream (Malard et al. 2006; Uehlinger et al. 2010). At the same time, increasing discharge also increases turbulence and hence the gas exchange through the water surface. The onset of snowmelt supplies the stream with oxygen because streamwater starts to equilibrate with atmospheric oxygen. Surface runoff, enriched in oxygen itself, further contributes to the oxygen balance in the streams. This period also constitutes a "window of opportunity" (Battin et al. 2004; Uehlinger et al. 2010) with low turbidity and hence elevated PAR for primary producers which may increase the daily amplitude in oxygen saturation.

### 3.5.2 Potential drivers of DO dynamics

*Glacier-fed stream.* Both quantile regression and PLS analysis revealed physical processes as the dominant control on oxygen dynamics in the glacier-fed stream. Very high discharge during snowmelt and particularly during ice melt in summer markedly influence the stream environment with impacts on DO saturation and its daily entropy. During these periods, the higher discharge, which is likely to increase turbulence, drastically increased the gas exchange rate (up to 6,000 d$^{-1}$). This enhancement in gas exchange likely drives the observed enrichment in streamwater oxygen after winter, as well as the constant daily oscillation of DO saturation values around 100% during high discharge. In fact, we argue that high values of daily oxygen entropy are linked to diurnal changes in discharge owing to the dynamics of snowmelt and glacier melt.

It is now increasingly understood that bubble mediated-gas exchange is typical for high-mountain streams (Ulseth et al. 2019; Hall and Ulseth 2019). High discharge in combination with the macroroughness of mountain streambeds increases turbulence to the point where the water surface continuously breaks and air is advected into the streamwater, dramatically increasing the air-water gas exchange (Zappa et al. 2007).

Flow-induced disturbance through bed scouring or local abrasion of biomass is a major control on the temporal and spatial dynamics of stream primary producers (Biggs et al. 1999). During high flow events, as shear stress exerted on the streambed rises towards the critical shear stress, coarser bed material is progressively mobilized thereby initiating bed scouring and transport (ref). Yet, even if there is not sufficient energy to move bedload, the shear stress applied to the benthic communities may be sufficient to scour biomass (e.g., Bond and Downes 2003; Katz et al. 2018). Our geomorphological analysis of the streambed suggests that both snowmelt and glacier-melt were critical in reworking the streambed in the glacier-fed stream. Streambed stability is influenced by the combination of the flow regimes, sediment size distribution, channel slope and riparian vegetation (Duncan et al. 1999; Schwendel et al. 2010; Peckarsky et al. 2014).

In high-mountain streams, bed roughness is typically higher than in low-gradient streams, with consequences for energy dissipation and the threshold of sediment movement (Schneider et al. 2015). A greater energy demand for sediment movement suggests that streambeds are less frequently mobilized in steep mountain streams than in low-gradient streams (Montgomery and Buffington 1997; Church 2006). For the case of the glacial stream studied here, high rates of sediment supply appear to be sufficient to prevent the development of armour and keeps resistance to entrainment relatively low. Thus, coupled with high discharges during snow and ice melt means high levels of streambed instability (Mao and Lenzi 2017). Extended periods of snow and ice melt significantly contribute to the annual bed load in nival and glacier-fed streams (Dell'Agnese et al. 2015; Schneider et al. 2016, Lane et al. 2017). This high rate of bed perturbation is likely to inhibit the development of benthic life in these streams (Uehlinger et al. 2010; Segura et al. 2011) and hence the GPP typical of more stable streams.

Besides inducing streambed movement, snowmelt and specifically ice melt can also mobilize fine sediments within the glacier forefield and its moraine depositions, which can drastically augment streamwater turbidity at both seasonal and diurnal scales (Clifford et al. 1995; Milner et al. 2017; Lane et al. 2017). High loads of fine suspended solids in the streamwater can constrain GPP via two mechanisms. On the one hand, abrasion by fine particles is a dominant physical mechanism removing periphyton (Hoyle et al. 2017). On the other, light within the streamwater is attenuated by the absorption and scattering by fine particles (Julian et al. 2008). It was shown, for instance, that high turbidity similar to that measured in the glacier-fed stream significantly lowered benthic GPP in the Colorado River, Grand Canyon, (Hall et al. 2015). The negative impacts of discharge and related turbidity on benthic algal biomass and GPP have been well documented in various other glacier-fed streams (Uehlinger et al. 1998; Hieber et al. 2001; Battin et al. 2004; Rott et al. 2006). Several studies have revealed the spring freshet and a short period in fall as "windows of opportunities" for benthic algal biomass and GPP as discharge and turbidity were low, streambed stable, and both temperature and UV radiation moderate during these periods (e.g., Battin et al. 2004, Hieber et al. 2001; Uehlinger et al. 2010).

In this context, we suggest that the increase in oxygen saturation along with higher daily entropy during the onset of snowmelt as channels become snow-free is a consequence of increasing GPP. As the melt season progresses, high levels of streambed movement coupled with reduced PAR availability likely impeded periphyton accrual and GPP. Therefore, we argue that physical drivers of DO dynamics prevailed over biological drivers during that period. However, it is noteworthy that in the event of GPP during that period, high gas exchange rates would have masked its effect on the oxygen dynamics variations (Guasch et al. 1998; Demars et al. 2011). As ice melt recedes in September, a decrease in both oxygen concentration and daily entropy indicates poor recovery of GPP in both consecutive years in the glacier-fed stream. Massive losses of benthic biomass during high flow in summer are often related to significant scouring (e.g., Rott et al. 2006). However, based on oxygen dynamics, we did not detect any major recovery in GPP in fall, which

contrasts from an autumnal window of opportunity observed in other glacier-fed streams (Uehlinger et al. 1998; Battin et al. 2004, Uehlinger et al. 2010). The recovery of benthic algal depends on the intensity of the flow-induced disturbance (Peterson 1994; Segura et al. 2011; Katz et al. 2018). In this sense, recovery of algal biomass and GPP photosynthetic rates following bed movement are influenced by other environmental factors such as temperature or light (Uehlinger and Naegeli 1998; Uehlinger 2000; Cronin et al. 2007; Segura et al. 2011). Our results suggest important biomass losses attributable to the prolonged disturbance throughout the melting seasons and to lack of favourable conditions thereafter.

*Krenal and nival streams.* During the snow-free periods, daily DO entropy followed the temporal variation of PAR at the stream bottom in both krenal and nival streams, and this in both years. Notably in 2017, we identified PAR as a major driver of the daily DO oxygen entropy in both streams, which suggests important contributions from GPP to the observed DO patterns. Due to the low turbidity in these two streams, water depth was likely the main controller of PAR extinction during the first phase of the snow-free period. As summer progresses into fall, baseflow decreased and streamwater became clearer. Thus, the reduction in PAR availability during this period was because of the lower angle of incident light, related mountain shading and reduction of day length. In the krenal stream, highest daily DO entropy was not associated with highest of PAR in 2017 after the snowmelt. Shallow and clear streamwater along with relatively high PAR prevalent in high-altitude regions may have inhibited photosynthesis as shown experimentally in high-Alpine streams (Wellnitz and Ward 2000). By definition, higher daily oxygen entropy reflects either an increase in the magnitude of the daily DO saturation and or a decrease in the magnitude of the daily DO saturation minimum. In this manner, an increase in daily oxygen entropy as summer progresses may be a consequence of the gradual shift towards low-oxygen groundwater dominated streamflow. In parallel, oxygen-consuming processes such as heterotrophic respiration in the stream surface and hyporheic sediments may further reduce the oxygen concentration.

In the nival stream, we did not find any indications of photoinhibition during the highest PAR registered during the snow-free period. In fact, a reduction in PAR late in the season appears to have an immediate negative effect on both oxygen concentration and daily DO entropy. Of the three study streams, the nival stream showed the most immediate response of streambed movement to increasing discharge. However, oxygen production in this stream seemed to respond more negatively to a reduction on PAR due to high-turbid events rather than to streambed disturbance. We suggest that during bedload events, with the absence of major turbidity, primary producers colonizing more stable patches of the streambed can potentially maintain oxygen production. On the contrary, high-turbidity events with or without associated bedload may have an integral effect on the extinction of PAR that affects the entire stream bottom.

### 3.5.3   What makes the energetic regime in Alpine streams unique?

Recent studies have revealed the seasonal patterns of ecosystem energetics across a broad range of streams (Bernhardt et al. 2018; Savoy et al. 2019). Using classifiers related to catchment characteristics and discharge, for instance, Savoy et al. (2019) identified two typologies of energetic regimes: streams with a peak productivity in spring or in summer. Clearly, such classifiers ultimately relate to the drivers of GPP, including light availability, as rooted in the River Continuum Concept (Vannote et al. 1980). Thus, the riparian canopy can reduce PAR reaching small streams draining forested catchments and hence their GPP, whereas water depth and turbidity suppress PAR and GPP further downstream (Vannote et al. 1980). Blaszczak et al. (2019) have recently shown streamwater turbidity as a modulator of GPP in urban streams through the attenuation of light reaching the streambed.

Based on daily DO entropy, our study expands the current list of stream energetics regimes, and sheds light on their drivers, including light and streambed movement (Figure 3.6). In fact, in high-mountain streams

above tree line, snow cover during winter, streamwater depth and turbidity, particularly during snow and ice melt in spring and summer, were major controls on PAR that reaches the bottom of three typical alpine streams. When periods of elevated PAR at the stream bottom were coupled with reduced bed movement, potential windows of opportunities emerged for GPP in spring but less so in fall in the glacier-fed stream. Between these windows, massive bed movement and turbidity depressed GPP such that no clear patterns in DO saturation and daily entropy emerged, except those that we attribute to daily changes in gas exchange rates, themselves modulated by fluctuations in discharge. Apparent ecosystem energetics in the nival stream followed the light regime outside the channel more closely because of low turbidity, and may hence be classified as a summer peak regime (*sensu* Savoy et al. 2019) with a minor peak during the freshet. The energetic regime in the krenal stream was shaped by an early and minor peak of apparent GPP during the freshet when turbidity was low and by an extended period of elevated apparent GPP after snowmelt when both bed movement and turbidity were low.
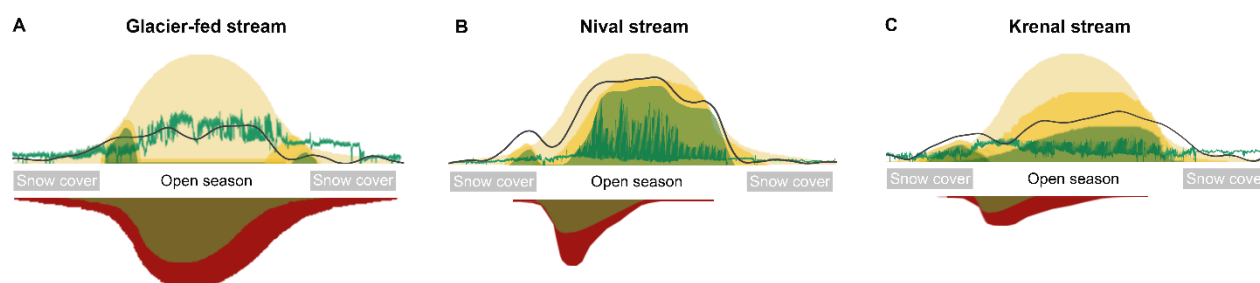


Figure 3.6 Conceptual model of three annual energetic regimes for streams with contrasted physical and hydro-logical regimes typical for high-alpine catchments: a glacier-fed (A), a nival (B) and a krenal stream (C). The meas-ured annual DO regimes (as both percentage of saturation and entropy) are the green and black lines, respec-tively. The annual pattern of potential solar radiation (i.e., radiation reaching the stream surface) is shown in light yellow while the actual incident solar radiation (i.e., radiation reaching the streambed bottom) in dark yel-low. The annual patterns associated to physical disturbances (i.e., streambed movement and turbidity) are shown in red and brown, respectively. In high-alpine streams, the interplay of both light and disturbance regimes drives the timing, magnitude and extent of productivity periods occurring at annual basis (i.e., maximum poten-tial for GPP).

Our findings suggest that in the high mountains, earth processes, such as glacier dynamics and sediment production and discharge modulate stream ecosystem energetics. Climate change is predicted to have major impacts on these modulators, particularly on glacier-fed streams that, as glaciers shrink, will shift towards nival and krenal-type ecosystems (e.g., Hotaling et al. 2017; Milner et al. 2017). Our comparative study suggests that this climate-driven transition in hydrology will also impact the energetics of these streams. We propose that, the favourable conditions (light, streambed stability) will extend towards early spring and late summer in krenal and nival streams due to an earlier and weaker freshet with reduced snowpack. Furthermore, glacier runoff beyond "peak water" (e.g., Huss and Hock 2018) in combination with reduced snowpack will decrease the discharge during spring and summer, but also on a diurnal scale (Lane and Nienow, 2019), and hence both the magnitude and duration of the flow-induced disturbance. A gradual decrease in glacial melt volume and the magnitude of diurnal flow peaks will reduce bed scouring and sediment transport and it remains to be seen whether these reductions are sufficient to reduce levels of turbidity and so increase GPP in the glacier-fed streams. Eventually, however, clear groundwater will come to dominate summer runoff in these streams, thereby enhancing PAR penetration to their bottom. In this event, benthic algal biomass may increase with a knock-on effect on benthic fauna community composition

(e.g., Cauvy-Frauníe et al. 2016) or on bryophytes that may even outcompete benthic algae (Milner et al. 2017). However, groundwater may not be able to sustain streamflow, increasing periods of intermittency (Paillex et al. 2019) with potentially detrimental consequences for primary producers in these streams.

Such shifts in ecosystem energetic regimes will have consequences for the temporal dynamics of carbon and nutrient transformation and retention. It is intuitive to assume that extended periods of GPP in high-mountain streams will reduce the downstream transport of nutrients, particularly phosphate, with yet unknown consequences for the downstream ecosystems.

# 3.6   References

Acuña, V., A. Wolf, U. Uehlinger, and K. Tockner. 2008. Temperature dependence of stream benthic respiration in an Alpine river network under global warming. Freshw. Biol. 53: 2076–2088. doi:10.1111/j.1365-2427.2008.02028.x

Allen, A. P., J. F. Gillooly, and J. H. Brown. 2005. Linking the global carbon cycle to individual metabolism. Funct. Ecol. 19: 202–213. doi:10.1111/j.1365-2435.2005.00952.x

Appling, A. P., J. S. Read, L. A. Winslow, and others. 2018. The metabolic regimes of 356 rivers in the United States. Sci. Data 5: 180292. doi:10.1038/sdata.2018.292

Battin, T. J., K. Besemer, M. M. Bengtsson, A. M. Romani, and A. I. Packmann. 2016. The ecology and biogeochemistry of stream biofilms. Nat. Rev. Microbiol. 14: 251–263. doi:10.1038/nrmicro.2016.15

Battin, T. J., A. Wille, R. Psenner, and A. Richter. 2004. Large-scale environmental controls on microbial biofilms in high-alpine streams. Biogeosciences 1: 159–171. doi:10.5194/bg-1-159-2004

Beniston, M., D. Farinotti, M. Stoffel, and others. 2018. The European mountain cryosphere: a review of its current state, trends, and future challenges. Cryosph. 12: 759–794. doi:10.5194/tc-12-759-2018

Berggren, M., and P. A. del Giorgio. 2015. Distinct patterns of microbial metabolism associated to riverine dissolved organic carbon of different source and quality. J. Geophys. Res. Biogeosciences 120: 989–999. doi:10.1002/2015JG002963

Berghuijs, W. R., R. A. Woods, and M. Hrachowitz. 2014. A precipitation shift from snow towards rain leads to a decrease in streamflow. Nat. Clim. Chang. 4: 583–586. doi:10.1038/NCLIMATE2246

Bernhardt, E. S., J. B. Heffernan, N. B. Grimm, and others. 2018. The metabolic regimes of flowing waters. Limnol. Oceanogr. doi:10.1002/lno.10726

Biggs, B. J. F., R. A. Smith, and M. J. Duncan. 1999. Velocity and Sediment Disturbance of Periphyton in Headwater Streams: Biomass and Metabolism. J. North Am. Benthol. Soc. 18: 222–241. doi:10.2307/1468462

Blaszczak, J. R., J. M. Delesantro, D. L. Urban, M. W. Doyle, and E. S. Bernhardt. 2019. Scoured or suffocated: Urban stream ecosystems oscillate between hydrologic and dissolved oxygen extremes. Limnol. Oceanogr. 64: 877–894. doi:10.1002/lno.11081

Boix Canadell, M., N. Escoffier, A. J. Ulseth, S. N. Lane, and T. J. Battin. 2019. Alpine Glacier Shrinkage Drives Shift in Dissolved Organic Carbon Export From Quasi-Chemostasis to Transport Limitation. Geophys. Res. Lett. 46: 8872–8881. doi:10.1029/2019gl083424

Bond, N. R., and B. J. Downes. 2003. The independent and interactive effects of fine sediment and flow on benthic invertebrate communities characteristic of small upland streams. Freshw. Biol. 48: 455–465. doi:10.1046/j.1365-2427.2003.01016.x

Brown, L. E., D. M. Hannah, and A. M. Milner. 2003. Alpine Stream Habitat Classification: An Alternative Approach Incorporating the Role of Dynamic Water Source Contributions. Arctic, Antarct. Alp. Res. 35: 313–322. doi:10.1657/1523-0430(2003)035[0313:ASHCAA]2.0.CO;2

Brown, L. E., A. M. Milner, and D. M. Hannah. 2007. Groundwater influence on alpine stream ecosystems. Freshw. Biol. 52: 878–890. doi:10.1111/j.1365-2427.2007.01739.x

Carbonneau, P. E., and J. T. Dietrich. 2017. Cost-effective non-metric photogrammetry from consumer-grade sUAS: implications for direct georeferencing of structure from motion photogrammetry. Earth Surf. Process. Landforms 42: 473–486. doi:10.1002/esp.4012

Carbonneau, P. E., S. N. Lane, and N. E. Bergeron. 2004. Catchment-scale mapping of surface grain size in gravel bed rivers using airborne digital imagery. Water Resour. Res. 40: n/a-n/a. doi:10.1029/2003WR002759

Cauvy-Fraunié, S., P. Andino, R. Espinosa, R. Calvez, D. Jacobsen, and O. Dangles. 2016. Ecological responses to experimental glacier-runoff reduction in alpine rivers. Nat. Commun. 7: 1–7. doi:10.1038/ncomms12025

Church, M. 2006. Bed material transport and the morphology of alluvial river channels. Annu. Rev. Earth Planet. Sci. 34: 325–354. doi:10.1146/annurev.earth.33.092203.122721

Clifford, N. J., K. S. Richards, R. A. Brown, and S. N. Lane. 1995. Scales of Variation of Suspended Sediment Concentration and Turbidity in a Glacial Meltwater Stream. Geogr. Ann. Ser. A, Phys. Geogr. 77: 45–65. doi:10.2307/521277

Cronin, G., J. H. McCutchan, J. Pitlick, and W. M. Lewis. 2007. Use of Shields stress to reconstruct and forecast changes in river metabolism. Freshw. Biol. 52: 1587–1601. doi:10.1111/j.1365-2427.2007.01790.x

Dell'Agnese, A., F. Brardinoni, M. Toro, L. Mao, M. Engel, and F. Comiti. 2015. Bedload transport in a formerly glaciated mountain catchment constrained by particle tracking. Earth Surf. Dyn. 3: 527–542.

Demars, B. O. L., and J. R. Manson. 2013. Temperature dependence of stream aeration coefficients and the effect of water turbulence: A critical review. Water Res. 47: 1–15. doi:10.1016/j.watres.2012.09.054

Demars, B. O. L., J. Russell Manson, J. S. Ólafsson, and others. 2011. Temperature and the metabolic balance of streams. Freshw. Biol. 56: 1106–1121. doi:10.1111/j.1365-2427.2010.02554.x

Dietrich, J. T. 2017. Bathymetric Structure-from-Motion: extracting shallow stream bathymetry from multi-view stereo photogrammetry. Earth Surf. Process. Landforms 42: 355–364. doi:10.1002/esp.4060

Dodds, W. K., K. Gido, M. R. Whiles, M. D. Daniels, and B. P. Grudzinski. 2015. The Stream Biome Gradient Concept: factors controlling lotic systems across broad biogeographic scales. Freshw. Sci. 34: 1–19. doi:10.1086/679756

Duncan, M. J., A. M. Suren, and S. L. Brown. 1999. Assessment of Streambed Stability in Steep, Bouldery Streams: Development of a New Analytical Technique. J. North Am. Benthol. Soc. 18: 445–456. doi:10.2307/1468377

Enquist, B. J., E. P. Economo, T. E. Huxman, A. P. Allen, D. D. Ignace, and J. F. Gillooly. 2003. Scaling metabolism from organisms to ecosystems. Nature 423: 639–42. doi:10.1038/nature01671

Eriksson, L., T. Byrne, E. Johansson, J. Trygg, and C. Vikström. 2006. Multi- and Megavariate Data Analysis, Basic Principles and Applications.

Gabbud, C., M. Bakker, M. Clémençon, and S. N. Lane. 2020. Hydropower flushing events cause severe loss of macrozoobenthos in Alpine streams. 2019. Water Resour. Res. doi:10.1029/2019WR024758

Gordon, N. D., T.A. McMahon, B. L. Finlayson, C. J. Gippel, and R. J. Nathan. 2004. Stream hydrology: An introduction for ecologists. Chichester: John Wiley

Guasch, H., J. Armengol, E. Martí, and S. Sabater. 1998. Diurnal variation in dissolved oxygen and carbon dioxide in two low-order streams. Water Res. 32: 1067–1074. doi:10.1016/S0043-1354(97)00330-8

Hall, R. O., and A. J. Ulseth. 2019. Gas exchange in streams and rivers. Wiley Interdiscip. Rev. Water 1–18. doi:10.1002/wat2.1391

Hall, R. O., C. B. Yackulic, T. A. Kennedy, M. D. Yard, E. J. Rosi-Marshall, N. Voichick, and K. E. Behn. 2015. Turbidity, light, temperature, and hydropeaking control primary productivity in the Colorado River, Grand Canyon. Limnol. Oceanogr. 60: 512–526. doi:10.1002/lno.10031

Hieber, M., C. T. Robinson, S. R. Rushforth, and U. Uehlinger. 2001. Algal Communities Associated with Different Alpine Stream Types. Arctic, Antarct. Alp. Res. 33: 447. doi:10.2307/1552555

Horgby, Å., M. Boix Canadell, A. J. Ulseth, T. W. Vennemann, and T. J. Battin. 2019. High-Resolution Spatial Sampling Identifies Groundwater as Driver of $CO_2$ Dynamics in an Alpine Stream Network. J. Geophys. Res. Biogeosciences 2019JG005047. doi:10.1029/2019JG005047

Hotaling, S., D. S. Finn, J. Joseph Giersch, D. W. Weisrock, and D. Jacobsen. 2017. Climate change and alpine stream biology: progress, challenges, and opportunities for the future. Biol. Rev. 92: 2024–2045. doi:10.1111/brv.12319

Hoyle, J. T., C. Kilroy, D. M. Hicks, and L. Brown. 2017. The influence of sediment mobility and channel geomorphology on periphyton abundance. Freshw. Biol. 62: 258–273. doi:10.1111/fwb.12865

Huss, M., and R. Hock. 2018. Global-scale hydrological response to future glacier mass loss. Nat. Clim. Chang. 8: 135–140. doi:s41558-017-0049-x

Hyndman, R., G. Athanasopoulos, C. Bergmeir, G. Caceres, L. Chhay, M. O'Hara-Wild, F. Petropoulos, S. Razbash, E. Wang, and F. Yasmeen. 2019. forecast: Forecasting functions for time series and linear models. R package version 8.9. http://pkg.robjhyndman.com/forecast

IPCC, 2019: Summary for Policymakers. In: IPCC Special Report on the Ocean and Cryosphere in a Changing Climate [H.-O. Pörtner, D.C. Roberts, V. Masson-Delmotte, P. Zhai, M. Tignor, E. Poloczanska, K. Mintenbeck, M. Nicolai, A. Okem, J. Petzold, B. Rama, N. Weyer (eds.)]. In press.

Julian, J. P., M. W. Doyle, S. M. Powers, E. H. Stanley, and J. A. Riggsbee. 2008. Optical water quality in rivers. Water Resour. Res. 44. doi:10.1029/2007WR006457

Katz, S. B., C. Segura, and D. R. Warren. 2018. The influence of channel bed disturbance on benthic Chlorophyll a: A high resolution perspective. Geomorphology 305: 141–153. doi:10.1016/j.geomorph.2017.11.010

Koenker, R. 2019. quantreg: Quantile Regression. R package version 5.51. https://CRAN.R-project.org/package=quantreg

Lane, S. N., M. Bakker, C. Gabbud, N. Micheletti, and J.-N. Saugy. 2017. Sediment export, transient landscape response and catchment-scale connectivity following rapid climate warming and Alpine glacier recession. Geomorphology 277: 210–227. doi:10.1016/j.geomorph.2016.02.015

Lane, S. N., and P. W. Nienow. 2019. Decadal-Scale Climate Forcing of Alpine Glacial Hydrological Systems. Water Resour. Res. 55: 2478–2492. doi:10.1029/2018WR024206

Malard, F., U. Uehlinger, R. Zah, and K. Tockner. 2006. FLOOD-PULSE AND RIVERSCAPE DYNAMICS IN A BRAIDED GLACIAL RIVER. Ecology 87: 704–716. doi:10.1890/04-0889

Mao, L., and M. A. Lenzi. 2007. Sediment mobility and bedload transport conditions in an alpine stream. Hydrol. Process. 21: 1882–1891. doi:10.1002/hyp.6372

Mevik, B. H., R. Wehrens, and K. H. Liland. 2019. pls: Partial Least Squares and Principal Component Regression. R package version 2.7-1. https://CRAN.R-project.org/package=pls

Milner, A. M., K. Khamis, T. J. Battin, and others. 2017. Glacier shrinkage driving global changes in downstream systems. Proc. Natl. Acad. Sci. 201619807. doi:10.1073/pnas.1619807114

Montgomery, D. R., and J. M. Buffington. 1997. Channel-reach morphology in mountain drainage basins. Geol. Soc. Am. Bull. 109: 596–611. doi:10.1130/0016-7606(1997)109<0596:CRMIMD>2.3.CO;2

Moog, D. B., and G. H. Jirka. 1999. Air-Water Gas Transfer in Uniform Channel Flow. J. Hydraul. Eng. 125: 3–10. doi:10.1061/(ASCE)0733-9429(1999)125:1(3)

Mulholland, P. J., C. S. Fellows, J. L. Tank, and others. 2001. Inter-biome comparison of factors controlling stream metabolism. Freshw. Biol. 46: 1503–1517. doi:10.1046/j.1365-2427.2001.00773.x

Naegeli, M. W., and U. Uehlinger. 1997. Contribution of the Hyporheic Zone to Ecosystem Metabolism in a Prealpine Gravel-Bed-River. J. North Am. Benthol. Soc. 16: 794–804. doi:10.2307/1468172

Paillex, A., A. R. Siebers, C. Ebi, J. Mesman, and C. T. Robinson. 2019. High stream intermittency in an alpine fluvial network: Val Roseg, Switzerland. Limnol. Oceanogr. lno.11324. doi:10.1002/lno.11324

Peckarsky, B. L., A. R. McIntosh, S. C. Horn, K. McHugh, D. J. Booker, A. C. Wilcox, W. Brown, and M. Alvarez. 2014. Characterizing disturbance regimes of mountain streams. Freshw. Sci. 33: 716–730. doi:10.1086/677215

Peterson, C. G., A. C. Weibel, N. B. Grimm, and S. G. Fisher. 1994. Mechanisms of benthic algal recovery following spates: comparison of simulated and natural events. Oecologia 98: 280–290. doi:10.1007/BF00324216

Rasmussen, J. J., A. Baattrup-Pedersen, T. Riis, and N. Friberg. 2011. Stream ecosystem properties and processes along a temperature gradient. Aquat. Ecol. 45: 231–242. doi:10.1007/s10452-010-9349-1

Raymond, P. A., C. J. Zappa, D. Butman, and others. 2012. Scaling the gas transfer velocity and hydraulic geometry in streams and small rivers. Limnol. Oceanogr. Fluids Environ. 2: 41–53. doi:10.1215/21573689-1597669

Riley, A. J., and W. K. Dodds. 2013. Whole-stream metabolism: strategies for measuring and modeling diel trends of dissolved oxygen. Freshw. Sci. 32: 56–69. doi:10.1899/12-058.1

Roberts, B. J., P. J. Mulholland, and W. R. Hill. 2007. Multiple Scales of Temporal Variability in Ecosystem Metabolism Rates: Results from 2 Years of Continuous Monitoring in a Forested Headwater Stream. Ecosystems 10: 588–606. doi:10.1007/s10021-007-9059-2

Robinson, C. T., U. Uehlinger, F. Guidon, P. Schenkel, and R. Skvarc. 2002. Limitation and retention of nutrients in alpine streams of Switzerland. SIL Proceedings, 1922-2010 28: 263–272. doi:10.1080/03680770.2001.11902585

Rode, M., A. J. Wade, M. J. Cohen, and others. 2016. Sensors in the Stream: The High-Frequency Wave of the Present. Environ. Sci. Technol. 50: 10297–10307. doi:10.1021/acs.est.6b02155

Rosa, J., V. Ferreira, C. Canhoto, and M. A. S. Graça. 2013. Combined effects of water temperature and nutrients concentration on periphyton respiration - implications of global change. Int. Rev. Hydrobiol. 98: 14–23. doi:10.1002/iroh.201201510

Rott, E., M. Cantonati, L. Füreder, and P. Pfister. 2006. Benthic Algae in High Altitude Streams of the Alps -- a Neglected Component of the Aquatic Biota. Hydrobiologia 562: 195–216. doi:10.1007/s10750-005-1811-z

Savoy, P., A. P. Appling, J. B. Heffernan, E. G. Stets, J. S. Read, J. W. Harvey, and E. S. Bernhardt. 2019. Metabolic rhythms in flowing waters: An approach for classifying river productivity regimes. Limnol. Oceanogr. 1–17. doi:10.1002/lno.11154

Schneider, J. M., D. Rickenmann, J. M. Turowski, K. Bunte, and J. W. Kirchner. 2015. Applicability of bed load transport models for mixed-size sediments in steep streams considering macro-roughness. Water Resour. Res. 51: 5260–5283. doi:10.1002/2014WR016417

Schneider, J. M., D. Rickenmann, J. M. Turowski, B. Schmid, and J. W. Kirchner. 2016. Bed load transport in a very steep mountain stream (Riedbach, Switzerland): Measurement and prediction. Water Resour. Res. 52: 9522–9541. doi:10.1002/2016WR019308

Schwendel, A. C., R. G. Death, and I. C. Fuller. 2010. The assessment of shear stress and bed stability in stream ecology. Freshw. Biol. 55: 261–281. doi:10.1111/j.1365-2427.2009.02293.x

Segura, C., J. H. McCutchan, W. M. Lewis, and J. Pitlick. 2011. The influence of channel bed disturbance on algal biomass in a Colorado mountain stream. Ecohydrology 4: 411–421. doi:10.1002/eco.142

Stoffel, M., and C. Corona. 2018. Future winters glimpsed in the Alps. Nat. Geosci. 11: 458–460. doi:10.1038/s41561-018-0177-6

Tamburrino, A., and J. S. Gulliver. 2002. Free-surface turbulence and mass transfer in a channel flow. AIChE J. 48: 2732–2743. doi:10.1002/aic.690481204

Thimijan, R., and R. Heins. 1983. Photometric, radiometric, and quantum light units of measure: a review of procedures for interconversion. Hortic Sci 18: 818–822.

Uehlinger, U. 2000. Resistance and resilience of ecosystem metabolism in a flood-prone river system. Freshw. Biol. 45: 319–332. doi:10.1046/j.1365-2427.2000.00620.x

Uehlinger, U., M. Naegeli, and S. G. Fisher. 2002. A heterotrophic desert stream? The role of sediment stability. West. North Am. Nat. 62: 466–473.

Uehlinger, U., and M. W. Naegeli. 1998. Ecosystem Metabolism, Disturbance, and Stability in a Prealpine Gravel Bed River. J. North Am. Benthol. Soc. 17: 165–178. doi:10.2307/1467960

Uehlinger, U., C. T. Robinson, M. Hieber, and R. Zah. 2010. The physico-chemical habitat template for periphyton in alpine glacial streams under a changing climate. Hydrobiologia 657: 107–121. doi:10.1007/s10750-009-9963-x

Uehlinger, U., R. Zah, and H. Bürgi. 1998. The Val Roseg project: Temporal and spatial patterns of benthic algae in an Alpine stream ecosystem influenced by glacier runoff. IAHS-AISH Publ. 248: 419–424.

Ulseth, A. J., R. O. Hall, M. Boix Canadell, H. L. Madinger, A. Niayifar, and T. J. Battin. 2019. Distinct air–water gas exchange regimes in low- and high-energy streams. Nat. Geosci. 12: 259–263. doi:10.1038/s41561-019-0324-8

Vannote, R. L., G. W. Minshall, K. W. Cummins, J. R. Sedell, and C. E. Cushing. 1980. The River Continuum Concept. Can. J. Fish. Aquat. Sci. 37: 130–137. doi:10.1139/f80-017

Vetsch D., A. Siviglia, F. Caponi, D. Ehrbar, E. Gerke, S. Kammerer, A. Koch, S. Peter, D. Vanzo, L. Vonwiller, M. Facchini, M. Gerber, C. Volz, D. Farshi, R. Mueller, P. Rousselot, R. Veprek, and R. Faeh. 2018. System Manuals of BASEMENT, Version 2.8. Laboratory of Hydraulics, Glaciology and Hydrology (VAW). ETH Zurich

Ward, J. V. 1994. Ecology of alpine streams. Freshw. Biol. 32: 277–294. doi:10.1111/j.1365-2427.1994.tb01126.x

Wellnitz, T. A., and J. V. Ward. 2000. Herbivory and irradiance shape periphytic architecture in a Swiss alpine stream. Limnol. Oceanogr. 45: 64–75. doi:10.4319/lo.2000.45.1.0064

Zappa, C. J., W. R. McGillis, P. A. Raymond, J. B. Edson, E. J. Hintsa, H. J. Zemmelink, J. W. H. Dacey, and D. T. Ho. 2007. Environmental turbulent mixing controls on air-water gas exchange in marine and aquatic systems. Geophys. Res. Lett. 34: L10601. doi:10.1029/2006GL028790

# Chapter 4   Regimes of primary production and their drivers in Alpine streams

Authors of this manuscrip are the following: Marta Boix Canadell, Lluís Gómez-Gener, Amber J. Ulseth, Mélanie Clémençon, Stuart N. Lane, Tom J. Battin.

M. B. C was involved in the fieldwork, conceived the study, analysed data and results and wrote the manuscript.

## 4.1    Abstract

Primary production is a fundamental ecosystem process that determines nutrient and carbon cycling, and trophic structure in streams. The magnitude and timing of gross primary production (GPP) are typically controlled by hydrology, light and grazers. GPP and its drivers in high-mountain streams remain elusive at present. We estimated GPP in streams typical for high-mountain catchments, namely a glacier-fed, groundwater-fed (krenal) and a snowmelt-fed (nival) stream. Using high-resolution sensor data over two years in combination with numerical simulations of stream hydraulics, we studied the periods of GPP characteristic for these streams, as well as their major drivers. Favourable windows for GPP were constrained to periods at the onset of the snowmelt and its recession, when photosynthetic active radiation (PAR) at the streambed and streambed stability facilitated GPP. During these widows of opportunity, GPP ranged from 0.004 g $O_2$ $m^{-2}$ $d^{-1}$ and 19.4 g $O_2$ $m^{-2}$ $d^{-1}$ across the three streams. GPP was controlled by the interplay of PAR at the stream bottom and the areal fraction of the streambed that moves owing to flow-induced shear. Our results highlight the capacity of primary producers to exploit the discrete and relatively predictable windows of opportunities in high-mountain streams. We propose that climate-driven change in snow and glacier melt reduction may ameliorate stream environmental conditions, thereby enhancing the potential autochthonous organic matter supply within the catchment.

## 4.2    Introduction

At ecosystem level, the transformation of dissolved inorganic carbon into organic matter by photosynthesis is estimated as ecosystem gross primary production (GPP). GPP represents a foundation for ecosystem ecology as it describes a major pathway for energy fixation (Odum 1956). In stream ecosystems, the carbon production by benthic primary producers can have a substantial impact on the food web, due to the preferential selection by aquatic consumers of the high-quality organic matter derived from them (e.g., Minshall 1978; Marcarelli et al. 2011). Such an autochthonous energy source is particularly important in streams draining high-mountain catchments above the treeline, where terrestrial supply of organic matter is typically low because of poorly developed soils and vegetation (e.g., Zah and Uehlinger 2001). In fact, it is well established that autotrophs are a primary food source for consumers across various alpine stream types (e.g., Zah et al. 2001; Füreder et al. 2003). Besides being consumed and respired, autotrophic biomass

can become transiently accumulated and stored within the ecosystem, or ultimately exported by the river flow or lost by non-biological oxidation (Lovett et al. 2006). Furthermore, at the ecosystem level, GPP regulates the uptake of nutrients and their downstream transport (Hall and Tank 2003; Lupon et al. 2016) but also has a part in other biogeochemical processes such as $CO_2$ exchange with the atmosphere (e.g., Hotchkiss et al. 2015; Rocher-Ros et al. 2019).

Primary production in high-mountain streams is generally associated with the benthic sediments, and is driven by diatoms, cyanobacteria, chrysophytes, green and red algae (Hieber et al. 2001; Fell et al. 2018; Niedrist et al. 2018), but also by lichens and mosses (Rott et al. 2006). The photosynthetic active radiation (PAR) available to primary producers at the streambed depends on season, water depth, suspended particles that influence turbidity, and on shading effects (e.g., catchment topography or the presence of ice or snow). Benthic life is particularly vulnerable to flow-induced movement and scouring of the streambed, as well as the abrasive impact of suspended particles and shear stress (e.g., Miller et al. 2009; Segura et al. 2011; Cullis et al. 2014; Hoyle et al. 2017). Therefore, along with PAR availability, the physical disturbance of the streambed has been recognized as major controls on GPP in stream ecosystems (e.g., Biggs et al. 1999; Uehlinger et al. 2002; Blaszczak et al. 2019). Recently, it was proposed that the description of sediment stability (Hoyle et al. 2017), driven by local shear stress and its interaction with the streambed structure (e.g., Gabbud et al. 2020), rather than simple flow metrics (e.g., discharge, flow velocity) should be considered to understand and predict benthic life in streams. This description is needed because of spatial (and temporal) variability in such interactions (Fuller et al. 2011). This recommendation is certainly important for better understanding the GPP regime in high-mountain streams, characterized by steep slopes, high bed movement and sometimes increased turbidity owing to their erosive forces. At the same time, the benthic communities in these streams have developed various adaptive traits to withstand the physical stress they are exposed (e.g., Biggs et al. 1999; Rott et al. 2006) and we still know relatively little on the precise conditions that lead to their scour.

Overall, our knowledge on the temporal dynamics of stream GPP and its controls has been greatly improved by the availability of affordable environmental sensors (e.g., Uehlinger 2006; Val et al. 2016; Arroita et al. 2018). Time series of daily GPP allow us both to reveal seasonal patterns of stream energetics (Bernhardt et al. 2018) and to classify streams into distinct regimes reflecting ecosystem phenology and the dynamics of key drivers (Bernhardt et al. 2018; Savoy et al. 2019). Due to the close connectivity between streams and their catchments, the terrestrial environment plays an important role in determining those GPP regimes (Bernot et al. 2010; Fuß et al. 2017). For instance, the presence of a deciduous canopy, whose relative importance varies with stream position in the catchment (Vannote et al. 1980), reduces light availability and thus constraining GPP (Hill et al. 2001; Roberts et al. 2007). Additionally, nutrient supply from urban and agricultural sources has the capacity to alter the magnitude of GPP (Griffiths et al. 2013; Arroita et al. 2018). Finally, floods caused by human management can reduce GPP due to an increase in streambed disturbance (Uehlinger et al. 2003). Unlike for lower altitude catchments, the seasonal riparian canopy is absent in undisturbed high-mountain streams, nutrients supply is limited, streamflow is dominated by an extended period of snowmelt and additional glacier-melt in case of glacierized catchments (Ward 1994) and glacial erosion leads to high turbidity during periods driven by ice melt. Therefore, we might expect that the major factors controlling GPP in high-mountain streams are more related to the hydrological and geomorphic nature of these landscapes including past and current glacial activity.

Snow-dominated and glacierized catchments are particularly vulnerable to global warming (Barnett et al. 2005; Beniston et al. 2018). Future scenarios suggest that increases in temperature are likely; to increase the probability that spring precipitation falls as rain and snow; to reduce snow accumulation at the end of the winter; and to drive an earlier onset of spring snowmelt (Hodgkins and Dudlley 2006; Stewart 2009;

Berghuijs et al. 2014). In basins where there is a glacier, temperature rise then has a double effect: ice begins to melt sooner because of a reduced snow cover, a more efficient process because ice has a lower albedo; and rising temperature leads to higher melt and higher runoff. Thus, in glaciated basins, and even if temperature is continuing to rise, runoff has been observed to be increasing under climate change (e.g. Lane et al. 2017) and daily hydrographs suggest ice melt that is more intense, starting earlier in the summer and lasting for longer into the autumn (Lane and Nienow 2019). This glacial subsidy (Collins 2008) lasts until a glacier shrinks sufficiently that it can no longer sustain summer flows and runoff declines and becomes dependent on the previous winter's snowfall rather than temperature. The point at which this occurs is commonly known as peak water (Huss and Hock 2018). These changes are thought likely to also impact the physicochemical characteristics of streams draining glacierized catchments (e.g., Milner et al. 2009; Milner et al. 2017). Despite unprecedented environmental change, the impact of changing hydrological regimes and associated controls on GPP in high-mountain streams remains elusive at present (Milner et al. 2017). Understanding the response of stream GPP is critical to evaluate the impact of global warming on autochthonous carbon fluxes and in high-mountain stream ecosystems.

In this study, we investigated temporal patterns and controls on GPP in a glacier-fed, groundwater-fed (krenal) and snowmelt-fed (nival) stream in the Swiss Alps. Recording relevant environmental parameters every 10 minutes over 21 months, we were able to estimate daily GPP for some periods of time in these streams. Using numerical simulations, we provide continuous estimates of sediment movement, as a proxy for streambed stability, in each stream. We hypothesized that PAR availability and streambed stability determined by the hydrological regime will shape productivity regimes characteristic for each stream. Our study represents a first attempt to describe productivity regimes in high-mountain streams and will provide insights into the implications of climate-driven hydrological changes for GPP in high-mountain streams.

## 4.3 Methods

### 4.3.1 Study sites

We conducted the study in three different Alpine streams chosen to reflect three different sources of water: glacier-fed stream (28 % glacier coverage), one snowmelt-fed stream (nival) and one groundwater-fed stream (krenal) (Table 4.1). All three streams drain high alpine catchments situated above the tree line (2384 ± 157 m a.s.l. to 2893 ± 399 m a.s.l.) where vegetation is dominated by sparsely vegetated areas with low productive grassland and shrubs. The channel-bed slopes are steep (6.5 ± 1.1 %) characteristic of streams that drain mountain terrains. The streambed in the study reach of the nival and glacier-fed streams is primarily composed of coarse gravel and cobbles. Streambed-sediment in the krenal stream was composed of finer sediments and had a dense mat of aquatic bryophytes covering stone surfaces.

In all three cases, the streams are completely or partially snow-covered in winter, such that they have long baseflow periods in winter, commonly dominated by groundwater sources. Spring discharge is dominated by melting snow in the non-glacierized catchments and the combination of both snow and ice-melt in the glacierized catchment; runoff peaking in spring and summer respectively. All three streams are also affected by summer storm events.

### 4.3.2 In situ long time series collection

At each of these streams, we deployed sensors to monitor streamwater dissolved $O_2$ (DO) concentration (mg/L) and temperature (ºC; miniDOT, Precision Measurement Engineering, Vista, California, USA), turbidity (NTU; Cyclops-7 Turbidity, Turner Designs) and water depth (mm; Odyssey Capacitance Logger, Dataflow Systems Ltd). At each stream we also monitored atmospheric pressure (mbar; Track-It™ Monarch

Instrument) and photosynthetic active radiation (PAR in Lux; Onset HOBO® Pendant) along the stream banks (1 m above ground). In order to measure the solar radiation that reaches the streambed, we installed additional PAR sensors at the streambed.

All parameters were continuously recorded at 10 min interval from 1 February 2017 to 15 October 2018. We visited each stream approximately monthly through the study period for sensor maintenance, data downloading, sampling for water chemistry analysis and collected rocks from the streambed to quantify benthic chlorophyll *a*. During the visit, we also measured in situ streamwater temperature and DO concentration with daily calibrated WTW multiparameter probes (Xylem Inc., USA). During winter, sampling was less frequent because snow restricted safe access to the streams.

Discharge ($m^3$/s) was estimated using slug-injections of sodium chloride as a conservative tracer (Gordon et al. 2004). Subsequently, rating curves between streamwater depth and discharge were established for each site using a power-law model by fitting a linear regression to natural log transformed data (glacier-fed stream: $R^2$=0.95; n=7; *P*<0.001; groundwater-fed stream: $R^2$=0.85; n=10; *P*<0.001; nival stream: $R^2$=0.93; n=8; *P*<0.001). Data gaps from sensor malfunctioning were extrapolated using discharge data from neighbouring gauging stations within the catchment (Boix Canadell et al. 2019). When data interpolation was not possible, variables derived from discharge are also therefore missing.

## 4.3.3   Water chemistry

Streamwater samples were analysed for soluble reactive phosphate (SRP), ammonium ($NH_4$), nitrate ($NO_3$) and dissolved organic carbon (DOC). SRP samples (~40 mL; n=2) and $NH_4$ samples (~20 mL; n=3) were collected using a 50 mL polyethylene syringe and filtered through precombusted GF/F glass fiber filters. Samples were stored on ice and analysed within 24 hours. SRP concentrations were measured using the ascorbic acid method (Murphy and Riley 1962) and $NH_4$ concentrations were measured using the orthophthalaldehyde fluorometric method (Holmes et al. 1999), as modified by Taylor et al. (2007). $NO_3$ concentration were measured on streamwater filtered with a 0.22-µm mixed cellulose ester membrane filter and using ion chromatography (ICS-3000 Dionex, USA). For DOC analysis, streamwater samples were filtered (precombusted GF/F filters, Whatman) into acid-washed, precombusted glass vials and analyzed using a Sievers M5310c TOC Analyzer (GE Analytical Instruments) (accuracy: ±2%, precision: <1%, detection limit: 22 µg C/L).

## 4.3.4   Benthic chlorophyll *a*

For each of the three streams, we collected samples for benthic chlorophyll *a* as a proxy for algal biomass. During site visits, we randomly collected 5 rocks along a 25-m section upstream of where the sensors were deployed. Collected rocks were transported to the laboratory and then kept frozen and analysed within one month. Biomass was removed from each stone with a wire brush and rinsed into a bucket. A volume known of the suspension was filtered through GF/F glass filters. Filters were subsequently transferred to individual centrifuge tubes filled with 5 mL ethanol (90% v/v), boiled at 76ºC for 10 min, and stored in the dark for 24h at 4ºC until analysed. Chlorophyll *a* was estimated by fluorometry (Arar and Collins 1997). Area values of chlorophyll *a* ($mg/m^2$) were calculated as described in Uehlinger (1991).

## 4.3.5   Modelling streambed movement

Time series of streambed movement used in this Chapter derive from Chapter 3. Therefore, methodology for this section is previously described in section 3.3.7 Modelling streambed stability.

## 4.3.6  Identification of snow-covered periods

A 10 cm layer of compacted snow covering the stream can reduce incident PAR by 96-98% (Jacobsen and Dangles 2017) and GPP can be strongly suppressed even if it is only covered by ice (Beaulieu et al. 2013). For this reason, for each stream we identified the snow-free periods for both years by combining satellite images with field observations and by inspecting time series of DO. Snow-free periods lasted 428 days across the study (2017: 6 April – 9 January; 2018: 18 May – 15 October) for the glacier-fed stream, 389 days (2017: 1 May – 9 January; 2018: 1 June – 15 October) for the krenal stream and 245 days (2017: 15 June – 15 November; 2018: 15 July – 15 October) for the nival stream.

## 4.3.7  Gross primary production (GPP) estimations

We used changes in streamwater DO concentration to estimate daily gross primary production (GPP) (g $O_2$ $m^{-2}$ $d^{-1}$) based on the single-station open-channel approach (Odum 1956), which relies on the fact that GPP, but also ecosystem respiration (ER) and physical air-water gas exchange are the dominant controls on the intra-daily dynamics of DO concentrations. We modelled time series of DO measured at 10-min frequency in each stream for the snow-free periods delimited using the following equation (Van de Bogert et al. 2007) in a mass-balance based approach:

$$\frac{dO_{i,d}}{dt} = \left(\frac{GPP_d}{\overline{z_{i,d}}} \times \frac{PPFD_{i,d}}{\overline{PPFD_d}}\right) + \left(\frac{ER_d}{\overline{z_{i,d}}}\right) + f_{i,d}(K600_d)(Osat_{i,d} - O_{i,d})$$

Equation 4.1

where $O_{i,d}$ is the modelled oxygen concentration on day d at time index i, and $dO_{i,d}/dt$ is a rate of concentration change. $GPP_d$ (GPP) and $ER_d$ (ER) are daily gross primary productivity and ecosystem respiration respectively (g $O_2$ $m^{-2}$ $d^{-1}$), while $K600_d$ (K600) is the daily gas exchange rate ($d^{-1}$) scaled to a Schmidt number of 600. The other variables are mean stream depth ($\overline{z_{i,d}}$, m) averaged over the width and length of the upstream reach; photosynthetic photon flux density ($PPFD_{i,d}$, µmol photons $m^{-2}$ $s^{-1}$); $\overline{PPFD_d}$ is the sum of observed $PPFD_{i,d}$ throughout the day; $f_{i,d}(K600_d)$ is a function that converts daily K600 to a stream temperature-specific gas exchange rate for DO (K $O_2$i,d, $d^{-1}$), and $Osat_{i,d}$ is the theoretical saturation concentration of $O_2$ if the water and air were in equilibrium.

For each stream, we estimated K600 from argon tracer gas injections (Ulseth et al. 2019). Argon releases were conducted throughout the year in order to capture the variability of the gas exchange rate during different flow conditions (i.e. baseflow, snow and glacier melt). To estimate K600 for every day of the entire study, we used stream specific log-log least-squared linear regressions between K600 and discharge data estimated in the field. Discharge (Q, $m^3/s$) and velocity (v, m/s) were calculated from sodium chloride slug releases during the day of the gas injection. We measured stream widths (n = 10) of the upstream reach and estimated mean stream depth assuming hydraulic continuity, that is, $\overline{z_{i,d}}$ = Q/wv. Further details on the estimation of K600, hydraulic and hydraulic geometry variables are provided in Ulseth et al. (2019).

In Equation 4.1, we used PAR reaching the streambed as $PPFD$. To do so, for the periods where we had measurements of water depth data, turbidity and PAR both at the stream surface and at the streambed, we calculated the coefficient of extinction of PAR ($K_d$, $m^{-1}$) using the following light attenuation function:

$$I_z = I_o exp^{-K_d \times z}$$

Equation 4.2

where $I_z$ is the PAR reaching the streambed, $I_o$ is the PAR reaching the stream surface and $z$ is the water depth (m) at the sensor location. In this case, we used the water depth data recorded from the water depth sensor which was deployed next to the PAR sensor. Next, we related $K_d$ to the corresponding value of the streamwater turbidity in order to obtain a $K_d$ for each time step as a function of turbidity. Finally, we applied the light attenuation function with the turbidity-specific $K_d$ to obtain the PAR reaching the benthic zone as a function of streamwater depth for each time step. We converted measured lux (lumens/m$^2$) to photosynthetic photon flux density (µmol m$^{-2}$ s$^{-1}$) for the 400-700 nm band dividing lux by a constant value of 54 given by Thimijan and Heins (1983).

Based on Equation 4.1, we estimated daily GPP for each stream using the *streamMetabolizer* package in the R software (Appling et al. 2018a). The streamMetabolizer package may implement several model variants. In this study we used the inverse modelling by maximum likelihood estimation (MLE) variant with the specific applied named 'm_np_oi_tr_plrckm.nlm'. Model specifications included a proportional (i.e. linear) response of GPP to light. Briefly, GPP was estimated with this variant by fitting Equation 4.1 relative to the measured DO data by choosing the parameters that minimized the normal negative log likelihood. The uncertainty on daily GPP estimates is reported as standard deviation. Despite the model also provides estimates on ER, this metabolic parameter was not the objective of this study, hence we do not show it here. Furthermore, extremely large values of ER as well as a significant relationship between ER and K600 (Figure SI 4.1) suggest that ER estimates are likely to be a model-artefact (i.e., model equifinality; Appling et al. 2018b) due to reaeration interference.

We further filtered the modelled estimates of GPP through the following criteria: (a) we excluded any physically impossible results (i.e., negative value of GPP), (b) we excluded estimates of GPP for periods when the stream was snow-covered, and (c) we excluded values of GPP for periods when K600 was beyond our field estimates of K600 (Figure SI 4.2). This specially affected the glacier-fed stream for nearly the entire melting season due to the extremely high gas-exchange rates associated with intense turbulence during this time. Additionally, analysis between oxygen dynamics and K600 in the glacier-fed stream (Chapter 3 of this thesis) indicated that daily oxygen concentrations were driven by gas exchange during the melting season in this stream, which along with high gas-exchange rates, likely would have resulted in large uncertainties in GPP estimates (McCutchan et al. 1998). Further missing values were due to data gaps from maintenance or malfunctioning of sensors. In total, we were able to estimate GPP for 145, 266 and 198 days for the glacier-fed, krenal and nival streams, respectively. Taking this into account, we argue that the GPP values presented in this study are highly representative of the productivity regimes across the three stream types.

## 4.3.8   Data analysis

For each stream, we examined the relationship between PAR at the streambed and GPP during the 2017 period conducting quantile regressions with the *quantreg* package in R (Koenker 2019). We additionally assessed the potential influence of daily mean of PAR at the streambed on modelled GPP during 2017 using generalized least squares (GLS). We estimated coefficients of the GLS model using the *gls* function from *nlme* package (Pinheiro et al. 2019). We included a temporal correlation structure defined by the residuals (autoregressive process of order 1, or AR(1)). Data pre-processing for GLS analysis included the standardization of all variables. We also visually explored the relationship between GPP and streambed movement for the period of 2017. For this, we used scatter plots with the percentage values of the

streambed movement arcsine square root transformed and using the measurement day and daily mean of PAR reaching the streambed as marker identifier. In glacier-fed and krenal streams we used the data collected after September 2017 and June 2017 respectively. All statistical analyses were conducted in R (version 3.6.1, R Development Core Team, 2019).

## 4.4    Results

### 4.4.1   Physical drivers : streambed movement and light availability

The dynamics of streambed movement largely followed the dynamics of discharge, particularly of snow and ice melt (Figure 4.1). In the glacier-fed stream, elevated discharge owing to snowmelt and ice melt lead to the highest values of streambed movement computed for all three streams for the entirety of the study period (Figure 4.1 ; average ± standard deviation: 1.4 ± 1.6 %; maximum values of 8.2% and 8.9% in 2017 and 2018, respectively). In the krenal and nival stream, increased streambed movement was related to the spring snowmelt. Because of its partially armoured streambed, the krenal stream exhibited the lowest values of streambed movement (0.02 ± 0.1 %). In this stream, owing to a greater snow pack in winter 2017/2018 (Stoffel and Corona 2018), streambed movement was more pronounced during the 2018 snowmelt (maximum of 1.2 %). In the nival stream, streambed movement averaged 0.2 ± 0.5 % and peaked during the 2017 snowmelt with 4.3 %; the 2018 values are missing because of sensor loss.

Discharge dynamics also influenced turbidity, which ultimately drove the PAR regimes of the thee streams (Figure 4.1). In the glacier-fed stream, high discharge and related turbidity (Table 4.1) attenuated on average 85 ± 16 % of the PAR reaching the stream surface. PAR at the streambed was typically lower than 2000 µmol m$^{-2}$ s$^{-1}$ during the study period. In contrast, PAR was attenuated by 54 ± 25 % in the krenal and by 36 ± 8 % in the nival stream. Overall, PAR at the streambed was higher in both the krenal (241 ± 471 µmol m$^{-2}$ s$^{-1}$) and nival (370 ± 0.5 µmol m$^{-2}$ s$^{-1}$) streams than in the glacier-fed stream (73 ± 187 µmol m$^{-2}$ s$^{-1}$). Extended snow cover in 2018 delayed the initial exposure of the streambed to PAR to late spring or early summer in all three streams.

| Stream | Lat. Long. | Altitude Site (m.a.s.l.) | Catchment Area (km$^2$) | % Vegetated | % Bare Rocks | % Glaciers and per-petual snow | Discharge (m$^3$/s) | Turbidity (NTU) |
|---|---|---|---|---|---|---|---|---|
| Glacier-fed | 45.930, 7.245 | 2148 | 18.1 | 25 | 48 | 28 | 0.9 ± 1.04 (0.1 – 6.3) | 86.7 ± 134.2 (0.2 – 2540) |
| Krenal | 45.928, 7.246 | 2161 | 3.1 | 65 | 35 | 0 | 0.07 ± 0.2 (0.004 – 1.7) | 3.6 ± 5.9 (0.2 – 83.6) |
| Nival | 45.894, 7.108 | 2027 | 4.0 | 61 | 39 | 0 | 0.2 ± 0.14 (0.01 – 0.9) | 8.8 ± 57.2 (0 – 1625) |

Table 4.1 Location and general catchment characteristics of the study streams. Shown are average values ± standard deviation. Minimums and maximums are given in parentheses. Discharge and turbidity values are subtracted from time series of 10-min frequency data. Minimums and maximums are given in parentheses.

## 4.4.2 Nutrients, DOC and benthic chlorophyll *a*

Streamwater nutrient ($NO_3$, $NH_4$ and SRP) and DOC concentrations were low in all three streams (Table 4.2). However, the concentrations of $NO_3$ (800 µg/L), $NH_4$ (31.1 µg/L) and SRP (54.15 µg P/L) were highest in the glacier-fed stream. In contrast, highest DOC concentrations (560 µg C/L) were found in the krenal stream. Throughout the study, the average benthic chlorophyll *a* ranged from 0.2 mg/m² in the glacier-fed, which also showed the lowest variability, and nival streams to 0.9 mg/m² in the krenal stream (Table 4.2). Maximum values of chlorophyll *a* in the glacier-fed stream were found in June 2017 (0.4 mg/m²) and in May 2018 (0.5 mg/m²). Maximum values in the krenal stream (1.2 mg/m² and 1.5 mg/m²) were found in August 2017 and September 2018 respectively. Maximum values of chlorophyll *a* were found both in July 2017 and 2018 (0.5 mg/m² and 0.7 mg/m² respectively).

| Stream | $NO_3$ (µg/ L) | $NH_4$ (µg/L) | SRP (µg/L) | DOC (µg/L) | Chl-*a* (mg/m²) | GPP (g $O_2$ m$^{-2}$ d$^{-1}$) |
|---|---|---|---|---|---|---|
| Glacier-fed | 615 ± 203.6 (n=6) | 18.1 ± 9.6 (n=7) | 14.5 ± 20.8 (n=6) | 207.9 ± 126.7 (n=8) | 0.2 ± 0.1 (n=7) | 1.52 ± 1.62 (0.01 – 6.25) |
| Krenal | 354 ± 220 (n=5) | 1.8 ± 0.7 (n=6) | 12.1 ± 12.6 (n=5) | 333.1 ± 217.9 (n=6) | 0.9 ± 0.5 (n=7) | 0.64 ± 0.59 (0.004 – 2.61) |
| Nival | 290 ± 84.5 (n=4) | 1.9 ± 0.5 (n=5 ) | 6.9 ± 4.8 (n=4 ) | 129.8 ± 26.3 (n=4 ) | 0.2 ± 0.3 (n=7) | 3.72 ± 3.4 (0.11 – 19.4) |

Table 4.2 Summary as mean ± standard deviation of major nutrients, chlorophyll *a* and gross primary production (GPP) of the three streams during the study period. Minimums and maximums are given in parentheses.

## 4.4.3 Patterns and drivers of stream GPP

During the periods when we were able to reliably compute GPP (see the methods section), GPP varied within and across the three streams (Figure 4.1). Overall, average GPP was higher in the nival stream, followed by the glacier-fed and the krenal streams (Table 4.2). Interannual patterns in GPP across the streams were evident, particularly in the glacier-fed and krenal streams, where the snow cover greatly reduced or annulled the pre-snowmelt peak productivity periods. Specifically, in the glacier-fed stream, in 2017, GPP reached maximum values (6.2 g $O_2$ m$^{-2}$ d$^{-1}$) before the 2017 snowmelt peak and decreased to ~ 2.0 g $O_2$ m$^{-2}$ d$^{-1}$ after the snowmelt and ice melt. During that same year in the krenal stream, GPP was similar before (2.6 g $O_2$ m$^{-2}$ d$^{-1}$) and after (2.6 g $O_2$ m$^{-2}$ d$^{-1}$) snowmelt (around June) and gradually decreased until snowfall covered the channel. The 2017 snow cover prevented measureable GPP until late spring in the nival stream. However, after the snowmelt peak, GPP rapidly reached 19.4 g $O_2$ m$^{-2}$ d$^{-1}$ in July and gradually decreased as summer and autumn progressed.

We compared daily GPP between 2017 and 2018 for those periods where data were available for both years. In the nival stream, during the period from 27 July to 14 October, GPP was lower (Wilcoxon test: p=0.005) in 2018 (2.18 ± 1.02 g $O_2$ m$^{-2}$ d$^{-1}$) than 2017 (3.33 ± 2.29 g $O_2$ m$^{-2}$ d$^{-1}$), whereas average daily PAR (Wilcoxon test: p=0.002) was higher during that same period in 2018 (386 ± 178 µmol m$^{-2}$ s$^{-1}$) than in 2017 (291 ± 193 µmol m$^{-2}$ s$^{-1}$). In the krenal stream, GPP was lower (Wilcoxon test: *P*<0.001) in 2018 (from 8 July

to 27 September) (0.14 ± 0.12 g $O_2$ m$^{-2}$ d$^{-1}$) than for the same period in 2017 (1.14 ± 0.47 g $O_2$ m$^{-2}$ d$^{-1}$), whereas average daily PAR was higher (Wilcoxon test: $P$<0.001) in 2018 (480 ± 151 µmol m$^{-2}$ s$^{-1}$) than in 2017 (290 ± 123 µmol m$^{-2}$ s$^{-1}$).

To explore these relationships between GPP and PAR at the streambed, we limited our analyses to the 2017 data as these are more complete. As expected, quantile regressions revealed positive relationships between GPP and PAR in all study streams (Figure 4.2). Owing to the varying dispersion of GPP with increasing PAR, the strength of the relationship (i.e., the slope of the regression line) consistently decreased from the 90th to 10th quantiles in all three streams. Furthermore, generalized least squares (GLS) analyses showed that the effect of PAR at the streambed on GPP was statistically significant ($P$<0.001) in all the three streams (Figure 4.2). GLS further revealed that the responsiveness of GPP to PAR was highest in the nival stream (coefficient: 0.422; 0.314 – 0.529 95% CI) compared to the glacier-fed (coefficient: 0.327; 0.217 – 0.436 95% CI) and krenal streams (coefficient: 0.313; 0.238 – 0.387 95% CI). When carefully checking the time series of daily GPP and PAR, we found that inverse dynamics occasionally emerged between GPP and PAR (Figure 4.3). This was particularly noticeable in the nival stream, where during short periods (from 29 September 2018 to 15 October 2018) daily GPP was highest with low PAR and minimal when PAR peaked (Figure 4.3, panel b). Similar patterns were found in the krenal stream (Figure 4.3, panel a), although less marked compared with the nival stream.

Streambed movement ranged from 0.12 to 1 %, from 0 to 0.013 % and from 0 to 1.6 % in the glacier-fed, krenal and nival stream, respectively, during the 2017 periods for which we have reliable GPP estimates (Figure 4.4). During these periods, bed movement declined as snowmelt receded in the krenal and nival streams, and as the influence of ice melt decreased in the glacier-fed stream. Along these trajectories, GPP was initially low in the nival stream when bed movement was still elevated (1.6 %) but peaked at intermediate levels (0.4 %) of streambed movement (Figure 4.4, panel e). Strikingly, after this peak GPP decreased with decreasing streambed movement towards late autumn, a pattern that mirrored that for PAR at the streambed (Figure 4.4, panel f). Streambed movement in the krenal stream was remarkably low compared to the other streams and yet it seemed to affect GPP (Figure 4.4, panel c). Elevated bed movement during snowmelt recession was loosely related to higher GPP when PAR was still relatively high (293 ± 127 µmol m$^{-2}$ s$^{-1}$). During baseflow in autumn when bed movement was zero, GPP was largely controlled by PAR (least-squared linear regression: y = 0.003x + 0.04; $R^2$=0.72; $P$<0.001). Elevated streambed movement inhibited GPP during late ice melt in the glacier-fed stream (Figure 4.4, panel a) — a constrain that became slightly relieved as bed movement receded and as long as PAR was high enough. When streambed movement was lowest (<0.2%), GPP was not related to PAR ($R^2$=4.68 x 10-6, $P$>0.05).
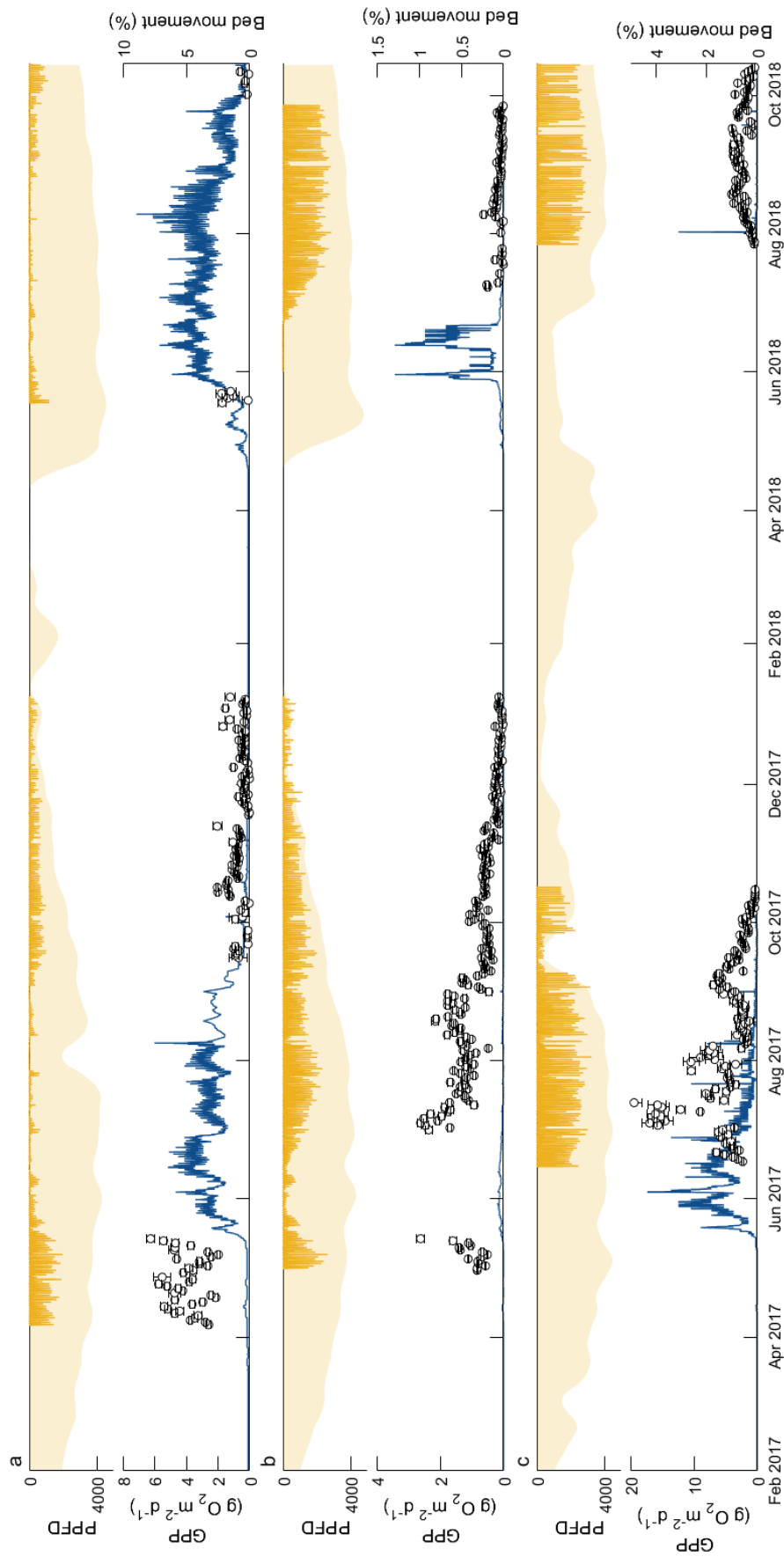
Figure 4.1 Time series of photosynthetically active radiation (PAR in PPFD; µmol m⁻² s⁻¹) reaching both the stream surface (light yellow) and the streambed (dark yellow), streambed movement percentage (blue) and daily gross primary production (GPP) in the glacier-fed (a), krenal (b) and nival (c) streams. Error bars of GPP values represent uncertainty on GPP estimation reported as standard deviations. PAR reaching the streambed only shown for periods where stream was not snow covered and with no missing data.
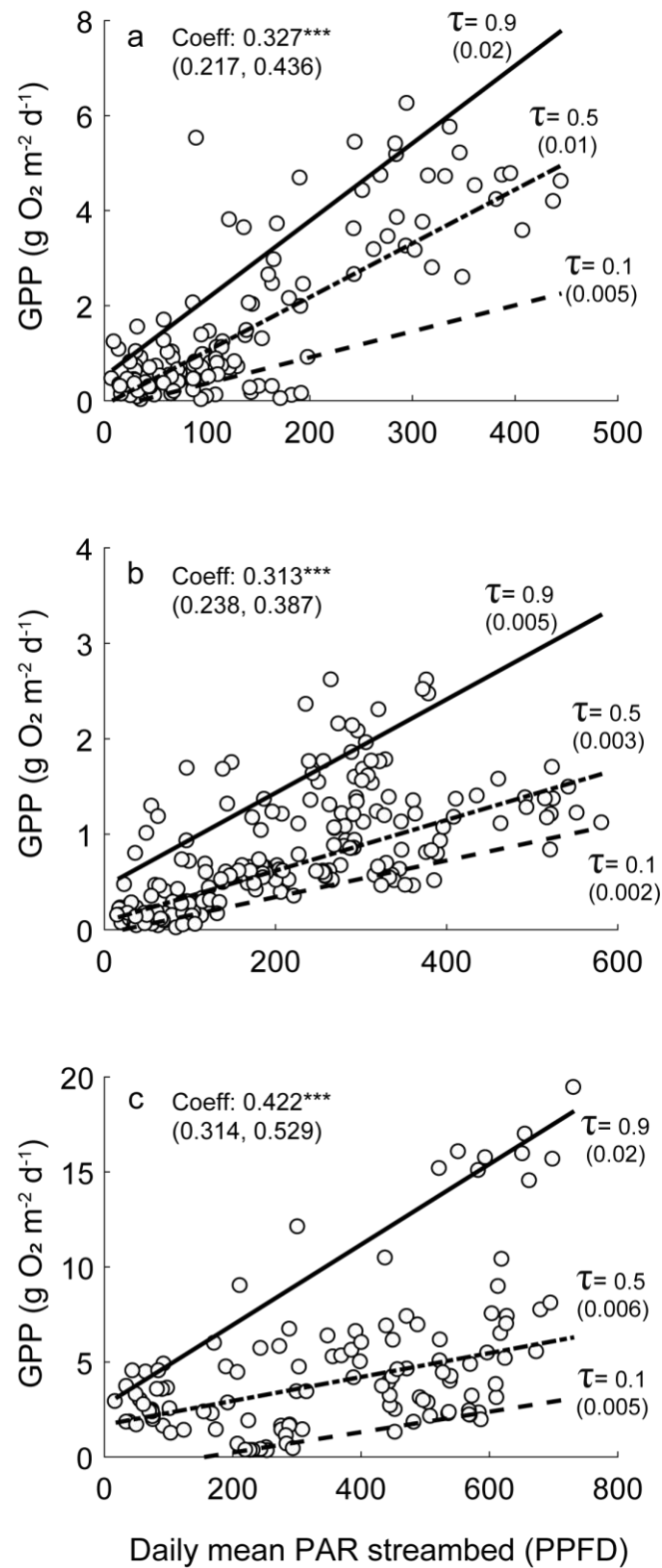
Figure 4.2 Relationship between daily gross primary production (GPP) and photosynthetically active radiation (PAR in PPFD; μmol m$^{-2}$ s$^{-1}$) reaching the streambed for 2017 in the glacier-fed (a), krenal (b) and nival (c) streams. The upper, middle and lower lines in each plot correspond to the 90th, 50th and 10th quantile regression of the data distribution respectively (slope of the regression is given in brackets). The standardized effect of PAR at the streambed on GPP obtained from GLS analysis is given for each site with the approximated 95% confidence intervals in brackets. Note: *** $P<0.001$.
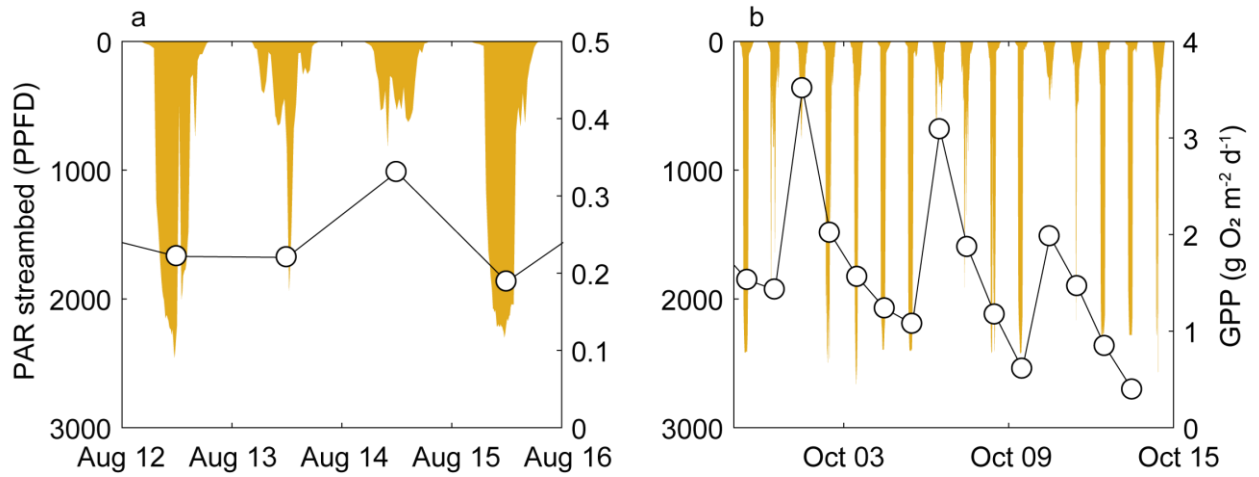
Figure 4.3 Daily gross primary production (GPP; open circles) and photosynthetically active radiation (PAR in PPFD; μmol m$^{-2}$ s$^{-1}$; dark yellow) dynamics during a window of four and fifteen days of 2018 in the krenal (a) and nival (b) streams respectively.
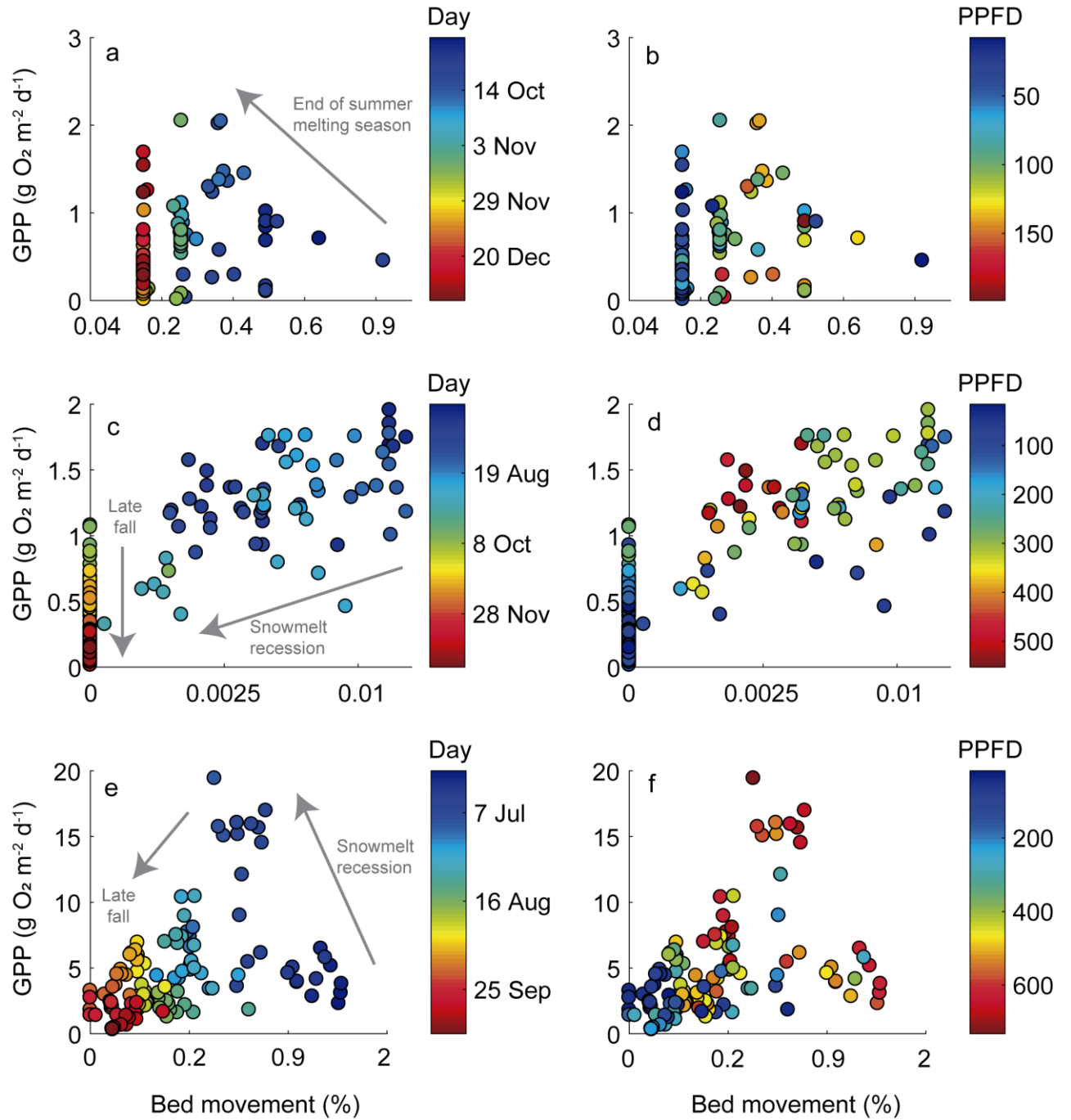
Figure 4.4 Scatter plots of gross primary production (GPP) and % of bed movement for a 2017 period in glacier-fed (a,b), krenal (c,d) and nival (e,f) streams. Symbols are coloured by day of the measurement (left panels) or by the value of photosynthetically active radiation (daily average of PAR in PPFD; µmol m$^{-2}$ s$^{-1}$) reaching the streambed during the specific day (right panels).

## 4.5    Discussion

### 4.5.1    Controls on GPP dynamics in Alpine streams

Our results indicate that PAR availability at the streambed is the dominant control on daily GPP at the three studied streams. These results support the well-established role of light in regulating GPP across streams of different size and draining catchments with varying land use (e.g., Mulholland et al. 2001). As embedded in the River Continuum Concept, variations in PAR supply and hence in GPP are modulated by the relative importance of riparian canopy shading from headwaters to large rivers (Vannote et al. 1980). In small forested streams, GPP seasonality is greatly influenced by the phenology of terrestrial vegetation (i.e., deciduous riparian forest) through rapid transitions in the light regime during the sequences of leaf out and litterfall periods (e.g., Acuña et al. 2004; Roberts et al. 2007; Bernhardt et al. 2018). In contrast, a reduction in light availability due to high levels of turbidity strongly covaries with primary production in larger rivers (Izagirre et al. 2008; Hall et al. 2015). For high-mountain streams above the tree line, snow cover during winter and sediment derived turbidity, particularly during ice melt in summer, shape different seasonal light regimes, thus obscuring these predicted longitudinal patterns observed elsewhere. In this study, we show that for the periods with reliable GPP estimates, PAR availability at the streambed was mostly determined by the hydrological and turbidity regimes, and a combination of day length and shift in solar angle, possibly accentuated by the steep-sided stream valleys where these streams are situated.

Benthic algae in high-mountain streams receive more PAR and UV radiation than in streams at lower altitudes (Jacobsen and Dangles 2017). Thus, despite strategies and adaptive mechanisms for alpine benthic algae to deal with high irradiance (Rott et al. 2006), it may still have an inhibitory effect on primary production (Aigner et al. 2018). High irradiance (> 2000 µmol m$^{-2}$ s$^{-1}$) had a negative effect on periphyton in a high-altitude stream (Wellnitz and Ward 2000), whereas light saturation appeared already around 200-500 µmol m$^{-2}$ s$^{-1}$ in streams at lower altitudes (Young and Huryn 1996; Mulholland et al. 2001). In accordance with Wellnitz and Ward (2000), higher PAR in 2018 (maxima above 2000 µmol m$^{-2}$ s$^{-1}$) likely impacted GPP in the krenal and particularly in the nival stream in this study. This effect became evident when a reduction in PAR intensities had an instantaneous positive effect in GPP (Figure 4.3).

Flow-related physical disturbance on the streambed is a major factor controlling in-stream primary production (Biggs et al. 1999). The principal mechanisms for high flows to impact benthic communities is via shear stress, abrasion and scouring from suspended particles, and burial and removal of benthic producers from substrate movement (Biggs et al. 2001). Besides increasing abrasion capacity, the mobilization of suspended particles during high flow events also results in a decrease in water clarity (Davies-Colley et al. 1992). In this study we found that by the end of the snowmelt season, the increase in GPP in the nival and glacier-fed stream was associated with a reduction in streambed disturbance. These results may suggest the existence of a stability threshold from where physical disturbance dominates over PAR availability on regulating GPP in these two streams. In the glacier-fed stream, the threshold of 1% of streambed movement (occurring at 0.7 m$^3$/s) was exceeded for the most part of the snow and glacier melting seasons (Figure 4.1), which along with high levels of turbidity, suggests primary production was highly suppressed during these periods. Uehlinger and Naegeli (1998) showed that stochastic streambed movement episodes consistently depressed GPP estimated throughout two years in a gravel-bed river. The effects of high streambed-moving events on GPP were also assessed by Uehlinger (2000) during 18 months in a pre-alpine Swiss river. This study showed that temporal patters of GPP reflected the occurrence of streambed movement events and that GPP could be reduced on average up to 53% compared to more stable periods. In the way, Cronin et al. (2007) also identified a discharge threshold at which GPP was suppressed to negligible values.

The effect of streamwater nutrient concentrations on daily GPP has yet not been determined fully. Studies have shown differing degrees and kinds of association between nutrients and GPP (Mulholland et al. 2001; Acuña et al. 2004; Roberts et al. 2007; Bernot et al. 2010). High-mountain streams tend to be nutrient-limited (Rott et al. 2006), but have strong temporal variation in $NO_3$, $NH_4$ and SRP concentrations, with alternating maxima in early spring and autumn (e.g., Füreder et al. 2001; Robinson et al. 2002; Tockner et al. 2002). Given our low sampling frequency, we could not capture such seasonal dynamics. However, annual median concentrations were in the same range as values previously reported for alpine streams (e.g., Robinson et al. 2002). When comparing streams, higher SRP concentrations in glacier-fed stream support a contribution of glacial melt to the phosphate pool (Füreder et al. 2001). Also, in catchments with the presence of a seasonal snowpack, snowmelt delivers $NO_3$ to the streams (Pellerin et al. 2012). Sources of $NO_3$ flushed during snowmelt include nitrification in surficial soils or atmospheric deposition during winter (Sebestyen et al. 2008). Thus, the delivery of $NO_3$ along with favourable PAR conditions may have facilitated GPP during the onset of snowmelt in the glacier-fed and krenal stream. Similarly, in the nival stream, the possible delivery of $NO_3$ extending throughout the snowmelt in combination with streambed stability and favourable light conditions may have enhanced GPP in the first half of July 2017. The sustained supply of nutrients in advanced stages of the snowmelt might also be responsible of the increased GPP in the krenal stream in July 2017 when the receding runoff from snowmelt was still able to mobilize fine sediment. However, in this stream, the beneficial effect of nutrient-rich waters is superimposed on top of the negative effect of streambed movement. Finally, a depletion of $NO_3$ from source areas (as seen in Pellerin et al. 2012) and from the biological activity itself (Hall and Tank 2003), could be responsible for the GPP drop after its peak in July 2017 in both the krenal and nival stream.

Biomass accumulation of benthic algae is a consequence of antecedent environmental conditions (e.g., PAR and nutrients) and streambed stability (e.g., Blaszczak et al. 2019). We found that the streambed in the krenal stream was more stable than in the other streams, and related this to large patches of bryophytes (Figure SI 4.3), which are known to armor the streambed (Duncan et al. 1999). In this sense, higher and prolonged stability conditions in the krenal stream could additionally explain the larger accumulation of benthic algal biomass. However, higher algal biomass in the krenal stream than in the glacier-fed and nival streams was not reflected in GPP. As showed by Guasch et al. (1995), elevated photoautotrophic biomass does not necessarily imply higher GPP; this can result from self-shading or mass transfer limitation. The community composition of benthic algal in high-mountain streams is regulated by the environmental harshness (e.g., Niedrist and Füreder 2018; Fell et al. 2018), with krenal and glacier-fed streams the most contrasted stream types in terms of community composition (Rott et al. 2006). The temporal variation in benthic community composition in alpine streams is additionally influenced by the light and streambed disturbance regimes of the benthic habitats (Wellnitz and Rader 2003). Despite not being investigated in this study, we hypothesize that differing photosynthetic efficiencies of the communities (e.g., bryophytes versus algae) in the three stream types could be responsible for the different levels of GPP observed. This would be corroborated by previous studies in a Mediterranean stream, where a change from a cyanobacterial-dominated to a green-algae dominated community resulted in an overall increase in photosynthetic capacity of the stream (Guasch et al. 1995). Differences in photosynthetic activity in response to PAR requirements have been also reported from experimental manipulations with common Alpine cyanobacterial communities (Aigner et al. 2018). In fact, bryophytes, as they are dominant in the krenal stream, were previously described to be less active per unit biomass than benthic algae (Ylla et al. 2007).

## 4.5.2   Phenology of GPP in high-mountain streams

The physicochemical and disturbance regime that each stream experiences determines the characteristic temporal pattern of ecosystem GPP, or phenology of GPP (Bernhardt et al. 2018). Our results suggest that light and flow-induced disturbance collectively shape the phenology of GPP in three Alpine streams. The favourable periods for GPP revealed in this study are in accordance with the more abundant studies of periphyton dynamics in glacier-fed and krenal streams (Battin et al. 2004; Uehlinger et al. 2010), that already identified early stages of snowmelt and the end of the glacier-melt as "windows of opportunity" for greater benthic algal growth.

Despite the perception that primary producers in high-mountain streams are likely to be most of the year under suboptimal conditions (Rott et al. 2006), GPP estimated in this study during the favourable "windows of opportunity" are bracketed between values reported from various stream ecosystem and background concentration of nutrients (Figure 4.5 ; Hoellein et al. 2013). Furthermore, the GPP that we measured in our three study streams agrees with previous studies on stream GPP measured in pre-alpine catchments, where daily GPP oscillated between 0.2 g $O_2$ m$^{-2}$ d$^{-1}$ and 12.6 g $O_2$ m$^{-2}$ d$^{-1}$ (Uehlinger and Naegeli 1998) and between 0.01 g $O_2$ m$^{-2}$ d$^{-1}$ and 29.1 g $O_2$ m$^{-2}$ d$^{-1}$ (Ulseth et al. 2018). Therefore, our results suggest a certain plasticity of primary producers to rapidly take advantage of the short environmental "windows of opportunity" in high-mountain streams.

Many aquatic consumers rely on the inputs of both autochthonous and allochthonous organic matter (Hall et al. 2001). Thus, the timing and duration of the rather predictable productivity peaks and allochthonous organic matter supply eventually determine the communities of consumers that maximally exploit the energetic resources available (Bernhardt et al. 2018). GPP values obtained in our three streams are comparable to other stream ecosystems and reinforce the role that in situ primary production has in sustaining food webs in high-mountain streams (Zah et al. 2001; Füreder et al. 2003). Furthermore, as stated by Füreder et al. (2001), recurring annual windows that are favourable for high-quality organic matter production may be also decisive in shaping the life histories and adaptive traits of the benthic invertebrates in high-mountain streams.
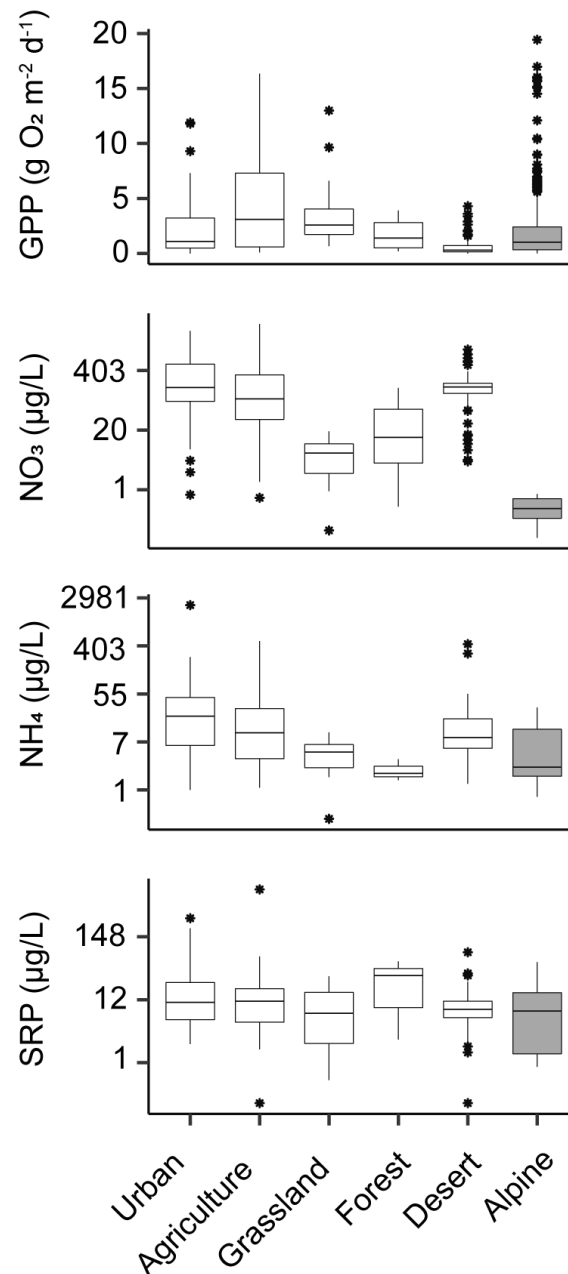
Figure 4.5 Boxplot and whisker plots summarizing daily GPP and major nutrients from this study (i.e., Alpine) and from different studies collected in Hoellein et al. (2013) data set (values only shown when discharge < 3 m³/s; total n = 182). Line within the box is the median, the box defines 25th and 75th percentiles, and the whiskers extend to the largest and lowest value no further than 1.5 times the box length.

### 4.5.3   Implications of climate change

Given the projections of changes in the hydrology of high-mountain streams owing to climate change, we tentatively propose scenarios of GPP regime change in these streams. Attempts to determine the direction and magnitude of the response of GPP regimes as a consequence of climate-driven hydrologic alteration have already been made (e.g., Marcarelli et al. 2010; Milner et al. 2017). Because of shifts in precipitation patterns from snow to rain (Berghuijs et al. 2014) and because of glacier shrinkage, the timing and magnitude of snowmelt and glacier-melt will change (Stewart et al. 2004; Huss and Hock 2018). This may shift the

timing and magnitude of the GPP as well. Once peak water is passed, lower runoff should result in a shallower water column and also lower turbidity as glacial erosion falls, such that PAR at the streambed may increase. Along with an amelioration of the conditions for primary production after peak water, changes in snowpack quantity and duration could cause a shift and an expansion in the current productivity periods towards early days in spring and later days in winter. As glacier influence decreases, bryophyte abundance may increase and compete with benthic algae (Milner et al. 2017).

This state may develop after peak water, but until then, glaciated basins are likely to be in a state of transience. As long as significant glacier cover is present, light attenuation in glacier-fed streams, glacially-driven high suspended sediment loads will be maintained. As summer melt is systematically occurring for longer in alpine glaciated basins (Lane and Nienow 2019), it is possible that periods of high turbidity are maintained for longer into the autumn, the second "window of opportunity". The latter is constrained ultimately be declining solar radiation during the autumn such that this second window becomes progressively squeezed as long as the basin contains a significant glacier coverage.

Our study paves the way to understanding the variation and controls on GPP in Alpine streams and highlights the capacity of primary producers to exploit the discrete and rather predictable windows of opportunity. An eventual alleviation from environmental harshness as runoff from snow and glacier melt decreases may lead to a greater production of autochthonous organic matter across high-mountain streams. However, in this scenario, other factors such as nutrient concentration or photoinhibition may additionally interact in limiting production. Throughout the continued measurement of productivity regimes in high-mountain streams, we will not only be able to better infer the future response of GPP to climate-driven changes, but also to assess its impact on the associated stream biogeochemistry and consumer production.

## 4.6      Figures supporting information
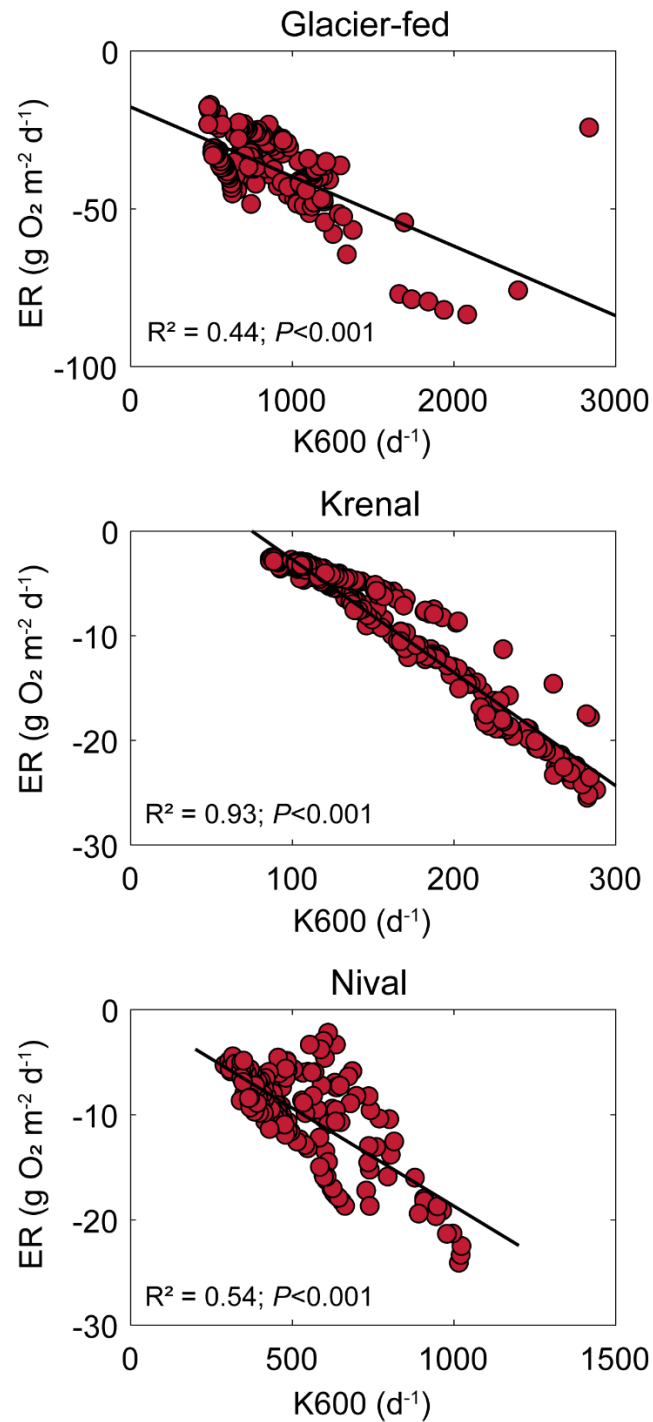


Figure SI 4.1 Relationship between K600 and ecosystem respiration (ER); K600 and ER were significantly linearly related in all stream sites and for the periods were we show GPP values.
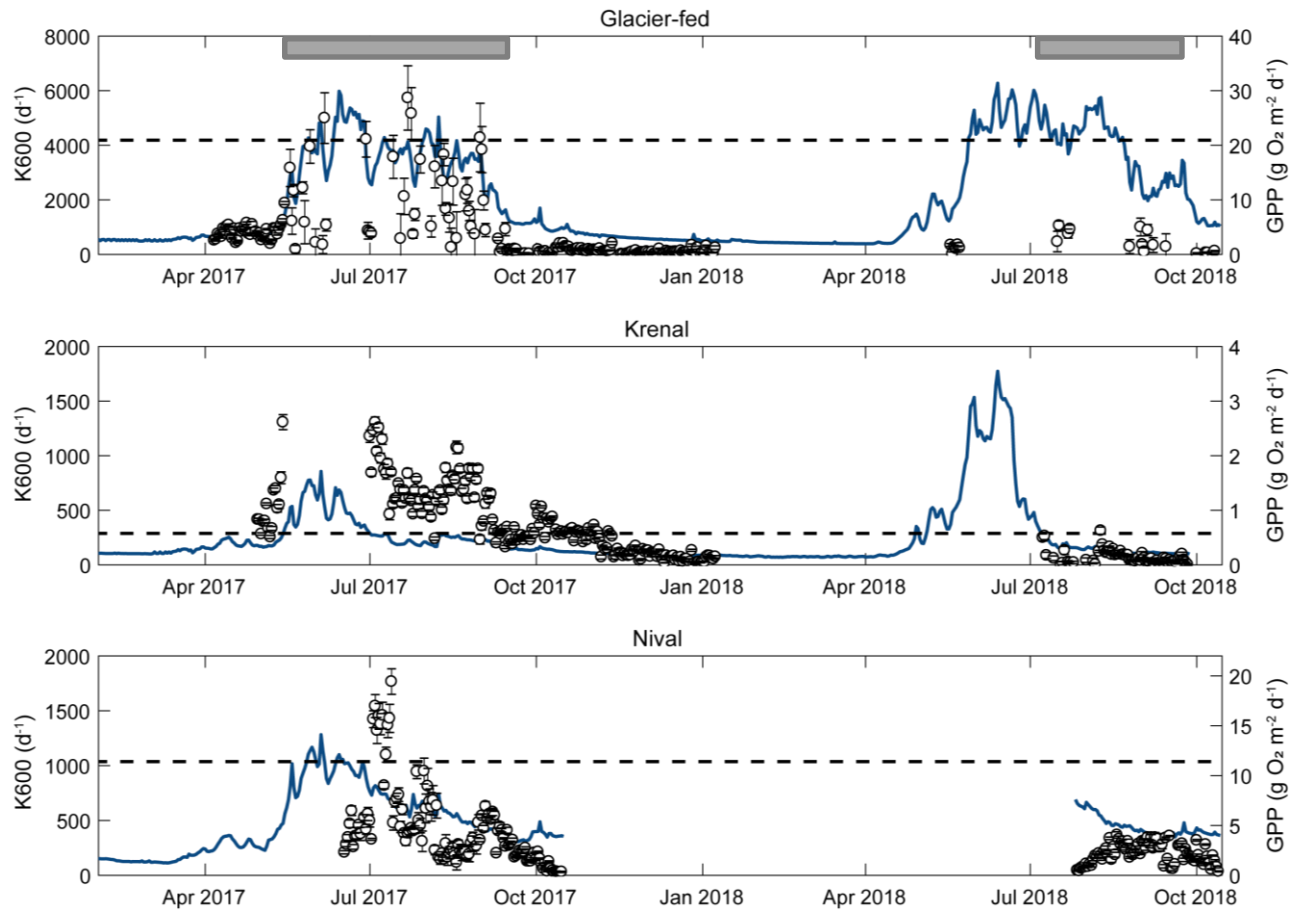
Figure SI 4.2 Time series of K600 (blue line) and GPP values estimated (white dots). Error bars of GPP values represent uncertainty on GPP estimation reported as standard deviation. Ashed line represents the maximum value of K600 measured in the field from argon releases and used as a filter for GPP values (see methods). For the glacier-fed stream, values during the melting seasons after the K600 filtering are presented (below grey bars). For the final analysis these values were subsequently also discarded due to the high error on the GPP estimations and likely attributable to high-reaeration rates.

Figure SI 4.3 Orthoimage of a section upstream from sensor station in krenal stream.

# 4.7    References

Acuña, V., A. Giorgi, I. Muñoz, U. Uehlinger, and S. Sabater. 2004. Flow extremes and benthic organic matter shape the metabolism of a headwater Mediterranean stream. Freshw. Biol. 49: 960–971. doi:10.1111/j.1365-2427.2004.01239.x

Aigner, S., K. Herburger, A. Holzinger, and U. Karsten. 2018. Epilithic Chamaesiphon (Synechococcales, Cyanobacteria) species in mountain streams of the Alps—interspecific differences in photo-physiological traits. J. Appl. Phycol. 30: 1125–1134. doi:10.1007/s10811-017-1328-7

Appling A. P., R. O. Hall, M. Arroita, and C. B. Yackulic. 2018a. streamMetabolizer: Models for estimating Aquatic Photosynthesis and Respiration. R package version 0. 10. 9. http://github.com/USGS-R/streamMetabolizer

Appling, A. P., R. O. Hall, C. B. Yackulic, and M. Arroita. 2018b. Overcoming Equifinality: Leveraging Long Time Series for Stream Metabolism Estimation. J. Geophys. Res. Biogeosciences 123: 624–645. doi:10.1002/2017JG004140

Arar E.J., and G. B. Collins. 1997. In vitro determination of chlorophyll a and pheophytin a in marine and freshwater algae by fluorescence. Cincinnati (OH): National Exposure Research Laboratory Office of Research and Development U.S. Environmental Protection Agency. (EPA publication; method no. 445.0). [cited 2014 Nov 21]. Available from: http://www.epa.gov/microbes/ documents/m445_0.pdf

Arroita, M., A. Elosegi, and R. O. Hall. 2018. Twenty years of daily metabolism show riverine recovery following sewage abatement. Limnol. Oceanogr. 1–16. doi:10.1002/lno.11053

Barnett, T. P., J. C. Adam, and D. P. Lettenmaier. 2005. Potential impacts of a warming climate on water availability in snow-dominated regions. Nature 438: 303–309. doi:10.1038/nature04141

Battin, T. J., A. Wille, R. Psenner, and A. Richter. 2004. Large-scale environmental controls on microbial biofilms in high-alpine streams. Biogeosciences 1: 159–171. doi:10.5194/bg-1-159-2004

Beaulieu, J. J., C. P. Arango, D. A. Balz, and W. D. Shuster. 2013. Continuous monitoring reveals multiple controls on ecosystem metabolism in a suburban stream. Freshw. Biol. 58: 918–937. doi:10.1111/fwb.12097

Berghuijs, W. R., R. A. Woods, and M. Hrachowitz. 2014. A precipitation shift from snow towards rain leads to a decrease in streamflow. Nat. Clim. Chang. 4: 583–586. doi:10.1038/NCLIMATE2246

Bernhardt, E. S., J. B. Heffernan, N. B. Grimm, and others. 2018. The metabolic regimes of flowing waters. Limnol. Oceanogr. 63: S99–S118. doi:10.1002/lno.10726

Bernot, M. J., D. J. Sobota, R. O. Hall, and others. 2010. Inter-regional comparison of land-use effects on stream metabolism. Freshw. Biol. 55: 1874–1890. doi:10.1111/j.1365-2427.2010.02422.x

Beniston, M., D. Farinotti, M. Stoffel, and others. 2018. The European mountain cryosphere: a review of its current state, trends, and future challenges. Cryosph. 12: 759–794. doi:10.5194/tc-12-759-2018

Biggs, B. J. F., R. A. Smith, and M. J. Duncan. 1999. Velocity and Sediment Disturbance of Periphyton in Headwater Streams: Biomass and Metabolism. J. North Am. Benthol. Soc. 18: 222–241. doi:10.2307/1468462

Biggs B. J. F., M. J. Duncan, A. M. Suren, and J.R. Holomuzki. 2001. The importance of bed sediment stability to benthic ecosystems of streams. GRAVEL-BED RIVERS V edited by M. Paul Mosley, New Zealand Hydrological Society Inc., Wellington. Page 423 – 449. ISBN 0 473 07486 9

Blaszczak, J. R., J. M. Delesantro, D. L. Urban, M. W. Doyle, and E. S. Bernhardt. 2019. Scoured or suffocated: Urban stream ecosystems oscillate between hydrologic and dissolved oxygen extremes. Limnol. Oceanogr. 64: 877–894. doi:10.1002/lno.11081

Boix Canadell, M., N. Escoffier, A. J. Ulseth, S. N. Lane, and T. J. Battin. 2019. Alpine Glacier Shrinkage Drives Shift in Dissolved Organic Carbon Export From Quasi-Chemostasis to Transport Limitation. Geophys. Res. Lett. 46: 8872–8881. doi:10.1029/2019gl083424

Collins, D. N. 2008. Climatic warming, glacier recession and runoff from Alpine basins after the Little Ice Age maximum. Ann. Glaciol. 48: 119–124. doi:10.3189/172756408784700761

Cronin, G., J. H. McCutchan, J. Pitlick, and W. M. Lewis. 2007. Use of Shields stress to reconstruct and forecast changes in river metabolism. Freshw. Biol. 52: 1587–1601. doi:10.1111/j.1365-2427.2007.01790.x

Cullis, J. D. S., L. F. Stanish, and D. M. McKnight. 2014. Diel flow pulses drive particulate organic matter transport from microbial mats in a glacial meltwater stream in the McMurdo Dry Valleys. Water Resour. Res. 50: 86–97. doi:10.1002/2013WR014061

Davies-Colley, R. J., C. W. Hickey, J. M. Quinn, and P. A. Ryan. 1992. Effects of clay discharges on streams. Hydrobiologia 248: 215–234. doi:10.1007/BF00006149

Duncan, M. J., A. M. Suren, and S. L. Brown. 1999. Assessment of Streambed Stability in Steep, Bouldery Streams: Development of a New Analytical Technique. J. North Am. Benthol. Soc. 18: 445–456. doi:10.2307/1468377

Fell, S. C., J. L. Carrivick, M. G. Kelly, L. Füreder, and L. E. Brown. 2018. Declining glacier cover threatens the biodiversity of alpine river diatom assemblages. Glob. Chang. Biol. 24: 5828–5840. doi:10.1111/gcb.14454

Fuller, R. L., S. Doyle, L. Levy, and others. 2011. Impact of regulated releases on periphyton and macroinvertebrate communities: The dynamic relationship between hydrology and geomorphology in frequently flooded rivers. River Res. Appl. 27: 630–645. doi:10.1002/rra.1385

Füreder, L., C. Schütz, M. Wallinger, and R. Burger. 2001. Physico-chemistry and aquatic insects of a glacier-fed and a spring-fed alpine stream. Freshw. Biol. 46: 1673–1690. doi:10.1046/j.1365-2427.2001.00862.x

Füreder, L., C. Welter, and J. K. Jackson. 2003. Dietary and Stable Isotope ($\delta$ 13C, $\delta$ 15N) Analyses in Alpine Stream Insects. Int. Rev. Hydrobiol. 88: 314–331. doi:10.1002/iroh.200390028

Fuß, T., B. Behounek, A. J. Ulseth, and G. A. Singer. 2017. Land use controls stream ecosystem metabolism by shifting dissolved organic matter and nutrient regimes. Freshw. Biol. 62: 582–599. doi:10.1111/fwb.12887

Gabbud, C., M. Bakker, M. Clémençon, and S. N. Lane. 2020. Hydropower flushing events cause severe loss of macro-zoobenthos in Alpine streams. 2019. Water Resour. Res. doi:10.1029/2019WR024758

Gordon, N. D., T.A. McMahon, B. L. Finlayson, C. J. Gippel, and R. J. Nathan. 2004. Stream hydrology: An introduction for ecologists. Chichester: John Wiley

Griffiths, N. A., J. L. Tank, T. V. Royer, S. S. Roley, E. J. Rosi-Marshall, M. R. Whiles, J. J. Beaulieu, and L. T. Johnson. 2013. Agricultural land use alters the seasonality and magnitude of stream metabolism. Limnol. Oceanogr. 58: 1513–1529. doi:10.4319/lo.2013.58.4.1513

Guasch, H., E. Martí, and S. Sabater. 1995. Nutrient enrichment effects on biofilm metabolism in a Mediterranean stream. Freshw. Biol. 33: 373–383. doi:10.1111/j.1365-2427.1995.tb00399.x

Hall, R. J. O., and J. L. Tank. 2003. Ecosystem metabolism controls nitrogen uptake in streams in Grand Teton National Park, Wyoming. Limnol. Oceanogr. 48: 1120–1128. doi:10.4319/lo.2003.48.3.1120

Hall, R. O., G. E. Likens, and H. M. Malcom. 2001. Trophic basis of invertebrate production in 2 streams at the Hubbard Brook Experimental Forest. J. North Am. Benthol. Soc. 20: 432–447. doi:10.2307/1468040

Hall, R. O., C. B. Yackulic, T. A. Kennedy, M. D. Yard, E. J. Rosi-Marshall, N. Voichick, and K. E. Behn. 2015. Turbidity, light, temperature, and hydropeaking control primary productivity in the Colorado River, Grand Canyon. Limnol. Oceanogr. 60: 512–526. doi:10.1002/lno.10031

Hieber, M., C. T. Robinson, S. R. Rushforth, and U. Uehlinger. 2001. Algal Communities Associated with Different Alpine Stream Types. Arctic, Antarct. Alp. Res. 33: 447. doi:10.2307/1552555

Hill, W. R., P. J. Mulholland, and E. R. Marzolf. 2001. Stream ecosystem responses to forest leaf emergence in spring. Ecology 82: 2306–2319. doi:10.1890/0012-9658(2001)082[2306:SERTFL]2.0.CO;2

Hodgkins, G. A., and R. W. Dudley. 2006. Changes in the timing of winter–spring streamflows in eastern North America, 1913–2002. Geophys. Res. Lett. 33: L06402. doi:10.1029/2005GL025593

Hoellein, T. J., D. A. Bruesewitz, and D. C. Richardson. 2013. Revisiting Odum (1956): A synthesis of aquatic ecosystem metabolism. Limnol. Oceanogr. 58: 2089–2100. doi:10.4319/lo.2013.58.6.2089

Holmes, R. M., A. Aminot, R. Kérouel, B. A. Hooker, and B. J. Peterson. 1999. A simple and precise method for measuring ammonium in marine and freshwater ecosystems. Can. J. Fish. Aquat. Sci. **56**: 1801–1808. doi:10.1139/f99-128

Hotchkiss, E. R., R. O. Hall Jr, R. A. Sponseller, D. Butman, J. Klaminder, H. Laudon, M. Rosvall, and J. Karlsson. 2015. Sources of and processes controlling $CO_2$ emissions change with the size of streams and rivers. Nat. Geosci. 8: 696–699. doi:10.1038/ngeo2507

Hoyle, J. T., C. Kilroy, D. M. Hicks, and L. Brown. 2017. The influence of sediment mobility and channel geomorphology on periphyton abundance. Freshw. Biol. 62: 258–273. doi:10.1111/fwb.12865

Huss, M., and R. Hock. 2018. Global-scale hydrological response to future glacier mass loss. Nat. Clim. Chang. 8: 135–140. doi:10.1038/s41558-017-0049-x

Izagirre, O., U. Agirre, M. Bermejo, J. Pozo, and A. Elosegi. 2008. Environmental controls of whole-stream metabolism identified from continuous monitoring of Basque streams. J. North Am. Benthol. Soc. 27: 252–268. doi:10.1899/07-022.1

Jacobsen, D., and O. Dangles. 2017. Ecology of High Altitude Waters, Oxford University Press.

Koenker, R. 2019. quantreg: Quantile Regression. R package version 5.51. https://CRAN.R-project.org/package=quantreg

Lane, S. N., M. Bakker, C. Gabbud, N. Micheletti, and J.-N. Saugy. 2017. Sediment export, transient landscape response and catchment-scale connectivity following rapid climate warming and Alpine glacier recession. Geomorphology 277: 210–227. doi:10.1016/j.geomorph.2016.02.015

Lane, S. N., and P. W. Nienow. 2019. Decadal-Scale Climate Forcing of Alpine Glacial Hydrological Systems. Water Resour. Res. 55: 2478–2492. doi:10.1029/2018WR024206

Lovett, G. M., J. J. Cole, and M. L. Pace. 2006. Is net ecosystem production equal to ecosystem carbon accumulation? Ecosystems 9: 152–155. doi:10.1007/s10021-005-0036-3

Lupon, A., E. Martí, F. Sabater, and S. Bernal. 2016. Green light: gross primary production influences seasonal stream N export by controlling fine-scale N dynamics. Ecology 97: 133–144. doi:10.1890/14-2296.1

Marcarelli, A. M., C. V. Baxter, M. M. Mineau, and R. O. Hall. 2011. Quantity and quality: unifying food web and ecosystem perspectives on the role of resource subsidies in freshwaters. Ecology 92: 1215–1225. doi:10.1890/10-2240.1

Marcarelli, A. M., R. W. Van Kirk, and C. V. Baxter. 2010. Predicting effects of hydrologic alteration and climate change on ecosystem metabolism in a western U.S. river. Ecol. Appl. 20: 2081–2088. doi:10.1890/09-2364.1

McCutchan, J. H., W. M. Lewis, and J. F. Saunders,. 1998. Uncertainty in the Estimation of Stream Metabolism from Open-Channel Oxygen Concentrations. J. North Am. Benthol. Soc. 17: 155–164. doi:10.2307/1467959

Miller, M. P., D. M. McKnight, J. D. Cullis, A. Greene, K. Vietti, and D. Liptzin. 2009. Factors controlling streambed coverage of Didymosphenia geminata in two regulated streams in the Colorado Front Range. Hydrobiologia 630: 207–218. doi:10.1007/s10750-009-9793-x

Milner, A. M., L. E. Brown, and D. M. Hannah. 2009. Hydroecological response of river systems to shrinking glaciers. Hydrol. Process. 23: 62–77. doi:10.1002/hyp.7197

Milner, A. M., K. Khamis, T. J. Battin, and others. 2017. Glacier shrinkage driving global changes in downstream systems. Proc. Natl. Acad. Sci. 201619807. doi:10.1073/pnas.1619807114

Minshall, G. W. 1978. Autotrophy in Stream Ecosystems. Bioscience 28: 767–771. doi:10.2307/1307250

Mulholland, P. J., C. S. Fellows, J. L. Tank, and others. 2001. Inter-biome comparison of factors controlling stream metabolism. Freshw. Biol. 46: 1503–1517. doi:10.1046/j.1365-2427.2001.00773.x

Murphy, J., and J. P. Riley. 1962. A modified single solution method for the determination of phosphate in natural waters. Anal. Chim. Acta **27**: 31–36. doi:10.1016/S0003-2670(00)88444-5

Niedrist, G. H., M. Cantonati, and L. Füreder. 2018. Environmental harshness mediates the quality of periphyton and chironomid body mass in alpine streams. Freshw. Sci. 37: 519–533. doi:10.1086/699480

Niedrist, G. H., and L. Füreder. 2018. When the going gets tough, the tough get going: the enigma of survival strategies in harsh glaical stream environments. Freshw. Biol. n/n. doi:10.1111/fwb.13131

Odum, H. T. 1956. Primary Production in Flowing Waters. Limnol. Oceanogr. 1: 102–117. doi:10.4319/lo.1956.1.2.0102

Pellerin, B. A., J. F. Saraceno, J. B. Shanley, S. D. Sebestyen, G. R. Aiken, W. M. Wollheim, and B. A. Bergamaschi. 2012. Taking the pulse of snowmelt: In situ sensors reveal seasonal, event and diurnal patterns of nitrate and dissolved organic matter variability in an upland forest stream. Biogeochemistry 108: 183–198. doi:10.1007/s10533-011-9589-8

Pinheiro, J., D. Bates, S. DebRoy, D. Sarkar, and R Core Team. 2018. *nlme: linear and nonlinear mixed effects models*. R package version 3.1-137, https://CRAN.R-project.org/package=nlme

Roberts, B. J., P. J. Mulholland, and W. R. Hill. 2007. Multiple Scales of Temporal Variability in Ecosystem Metabolism Rates: Results from 2 Years of Continuous Monitoring in a Forested Headwater Stream. Ecosystems 10: 588–606. doi:10.1007/s10021-007-9059-2

Robinson, C. T., U. Uehlinger, F. Guidon, P. Schenkel, and R. Skvarc. 2002. Limitation and retention of nutrients in alpine streams of Switzerland. SIL Proceedings, 1922-2010 28: 263–272. doi:10.1080/03680770.2001.11902585

Rocher-Ros, G., R. A. Sponseller, A. Bergström, M. Myrstener, and R. Giesler. 2019. Stream metabolism controls diel patterns and evasion of CO 2 in Arctic streams. Glob. Chang. Biol. gcb.14895. doi:10.1111/gcb.14895

Rott, E., M. Cantonati, L. Füreder, and P. Pfister. 2006. Benthic Algae in High Altitude Streams of the Alps -- a Neglected Component of the Aquatic Biota. Hydrobiologia 562: 195–216. doi:10.1007/s10750-005-1811-z

Savoy, P., A. P. Appling, J. B. Heffernan, E. G. Stets, J. S. Read, J. W. Harvey, and E. S. Bernhardt. 2019. Metabolic rhythms in flowing waters: An approach for classifying river productivity regimes. Limnol. Oceanogr. 1–17. doi:10.1002/lno.11154

Sebestyen, S. D., E. W. Boyer, J. B. Shanley, C. Kendall, D. H. Doctor, G. R. Aiken, and N. Ohte. 2008. Sources, transformations, and hydrological processes that control stream nitrate and dissolved organic matter concentrations during snowmelt in an upland forest. Water Resour. Res. 44: 1–14. doi:10.1029/2008WR006983

Segura, C., J. H. McCutchan, W. M. Lewis, and J. Pitlick. 2011. The influence of channel bed disturbance on algal biomass in a Colorado mountain stream. Ecohydrology 4: 411–421. doi:10.1002/eco.142

Stewart, I. T. 2009. Changes in snowpack and snowmelt runoff for key mountain regions. Hydrol. Process. 23: 78–94. doi:10.1002/hyp.7128

Stewart, I. T., D. R. Cayan, and M. D. Dettinger. 2004. Changes in Snowmelt Runoff Timing in Western North America under a `Business as Usual' Climate Change Scenario. Clim. Change 62: 217–232. doi:10.1023/B:CLIM.0000013702.22656.e8

Stoffel, M., and C. Corona. 2018. Future winters glimpsed in the Alps. Nat. Geosci. 11: 458–460. doi:10.1038/s41561-018-0177-6

Taylor, B., C. Keep, R. Hall, B. Koch, L. Tronstad, A. Flecker, and A. Ulseth. 2007. Improving the fluorometric ammonium method: Matrix effects, background fluorescence, and standard additions. J. North Am. Benthol. Soc. - J N Amer Benthol Soc **26**: 167–177. doi:10.1899/0887-3593(2007)26[167:ITFAMM]2.0.CO;2

Thimijan, R., and R. Heins. 1983. Photometric, radiometric, and quantum light units of measure: a review of procedures for interconversion. Hortic Sci 18: 818–822.

Tockner, K., F. Malard, U. Uehlinger, and J. V. Ward. 2002. Nutrients and organic matter in a glacial river-floodplain system (Val Roseg, Switzerland). Limnol. Oceanogr. 47: 266–277. doi:10.4319/lo.2002.47.1.0266

Uehlinger, U. 1991. Spatial and temporal variability of the periphyton biomass in a prealpine river (Necker, Switzerland). Archiv Fur Hydrobiologie 123: 219–237

Uehlinger, U. 2000. Resistance and resilience of ecosystem metabolism in a flood-prone river system. Freshw. Biol. 45: 319–332. doi:10.1046/j.1365-2427.2000.00620.x

Uehlinger, U. 2006. Annual cycle and inter-annual variability of gross primary production and ecosystem respiration in a floodprone river during a 15-year period. Freshw. Biol. 51: 938–950. doi:10.1111/j.1365-2427.2006.01551.x

Uehlinger, U., B. Kawecka, and C. T. Robinson. 2003. Effects of experimental floods on periphyton and stream metabolism below a high dam in the Swiss Alps (River Spöl). Aquat. Sci. 65: 199–209. doi:10.1007/s00027-003-0664-7

Uehlinger, U., M. Naegeli, and S. G. Fisher. 2002. A heterotrophic desert stream? The role of sediment stability. West. North Am. Nat. 62: 466–473.

Uehlinger, U., and M. W. Naegeli. 1998. Ecosystem Metabolism, Disturbance, and Stability in a Prealpine Gravel Bed River. J. North Am. Benthol. Soc. 17: 165–178. doi:10.2307/1467960

Uehlinger, U., C. T. Robinson, M. Hieber, and R. Zah. 2010. The physico-chemical habitat template for periphyton in alpine glacial streams under a changing climate. Hydrobiologia 657: 107–121. doi:10.1007/s10750-009-9963-x

Ulseth, A. J., E. Bertuzzo, G. A. Singer, J. Schelker, and T. J. Battin. 2018. Climate-Induced Changes in Spring Snowmelt Impact Ecosystem Metabolism and Carbon Fluxes in an Alpine Stream Network. Ecosystems 21: 373–390. doi:10.1007/s10021-017-0155-7

Ulseth, A. J., R. O. Hall, M. Boix Canadell, H. L. Madinger, A. Niayifar, and T. J. Battin. 2019. Distinct air–water gas exchange regimes in low- and high-energy streams. Nat. Geosci. 12: 259–263. doi:10.1038/s41561-019-0324-8

Val, J., R. Pino, E. Navarro, and D. Chinarro. 2016. Addressing the local aspects of global change impacts on stream metabolism using frequency analysis tools. Sci. Total Environ. 569–570: 798–814. doi:10.1016/j.scitotenv.2016.06.178

Van de Bogert, M. C., S. R. Carpenter, J. J. Cole, and M. L. Pace. 2007. Assessing pelagic and benthic metabolism using free water measurements. Limnol. Oceanogr. Methods 5: 145–155. doi:10.4319/lom.2007.5.145

Vannote, R. L., G. W. Minshall, K. W. Cummins, J. R. Sedell, and C. E. Cushing. 1980. The River Continuum Concept. Can. J. Fish. Aquat. Sci. 37: 130–137. doi:10.1139/f80-017

Ward, J. V. 1994. Ecology of alpine streams. Freshw. Biol. 32: 277–294. doi:10.1111/j.1365-2427.1994.tb01126.x

Wellnitz, T. A., and J. V. Ward. 2000. Herbivory and irradiance shape periphytic architecture in a Swiss alpine stream. Limnol. Oceanogr. 45: 64–75. doi:10.4319/lo.2000.45.1.0064

Wellnitz, T., and R. B. Rader. 2003. Mechanisms influencing community composition and succession in mountain stream periphyton: interactions between scouring history, grazing, and irradiance. J. North Am. Benthol. Soc. 22: 528–541. doi:10.2307/1468350

Ylla, I., A. M. Romaní, and S. Sabater. 2007. Differential effects of nutrients and light on the primary production of stream algae and mosses. Fundam. Appl. Limnol. / Arch. für Hydrobiol. 170: 1–10. doi:10.1127/1863-9135/2007/0170-001

Young, R. G., and A. D. Huryn. 1996. Interannual variation in discharge controls ecosystem metabolism along a grassland river continuum. Can. J. Fish. Aquat. Sci. 53: 2199–2211. doi:10.1139/f96-186

Zah, R., P. Burgherr, S. M. Bernasconi, and U. Uehlinger. 2001. Stable isotope analysis of macroinvertebrates and their food sources in a glacier stream. Freshw. Biol. 46: 871–882. doi:10.1046/j.1365-2427.2001.00720.x

Zah, R., and U. Uehlinger. 2001. Particulate organic matter inputs to a glacial stream ecosystem in the Swiss Alps. Freshw. Biol. 46: 1597–1608. doi:10.1046/j.1365-2427.2001.00847.x

# Chapter 5   Summary and Conclusions

## 5.1    Achieved results

In this thesis, with the use of high-frequency time series data I explored carbon fluxes and ecosystem energetics in high-mountain streams. First chapter of the thesis is focused on dissolved organic carbon export and its response to hydrology, while the second and third focused on identifying the processes that dominate ecosystem functioning and the quantification and delimitation of the productivity regimes in three Alpine stream types.

Despite the acknowledged role of both snowmelt and glacier melt in delivering DOC to the stream, the annual DOC flux behaviour from alpine landscapes are poorly understood. In Chapter 2, I studied DOC yield response to runoff in twelve streams with different glacier and vegetation coverage in their catchments. The acquisition of high frequency time series of chromophoric dissolved organic carbon as a proxy of DOC concentration allowed me to study the DOC flux behaviour and its drivers during one hydrological year. Through the analysis of the slope from the relationship between DOC yield and runoff I could establish that from glacierized to non-glacierized catchments, hydrologic flow and not DOC sources determined DOC flux behaviour. DOC source availability was related to vegetation coverages across catchments, which in the case of glacierized catchments, was linked to the historical glacier retreat.

In Chapter 3, I determined the occurrence of biological and physical processes in shaping dissolved oxygen concentration patterns in three Alpine stream types. For this, I made use of two years of oxygen time series concentration (in terms of saturation) from three streams with contrasting hydrological regimes: glacier-, snowmelt- and groundwater-fed. Later, I related dissolved oxygen dynamics with its potential drivers: light availability at the streambed, air-water gas exchange, turbidity, discharge and streambed stability. The findings showed that the different hydrological regimes, through the effect of disturbance, light limitation and turbulence regimes, determined the characteristic daily and seasonal oxygen patterns across Alpine stream types. The use of Shannon entropy to describe daily variability of dissolved oxygen proved to be a useful measure to explore the temporal dynamics of streamwater dissolved oxygen and to infer information on the ecosystem energetics and on the potential drivers.

Finally, in Chapter 4, I estimated gross primary production (GPP) for the potential productivity periods revealed in Chapter 3. In each stream, favourable periods for GPP were constrained by the light available at the streambed and disturbance conditions that were mostly determined by the hydrological and turbidity regime. GPP values reported in this chapter highlight the capacity of primary producers to exploit the finite favourable periods for GPP in high-mountain streams.

## 5.2    Conclusions and outlook

Climate change is predicted to have major impacts on high-mountain hydrological regimes, particularly on glacier-fed streams that, as glaciers shrink and glacier melt contribution decreases, will shift towards nival and krenal-type stream ecosystems (Beniston et al. 2018). Therefore, it is of critical importance to identify the effect of the hydrological regimes in high-mountain catchments on stream biogeochemistry and ecosystem functioning to anticipate the effect of those changes on carbon fluxes. Investigating the effect

of the hydrological alterations on biogeochemistry and ecosystem functioning would ideally involve examining trends over long term time series. In this thesis, due to the absence of extensive long term measurements, a space-for-time substitution approach was used to propose scenarios of change of the behaviour of the DOC fluxes and of the productivity regimes in high-mountain streams.

In glacierized catchments, glacier dynamics, sediment production and glacier runoff modulated both the chemostatic behaviour of DOC yield and the stream ecosystem energetics. As glaciers shrink, runoff generated from ice melt initially increases until a "peak water" is reached, beyond which it diminishes until the ice mass has disappeared (Huss and Hock 2018). In the scenario before "peak water", I first assume an associated increase in DOC yield due to an increase in glacier runoff. As for the windows of opportunity for primary production, the more layers of contraint and the degree of correlation among them and among discharge will reduce predictability of the windows of opportunity for primary production. Also, intraannual variation in each of the constraints will add uncertainty to those predictions. With this is mind and in the scenarion before "peak water", I suggest an increase in glacier environmental harshness caused by an increase in glacier melt and an associated increase therefore of streambed disturbance and streamwater turbidity. Due to warmer temperatures, summer harsh conditions will be extended towards further days in summer and autumn. This scenario, will narrow the second window of opportunity favourable for primary producers and overall in-stream primary production may decrease. As glaciers become smaller, a gradual decrease of glacier runoff after the "peak water" may alleviate the summer period from flow-induced disturbance. However, with a yet present glacier, glacier contribution to the suspended load of sediment may still cause a reduction of the light available at the streambed. As glacier shrink, runoff production from ice melt directly feeding into the stream channel will diminish and thereby the DOC yield as well. In this scenario, new hydrological flow paths through the catchment may diversify the delivery of DOC from different sources to the stream. Eventually, some glaciers will completely disappear (Huss and Fischer 2016), thus proportional groundwater contributions to streamflow will increase. Clearer water and better stability conditions due to lower discharge will create a favourable summer physical template that may enhance primary production activity. However, under this new scenario, other factors such as nutrient limitation, photoinhibition or flow intermittency might play a more important role regulating productivity regimes.

In snowmelt-driven catchments, I propose that a reduction in the snowpack duration and accumulation will shift towards early spring the window of opportunity for primary production occurring at the very onset of the snowmelt. Also, a reduction in the time that the stream remains snow covered will expand towards early spring and late winter the favourable environmental period for GPP to occur. Across high-mountain streams, the now extended mild physical template may lead to an overall greater production of autochthonous organic matter. A shift from snow- towards rain-dominated regime is likely to negatively impact the snowmelt-associated DOC delivery to the stream and also may alter the nutrient supply occurring during this period. These changes will be accompanied by alterations in plant communities and soil properties due to warmer temperatures (Mayor et al. 2017) that will eventually impact soil organic carbon sources and their distribution within high-mountain catchments.

Both the lateral DOC fluxes and primary production patterns and estimates reported in this thesis represent energy inputs that support high-mountain stream ecosystems. Consumers within the stream, from microorganisms to invertebrate macrofauna, decompose and consume these supplies of organic carbon, ultimately respiring and converting some fraction to $CO_2$. The consumption of organic matter from both the autotrophic and heterotrophic component is quantified by the estimation of ecosystem respiration (ER), the second process that constitutes ecosystem metabolism. Additional ER estimations and their balance with GPP could inform us about the trophic state of the stream (Dodds and Cole 2007) and to which extent

the energy inputs, both allochthonous and autochthonous, are used within a stream (Webster and Meyer 1997). Scenarios of an increase in primary production like the ones suggested in this thesis would increase autochthonous organic matter yield, which eventually, would be respired proportionally (Staehr et al. 2012). A scenario towards hydrological transport limiting DOC export from the catchment rather than terrestrial DOC sources could ultimately enhance stream respiration via microbial communities. Last but not least, a shift in the temporal patterns of the allochthonous and autochthonous inputs, confined to hydrological events and environmental favourable periods respectively, would likely impact the respective communities of consumers whose life-history is associated with those and rather predictable energetic inputs.

Overall, the results presented in this thesis can be seen as a first step in the assessment of lateral DOC fluxes and productivity regimes in Alpine streams across a gradient of glacier coverage and through the use of data at high temporal resolution. Also, they are thought to contribute to our understanding of how global warming, through the alteration of hydrological regimes and stream's physicochemical template, is altering stream ecosystem biogeochemistry and function and the overall role of alpine streams in the global carbon cycle.

## 5.3    References

Beniston, M., D. Farinotti, M. Stoffel, and others. 2018. The European mountain cryosphere: a review of its current state, trends, and future challenges. Cryosph. 12: 759–794. doi:10.5194/tc-12-759-2018

Dodds, W. K., and J. J. Cole. 2007. Expanding the concept of trophic state in aquatic ecosystems: It's not just the autotrophs. Aquat. Sci. 69: 427–439. doi:10.1007/s00027-007-0922-1

Huss, M., and M. Fischer. 2016. Sensitivity of very small glaciers in the Swiss Alps to future climate change. Front. Earth Sci. 4: 1-17. doi:10.3389/feart.2016.00034

Huss, M., and R. Hock. 2018. Global-scale hydrological response to future glacier mass loss. Nat. Clim. Chang. 8: 135–140. doi:10.1038/s41558-017-0049-x

Mayor, J. R., N. J. Sanders, A. T. Classen, and others. 2017. Elevation alters ecosystem properties across temperate treelines globally. Nature 542: 91–95. doi:10.1038/nature21027

Staehr, P. A., J. M. Testa, W. M. Kemp, J. J. Cole, K. Sand-Jensen, and S. V. Smith. 2012. The metabolism of aquatic ecosystems: History, applications, and future challenges. Aquat. Sci. 74: 15–29. doi:10.1007/s00027-011-0199-2

Webster, J. R., and J. L. Meyer. 1997. Stream Organic Matter Budgets: An Introduction. J. North Am. Benthol. Soc. 16: 3–13. doi:10.2307/1468223

# Curriculum Vitae

# Marta Boix Canadell

Biologist and freshwater ecologist with a variety of professional experiences in environmental management and research

@ mboixcan@gmail.com

📞 +41 76 778 64 05

📍 Route de la Plaine 5, 1022 Chavannes-près-Renens, Switzerland

## WORK AND RESEARCH EXPERIENCE

**Dec 2015 - Jan 2020**

### Doctoral Assistant
#### Stream biofilm and ecosystem research laboratory
École Polytechnique Fédérale de Lausanne, EPFL (Switzerland)

- Studied impact of global warming on Alpine stream biogeochemistry
- Collected in the field and subsequently analysed time series of discharge, streamwater physicochemical parameters and geomorphological data to investigate carbon export and production across a range of Alpine hydrologic regimes

**May 2013 – May 2015**

### Research Assistant

National University of Singapore (Singapore)

- Participated in design and operation of a National Biological Monitoring Program for the study of the quality of Singapore's freshwaters (reservoirs and waterways)
- Collected environmental in situ data and benthic macroinvertebrates
- Analysed and interpreted data to assess water ecological status
- Produced technical and research reports

**May - Aug 2012**

### Field Technologist

Alberta Biodiversity Monitoring Institute - Alberta Innovates Technology Futures (Canada)

- Surveyed terrestrial and aquatic ecosystems for field data collection: aquatic macroinvertebrates, birds, forest stand composition, soil, plants and wetland vegetation mapping
- Sorted and identification of collected specimens: aquatic invertebrates

**Sept - Dec 2010**
**Aug 2008 - Jan 2010**

### Wildlife Biologist

Game and Fish Department - Catalan Environmental Council (Spain)

- Organized and executed fieldwork campaigns for the wild rabbit (*Oryctolagus cuniculus*) and red partridge (*Alectoris rufa*) genetic and population study
- Participated in writing final results

| | |
|---|---|
| Nov 2006 - Jul 2008 | **Wastewater Technician** |
| | Catalan Water Agency - Catalan Environmental Council (Spain) |

- Evaluated wastewater treatment systems of industries in fulfilment of domestic
  and international legislation and tailored efforts to the characteristics of the activity
- Provided technical and legal advice to industries and citizens
- Wrote official wastewater reports of the industries and farms evaluated

## EDUCATION

| | |
|---|---|
| Dec 2015 – Jan 2020 | **Doctoral Program in Civil and Environmental Engineering**<br>Stream Biofilm and Ecosystem Research Laboratory<br>École Polytechnique Fédérale de Lausanne (EPFL) |
| Sept 2010 - Sept 2011 | **Master's Degree in Fundamental and Applied Ecology**<br>University of Barcelona and University of Girona |
| Jan 2007 – May 2007 | **Postgraduate Course in Geographical Information Systems (GIS)**<br>University of Lleida |
| Sept 2001 - Sept 2006 | **Bachelor's Degree in Biology**<br>University of Barcelona |

## PERSONAL SKILLS

**Technical skills**
- Highly competent in data handling, analysis and visualization using R and Matlab
- Highly experienced in Geographical Information Systems (ArcGIS)
- Professional command with Microsoft Office™ tools
- Bibliographic research using ISI Web of Knowledge
- Proven experience in data collection and monitoring

**Soft skills**
- Strong organization, research and analytical skills
- Positive attitude and ability to work independently or as a part of a team
- Highly motivated in learning and acquiring new knowledge

**Languages**
- Spanish – Mother Tongue
- English – Professional
- French – Intermediate

**Others**
- Driving licence (B)

**Boix Canadell, M.**, Escoffier, N., Ulseth, A. J., Lane, S. N., & Battin, T. J. (2019). Alpine glacier shrinkage drives shift in dissolved organic carbon export from quasi-chemostasis to transport-limitation. *Geophysical Research Letters,* 46(15), 8872-8881. https://doi.org/10.1029/2019gl083424

Ulseth, A. J., Hall, R. O., **Boix Canadell, M**., Madinger, H. L., Niayifar, A., & Battin, T. J. (2019). Distinct air-water gas exchange regimes in low- and high-energy streams. *Nature Geosciences*, 12(4), 259-263. https://doi.org/10.1038/s41561-019-0324-8

Horgby, Å., **Boix Canadell, M.**, Ulseth, A. J., Vennemann, T. W., & Battin, T. J. (2019). High-resolution spatial sampling identifies groundwater as driver of $CO_2$ dynamics in an Alpine stream network. *Journal of Geophysical Research: Biogeosciences*, 124. https://doi.org/10.1029/2019JG005047

Kneib, M., Cauvy-Fraunié, S., Escoffier, N., **Boix Canadell, M.**, Horgby, Å., & Battin, T. J. (2020). Glacier retreat changes diurnal variation intensity and frequency of hydrologic variables in Alpine and Andean streams. *Journal of Hydrology*, 583, https://doi.org/10.1016/j.jhydrol.2020.124578